Mechanisms of Cross-Modal Refinement by Visual Experience

Dissertation Advisor: Takao K. Hensch Daniel Mahefasoa Brady

Mechanisms of Cross-Modal Refinement by Visual Experience

Abstract

Alteration of one sensory system can have striking effects on the processing and organization of the remaining senses, a phenomenon known as cross-modal plasticity. The goal of this thesis was to understand the circuit basis of this form of plasticity.

I established the mouse as a model system for studying cross-modal plasticity by comparing population activity in visual cortex between animals reared in complete darkness from birth (DR) to those housed in a normal light/dark environment (LR). I found that secondary visual cortex (V2L) responds much more strongly to auditory stimuli in DR than LR. I provide evidence that there is a sensitive period for cross-modal responses that ends in early adulthood. I also show that exposure to light later in life reduces V2L auditory activity to LR levels.

I recorded single units to show that there is a higher percentage of auditory responsive neurons in DR V2L. In collaboration with Lia Min in Michela Fagiolini's laboratory, we discovered that this was associated with an increase in

the number of projections from auditory thalamus and auditory cortex. We also provide evidence that V2L is multimodal from birth and becomes less so with visual experience.

I examined several molecular pathways that are affected by dark-rearing to see if they are involved in cross-modal plasticity. I found that Nogo receptor (NgR), Lynx1, and Icam5 signaling all play a fundamental role in controlling the duration of plasticity. I also show that the hyperconnectivity in NgR -/- and DR mice leads to an increase in multisensory enhancement.

In primary visual cortex, cross-modal influences were much weaker. Similar to V2L, the distribution of cell types was affected by NgR signaling. I also found that both the range of cross-modal influence and its sign (excitatory or inhibitory) is dependent on visual experience. Finally, I show that NgR signaling and the maturation of inhibitory circuits affect these two properties.

Together, these results provide evidence of the molecular mechanisms underlying cross-modal plasticity. We believe that this will further our knowledge of how to improve rehabilitation strategies after loss of a sensory system.

Acknowledgements

To my parents, Michael, and Naira for their unconditional love and support

To Richard and Jon for being the best housemates

To Brett, Kevin, and Tim for their availability in imbibing

To Stacy, Richard, Andrew, Ryan, and Moriko for being my gang in New York

To the ocean and surfing for keeping me sane

Oh, and to every colleague and advisor I have ever had that made me the scientist I am today…

Table of Contents

Chapter 1

Introduction

The human brain has a remarkable capacity to reorganize itself in response to surrounding external experience (Hensch, 2004). Experience can influence cortical representations of fingers based on musical training (Pantev et al., 2001), how sounds are perceptually categorized for language (Kuhl, 2004), and can even allow large areas of brain to compensate for lost functions after insult and injury (Anderson et al., 2011). The strength of this 'plasticity' is dependent on both the efficacy of the pertinent training paradigm and when it is employed (Will et al., 2004). In most cases, the earlier the better, as multisensory processing is dependent on age of cochlear implantation (Schorr et al., 2005), language processing on age of hearing loss identification in deaf children (Yoshinaga-Itano et al., 1998), and cognitive recovery on age of social immersion (Nelson et al., 2007). This has led to the idea that there are critical or sensitive periods for cortical plasticity during brain development that consolidate early life experience (Hensch, 2005). Much work over the last few decades has been dedicated to understanding the anatomical, physiological, and molecular mechanisms that underlie the induction, duration, and closure of critical periods across brain regions. The hope is that one day improved early diagnoses of brain function coupled with the reopening of plasticity in relevant brain areas will help

rehabilitation strategies at any age, whether the impairment stems from low level malformations such as the occlusion of vision to higher order deficits that underlie complex neurodevelopmental and cognitive disorders.

Mechanisms of critical period plasticity

Ocular dominance plasticity has long been the leading model to study plasticity, as there is a clear critical period for binocular vision early in life (Hubel et al., 1977). Monocular occlusion leads to a behavioral reduction in responses to the deprived eye, an effect that is mediated in primary visual cortex (Prusky et al., 2000). Over a decade ago, the first direct experimental control over the induction of ocular dominance plasticity was achieved by altering local circuit excitation/inhibition (E/I balance) (Hensch et al., 1998b). Subsequent experiments showed that the potential for plasticity is retained throughout life until an inhibitory threshold is attained (Fagiolini & Hensch, 2000). More specifically, it is the late maturation of inhibitory Parvalbumin-positive large basket (PV) cells that mediates this form of plasticity (Fagiolini et al., 2004). Whether PV cells control the opening of critical periods for other receptive field properties across multiple sensory domains is unclear and is an active area of research.

The maturation of excitatory circuits has also been implicated in critical period induction. For many years, homosynaptic plasticity at excitatory synapses alone was thought to control ocular dominance plasticity, but experimental manipulations failed to produce changes *in vivo* (Hensch & Stryker, 1996; Hensch et al., 1998a; Renger et al. 2002). However, mice with immature

excitatory circuits arising from targeted gene-disruption of NR2A, a subunit of the *N*-methyl-*D*-aspartate (NMDA) glutamate receptor, fail to develop orientation selectivity despite normal visual experience (Fagiolini et al., 2003). Thus, the maturation of inhibitory and excitatory circuits controls separable features of visual cortical plasticity.

Rapid functional plasticity is converted to long lasting structural changes by a variety of pre- and postsynaptic mechanisms. Axonal outgrowth is inhibited when presynaptic Nogo receptors and PirB receptors bind to oligodendrocyte-released Nogo, OMgp, and MAG (Atwal et al., 2008; Schwab, 2010). This, in turn, consolidates functional circuits and reduces plasticity (McGee et al., 2005; Syken et al., 2006). Postsynaptically, monocular deprivation increases proteolytic (tPA-plasmin) activity (Mataga et al., 2002), leading to increased dendritic spine motility (Oray et al., 2004). This is followed by transient elimination and regrowth of spines in favor of the non-deprived eye (Mataga et al., 2004). Along these lines, accelerating the maturation of dendritic spines by deletion of intracellular adhesion molecule 5 (Icam5) accelerates the window of plasticity for auditory thalamocortical connectivity (Barkat et al., 2011).

Finally, molecular brakes on modulatory systems play an active role in suppressing plasticity in adulthood. Depletion of catecholamines by the administration of 6-OH-dopamine, which selectively destroys dopaminergic and noradrenergic neurons, prevents ocular dominance plasticity in kittens (Kasamatsu & Pettigrew, 1976; Bear et al., 1983). Chronic administration of fluoxetine, a selective serotonin reuptake inhibitor, can restore plasticity in adult

visual cortex by increasing the expression of brain-derived neurotrophic factor, which had previously been implicated in developmental plasticity (Hanover et al., 1999), and decreasing intracortical inhibition (Vetencourt et al., 2008). Finally, negative regulation of cholinergic modulation by Lynx1 facilitates E/I balance and prevents ocular dominance plasticity in adulthood (Morishita et al., 2010). While many studies over the last forty years have uncovered mechanisms underlying plasticity within a sensory domain, how sensory experience affects the processing and organization across sensory modalities is much less clear.

Plasticity at multisensory convergence zones

Interactions with the real world rarely involve a single sensory system. In the brainstem, information from multiple sensory modalities converges at the superior colliculus (also referred to as the optic tectum) to direct eye movements and orienting behavior (Sprague, 1972; Stein et al., 1980; Meredith et al., 1983). This feature is a hallmark in a wide range of species, from mammals (Stein et al., 1980) to birds (Knudsen, 1983), reptiles (Hartline et al., 1978), and fish (Roeser & Baier, 2003).

Multisensory integration in the tectum is sculpted by experience. Vision guides the adjustment of auditory localization after monaural occlusion (Knudsen & Knudsen, 1985) or prism rearing in barn owls (Knudsen & Knudsen, 1989a; Knudsen & Knudsen, 1989b), shifting the auditory spatial tuning of tectal neurons to displaced visual receptive field locations (Knudsen & Brainard, 1991). The degree of visual field displacement is also dependent on the age of the animal at prism exposure; maximal shifts occurred only if prism experience began before

21 days of age. Furthermore, recovery to accurate sound localization after the restoration of normal vision only occurred in animals that had their prisms removed before 200 days of age (Knudsen & Knudsen, 1990). Mechanistically, NMDA receptors preferentially mediate the expression of novel neuronal responses induced by experience (Feldman et al., 1996) while inhibitory circuits functionally suppress the original map (Zheng & Knudsen, 1999). This early prismatic experience leaves an enduring anatomical trace long after normal sensory experience has been restored (Likenhoker et al., 2005), which might explain the increased capacity for plasticity in adulthood seen in these animals (Knudsen, 1998).

In mammals, visual and auditory representations in the superior colliculus (SC) are also dependent on age and experience (King et al., 1988; Wallace & Stein, 1997b), and the of interactions between multisensory cortex and SC has been closely studied. In cats, integration in the SC is dependent on input from the anterior ectosylvian sulcus (AES) (Wallace et al., 1993; Wallace & Stein, 1994a). This cortical zone contains unisensory and multisensory responsive cells that respond to auditory, visual, and somatosensory stimuli (Wallace et al., 1992; Jiang et al., 1994). Reversible deactivation of AES reduces characteristic multisensory response enhancement without affecting a neuron's modality specific response (Jiang et al., 2001) Traditionally, this sort of multisensory integration was thought to occur in higher-order association cortices after extensive unisensory processing (Felleman & Van Essen, 1991). More recent work has shown that multisensory integration can occur in areas previously

deemed ‘unisensory.’ Visual and somatosensory processing has been reported in early auditory areas (Foxe et al., 2000; Schroeder & Foxe, 2002; Brosch et al., 2005), and individual neurons in cat visual cortex can be driven by auditory stimuli (Morrell, 1972). These results have led some to question traditional views of cortical parcellation (Wallace et al., 2004), instead promoting the idea that most, if not all, of the neocortex is multimodal when interacting with the real world (Ghazanfar & Schroeder, 2006). It is possible that plasticity at these cross-modal synapses across lower and higher cortical regions may lead to compensation after total loss of a sensory system, a process known as cross-modal plasticity.

Compensation after loss of a sensory system

For many years, anecdotal evidence has suggested that loss of a sensory system leads to perceptual facilitation in the remaining modalities. Indeed, recent studies have shown improvements in tactile-discrimination thresholds (Goldreich & Kanics, 2003), sound localization (Lessard et al., 1998), and speech discrimination in the blind (Amedi et al., 2003). Along these lines, deaf people have enhanced vibro-tactile sensitivity (Levänen et al., 1998), improved face processing (McCullough & Emmorey, 1997), and perform better at peripheral visual tasks than hearing subjects (Bavelier et al., 2000). Moreover, improvements are greatest for those that become deaf or blind early in life (Bavelier & Neville, 2002).

It is believed that these behavioral improvements stem from two distinct neuronal mechanisms. First, perceptual facilitation could manifest itself by improved processing within the brain regions responsible for that modality. Along

these lines, functional expansion and reorganization of somatosensory (Pascual-Leone & Torres, 1993; Sterr et al., 1998) and auditory cortices (Elbert et al., 2002) have been reported in the blind. Cats deprived of vision early in life show supernormal growth of their facial vibrissae, and whisker representation in the somatosensory cortical barrel field is enlarged in enucleated mice (Rauschecker et al., 1992). It is important to note that not every study has agreed with this hypothesis; work with deaf humans has shown little functional or structural reorganization in occipital cortex in response to visual stimuli (Fine et al., 2005). Of course, negative results are difficult to interpret and methods used to detect these differences in humans (typically functional magnetic resonance imaging) have poor spatial and temporal resolution (Menon & Kim, 1999).

The second mechanism suggests cortical reorganization across sensory systems. A multitude of evidence supports this hypothesis: occipital cortex in the blind has been reported to respond to braille reading (Sadato et al., 1996), auditory motion perception (Poirier et al., 2006), verbal language processing (Bedny et al. 2011), and even during an olfactory discrimination task (Kupers et al., 2011). Similarly, visual activity in auditory cortex has been reported in deaf subjects (Nishimura et al., 1999).

These effects are not restricted to indirect measurements of population activity, as many studies across multiple animal models have recorded cross-modal responses at the level of individual neurons (Sur et al., 1988; Rauschecker 2002; Bronchti et al., 2002; Meredith & Lomber, 2011). In cats, AES can have the visual area completely taken over by non-visual inputs after early binocular

deprivation (Rauschecker & Korte, 1993; Korte & Rauschecker, 1993; Rauschecker 1995; Rauschecker 1996). Early enucleation expands the cortical space dedicated to processing auditory and somatosensory information in opossums, particularly at the borders of visual cortex (Kahn & Krubitzer, 2002). The exact nature and spread of these reorganizations have varied due to differences in type of sensory loss, discrimination task, and neurophysiological method, and as such, cross-modal plasticity has been reported in areas ranging from primary and secondary sensory cortices to multimodal parietal and frontal regions (Merabet & Pascual-Leone, 2010).

Similar to other modes of plasticity within sensory systems, cross-modal reorganization is age-dependent. Only people who lose their vision early in life exhibit cross-modal responses in lower (Sadato et al., 2002; Burton et al., 2002a; Burton et al., 2002b) or higher occipital regions (Bedny et al., 2010). However, a recent study in ferrets suggests that adult deafness can induce somatosensory responses in auditory cortex (Allman et al., 2009). These results might be specific to the method of deafness induced (kanamycin and ethacrynic acid), as this form of cochlear damage causes auditory deafferentation of the cochlear nucleus, allowing already existent non-auditory input to dominate in auditory cortex (Zeng et al., 2009).

Ectopic activity is not merely a reflection of processing elsewhere (the mirror hypothesis), but is functionally relevant. A series of studies using transcranial magnetic stimulation (TMS) to temporarily disrupt neuronal activity in the occipital cortex of the blind have reported disruptions in Braille reading

(Cohen et al., 1997), the induction of phantom Braille percepts (Ptito et al., 2008), and reduced verb generation performance (Amedi et al., 2004). It is important to point out that TMS studies should be taken with a grain of salt. Previously, this method was thought to act as a 'virtual' lesion over an area of cortex. Recent work, however, suggests a much more complicated activity pattern involving long-range connections across multiple brain networks (Garcia et al., 2011). Perhaps more convincingly, there is a case study of a congenitally blind woman that became alexic for Braille after suffering from bilateral occipital stroke (Hamilton et al., 2000). Recently, behavioral enhancements in visual processing by congenitally deaf cats were abolished after cooling specific regions of auditory cortex (Lomber et al., 2010; Meredith et al., 2011). Thus, cross-modal plasticity is both age dependent and functionally relevant.

Circuits and signaling mechanisms underlying cross-modal plasticity

While the phenomenon of cross-modal plasticity has been known for some time, the circuit and signaling mechanisms underlying this process remain largely unknown. The early but not late blind have thicker visual cortices than sighted controls, suggesting reduced pruning during a developmental critical period (Jiang et al., 2009). Whether this is a reflection of intra- or intermodal connections is unclear, as they could not be differentiated. Dynamical causal modeling of fMRI, an indirect method of linking activity across brain regions, has supported direct auditory-visual intracortical connections (Klinge et al., 2010). However, another study suggested indirect intracortical connections as the main pathway for somatosensory-visual interactions (Fujii et al., 2009).

Animal studies provide support for aberrant structural connectivity after sensory deprivation. Early bilateral retinal ablation in monkeys (Rakic et al., 1991) and opossums (Kahn & Krubitzer, 2002) leads to a novel cytoarchitectonic area between primary and secondary visual cortices with a unique laminar structure and neurons that respond to auditory and somatosensory stimuli. Animals that are anophthalmic (Doron & Wollberg, 1994; Laemle et al. 2006) have aberrant projections from auditory subcortical structures to visual cortex, although this claim is sometimes disputed (Chabot et al., 2008). Retinal projections rerouted to thalamic somatosensory (Frost & Metin, 1985) or auditory nuclei (Roe et al., 1990; Sharma et al., 2000; Ptito et al., 2001) early in life form functional visual maps in primary somatosensory or auditory cortex. Similarly, congenitally deaf mice have retinal projections to auditory thalamus and brainstem (Hunt et al., 2005).

In these studies, it is unclear if cross-modal projections are initially present and later pruned with normal visual experience or whether ectopic outgrowth occurs due to a lack of coherent visual activity. A handful of anatomical studies support the former idea. Cross-modal connections have been found between auditory and visual cortices in kittens reared in a normal light environment (Dehay et al., 1988; Innocenti et al. 1988). This input is pruned to low but still existent levels in adulthood (Hall & Lomber, 2008). In rats, a transient connection between auditory thalamus and primary somatosensory cortex has been reported, and which be stabilized by whisker deprivation (Nicolelis et al., 1991).

Unfortunately, these studies lacked physiology, so it is unclear whether these early connections are functional.

At a finer scale, the molecular mechanisms underlying cross-modal plasticity are almost totally unknown. **The goal of my thesis is to understand the molecular mechanisms underlying cross-modal plasticity. More specifically, I aim to uncover how cross-modal activity arises and the mechanisms that are responsible for its experience-dependent regulation.**

To answer these questions, I employed the following strategy:

1. I established the mouse as a model system for studying cross-modal plasticity. Based on previous work and the expertise in my lab, I chose to use dark-rearing as a form of visual deprivation and probe multimodal responses with light and auditory stimuli.
2. I first used riboflavin imaging, a measure of neuronal population activity (Reinert et al., 2004), to monitor cross-modal responses over the entire visual cortex.
3. Once regions of cross-modal plasticity were identified, I used extracellular single-unit recordings to understand the behavior of individual neurons.
4. In collaboration with Lia Min in Michela Fagiolini's lab, we performed anatomical experiments to determine the origin of cross-modal inputs.
5. I examined genetically engineered mice to uncover the role of specific signaling pathways controlling cross-modal plasticity.

6. Finally, I explored some of the functional consequences of cross-modal reorganization by comparing multisensory interactions in sighted, visually deprived, and genetically engineered mice.

Overall, I seek to provide a framework in understanding the anatomical, circuit, and signaling pathways that underlie cross-modal plasticity. By doing so, I hope to further our knowledge of how to restore or retune neuronal circuits after loss of a sensory system.

Chapter 2

Materials and Methods

Animals and Rearing Conditions

Experiments were performed on the C57BL/6 inbred strain of the house mouse (*Mus musculus*) born and raised in standard mouse cages with food and water *ad libitum*. Males and females were inspected for any physical malformations and had to be within an appropriate weight range for their age (juvenile >9 g, adults 18-35 g). Light-reared mice (LR) were housed in the normal mouse facility on a 12-hour light/dark cycle. Eye opening occurred around postnatal day 12 (P12). Our first set of imaging and recordings of LR took place around the age of P25, when visual receptive field properties are becoming functionally mature (Hensch, 2004). We also imaged animals during early adulthood around P45. Finally, we imaged after P60, when mice are fully sexually mature (Fig. 2.1a).

Visual deprivation was achieved by placing mice in a specially designed room under 24-hours of complete darkness. We used three dark rearing protocols. In the first protocol, animals were placed in darkness at birth (DR or DR P0), P25 (DR P25), or P45 (DR P45), and imaged or recorded shortly after reaching adulthood (Fig. 2.1b, top panel). In the second protocol, adults were placed in the dark room for at least two months (Late DR) (Fig. 2.1b, middle panel). Finally, animals were raised in darkness from birth and then exposed

Figure 2.1 | Developmental timeline of the mouse visual system and dark rearing protocols

(a) Schematic of the developmental timeline of the mouse visual system. Eye opening occurs at P12. Visual receptive field properties become functionally mature between P20-P30. Mice are sexually mature adults after P60. Arrows at P25, P45, and >P60 indicate times of imaging and/or recording in LR animals.

(b) Mice were placed in 24hr of darkness at P0, P25, or P45 (arrows) until imaged in adulthood (top panel). Adults placed in the darkness were raised in a normal LR environment until adulthood and then placed in darkness for at least two months before imaging (middle panel). DR mice exposed to light were dark-reared from birth until adulthood. They were imaged after being placed in a normal LR environment for 2-3 weeks (bottom panel).

a.

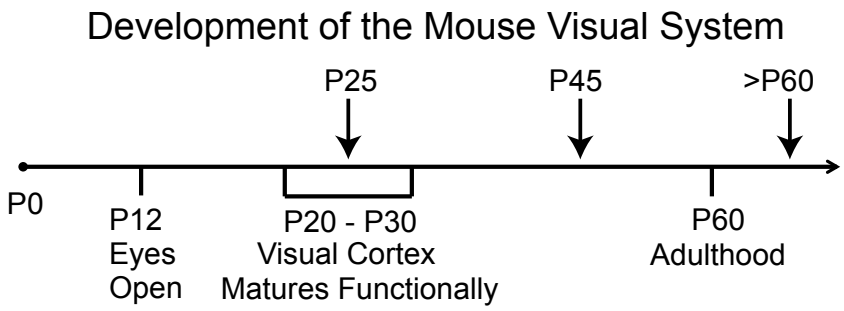

b.

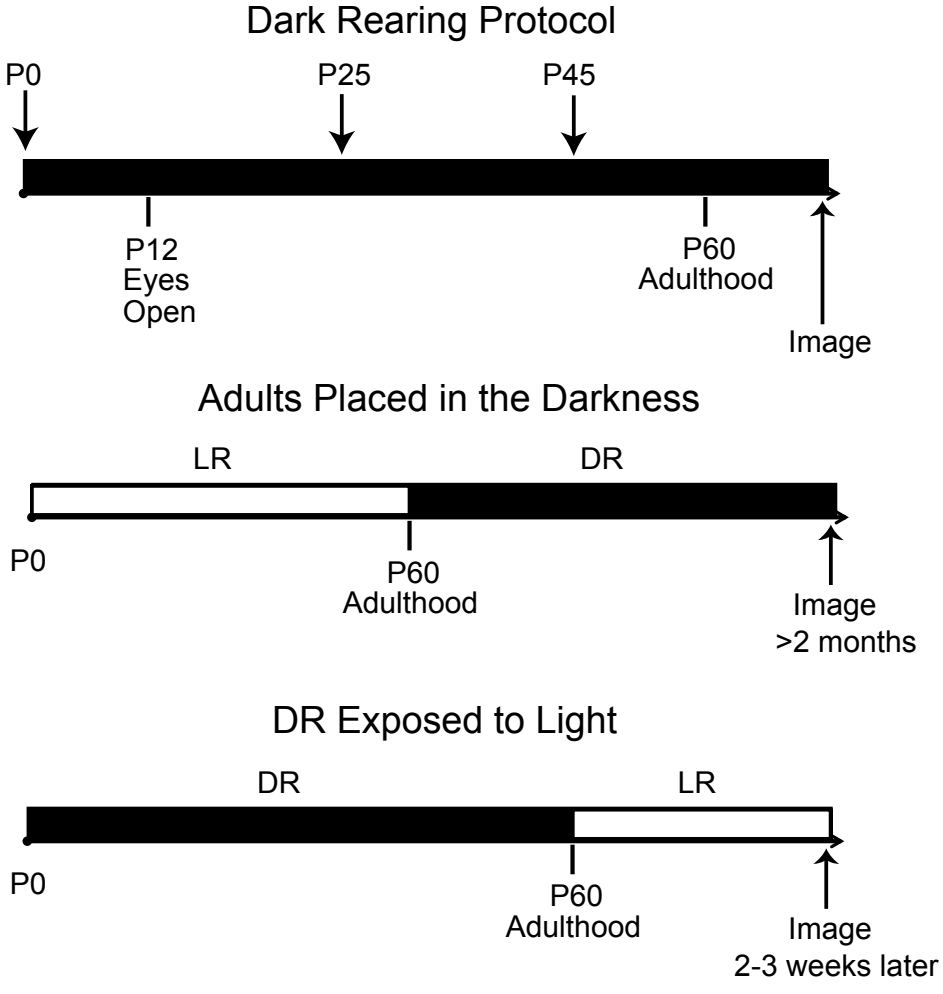

DR = Dark Reared (24 hours darkness)
LR = Light Reared (12 hrs light/ 12 hrs dark)

Figure 2.1 (Continued)

to a normal light/dark cycle for 2-3 weeks (DR + Light) (Fig. 2.1b, bottom panel). All procedures and protocols were approved by the Children's Hospital Boston animal care committee and were in accordance with the guidelines of the National Institute of Health and the Society of Neuroscience.

Surgical Preparations and Stimuli for Anesthetized Recordings

Surgical Preparations

For riboflavin imaging and single-unit recordings, mice were transiently anesthetized with isoflurane gas (3.5% with O_2), their weight was measured, and appropriate amounts of Nembutal (50 mg/kg, intraperitoneal injection - for a longer lasting and more stable anesthetic state), Chlorprothixene (0.2 mg, intramuscular injection of the left thigh - to relax the muscles), and Atropine (0.3 mg, subcutaneous injection – to dilate the pupils, open airways, and reduce mucus production) were administered. A tube providing supplemental Nembutal (1 mg/ml for juveniles, 5 mg/ml for adults, as indicated) was inserted into the peritoneal cavity to maintain anesthesia throughout the recording session. To maintain proper respiration with our stereotaxic equipment, we inserted a custom L-shaped borosilicate glass tube (1.0 mm outer diameter, 0.75 mm inner diameter) into the trachea. The head was fixed using a standard mouse stereotaxic frame albeit in a slightly modified manner so as not to occlude the ears. Use of the palate bar and nose clamp were normal, but the ear bars were applied firmly against the orbital bones underneath the eyes. Under sterile conditions, the skin on top of the skull was removed. Drilling along the lamboid,

bregmatic, and sagittal sutures until they met at the squamosal plate exposed all of right and/or left visual cortex. The dura was left intact and the surface of the brain kept moist by a combination of saline and 3% agarose gel. For imaging, a coverslip was fixed to provide a clear window over visual cortex. Throughout the imaging and recording sessions, the animal breathed O_2 and its temperature was kept at 37.5°C using a heating pad and rectal thermometer. The eyelids were trimmed and the corneas covered with silicone oil to prevent drying. In a few cases, the eyes became dry enough to form a thin opaque film over the cornea. These experiments were immediately interrupted and eyes were flushed with saline until the film dissolved. At the end of the experiment, mice were euthanized with an overdose of Nembutal.

Stimuli

The visual stimulus was a 5 mm red light-emitting diode (λ = 630 nm, luminance = 12 cd/m^2). The auditory stimulus was a free field 4.4 kHz piezo buzzer at 70 dB. For imaging experiments, both stimuli were placed 10 cm away at 30° azimuth towards the contralateral eye and turned on for one second during each trial. For single-unit experiments, moving bars of light were used to determine the receptive field location of a given penetration. The LED and buzzer were then placed 10 cm away at the appropriate angle.

Riboflavin Imaging and Analysis

Cortical images (128 x 168 pixels after binning) of endogenous green fluorescence (λ = 500-550 nm) in blue light (λ = 470-490 nm) were recorded at

nine frames/second using a cooled CCD camera system attached to a dissecting microscope. Each trial lasted for 10s and was composed of three epochs: pre-stimulation for 3s, light and/or tone stimulation for 1s, and post-stimulation for 5s. After each trial, there was an 11s resting period to allow for the processing of images (Metamorph® from Molecular Devices®). Thirty trials (one run) were added together and pixel values were divided by the number of trials (Fig. 2.2a). Images were normalized with respect to a reference (average of the first twenty frames, Fig. 2.2b) and passed through a low-pass square filter (10 x 10 pixels) to improve image quality (Fig. 2.2c). Finally, the normalized images were transformed to a pseudocolor scale (Fig. 2.2d).

Imaging Analysis

Several 30-trial runs of each stimulus (visual, auditory, and blank) were averaged together to reduce noise. To correct photobleaching over the length of a trial, average visual and auditory movies were divided by the average blank. Regions of interest (primary and secondary visual cortices as determined by stereotaxic coordinates) were demarcated by circular windows (1 mm in diameter) and compared to a reference region outside of the brain (Fig. 2.3a). Timelines of relative fluorescence changes in ROIs were calculated by subtracting ROI values with the reference. The peak amplitude was calculated by taking the ROI timeline and averaging the frames one second around the peak after stimulation (Fig. 2.3b). Animals with V1 visual peak amplitudes less than 0.5% $\Delta F/F_0$ were excluded from analysis because it was likely that their visual system was compromised or there were problems with the anesthesia.

Figure 2.2 | Riboflavin imaging process

(a) Still image from an original riboflavin fluorescence movie after 30 trials (1 run) of visual + auditory stimulation in an adult anesthetized C57BL/6 DR mouse (A – anterior, P – posterior, L – lateral, M – medial).

(b) Resultant image after dividing part (a) with the average of the first 20 frames before stimulation. Bright white spots indicate responsive primary and secondary visual cortices.

(c) Smoothed image of part (b) after low-pass square filtering (10 x 10 pixels).

(d) Pseudocoloring of part (c) gives the final image ready for analysis.

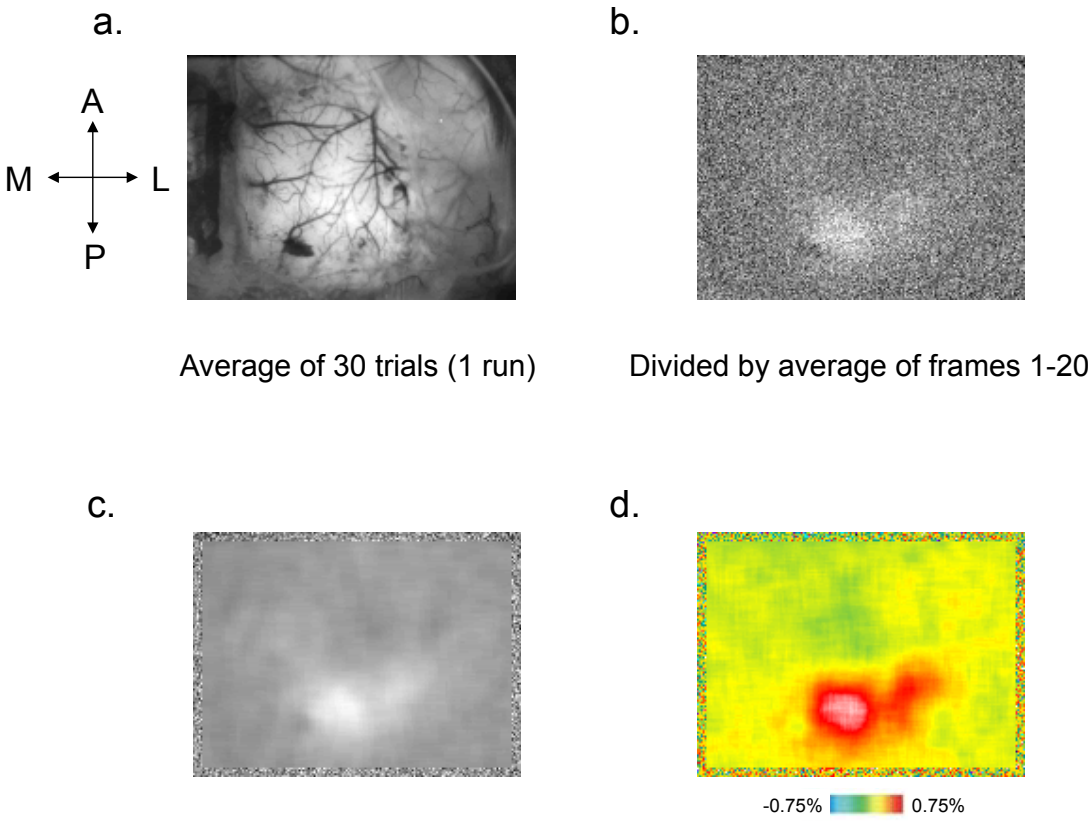

Figure 2.2 (Continued)

Figure 2.3 | Riboflavin imaging analysis

(a) Primary visual cortex (V1), secondary visual cortex (V2L), and a reference area outside of the brain were demarcated by small circles (1mm in diameter) in the original fluorescence movie (left bottom panel) and transferred to the processed pseudocolor images (left top panel). Average pixel intensity (arbitrary units) over a given region was recorded in each frame of the movie (right panel). Arrow denotes onset of stimuli.

(b) Intensity values from part (a) were converted to $\Delta F/F_0$ (F_0 = average intensity before stimulation, ΔF = current pixel intensity - F_0). The peak after stimulation was found (black circle) and peak amplitude response calculated by averaging intensity values 0.5s around the peak.

a.

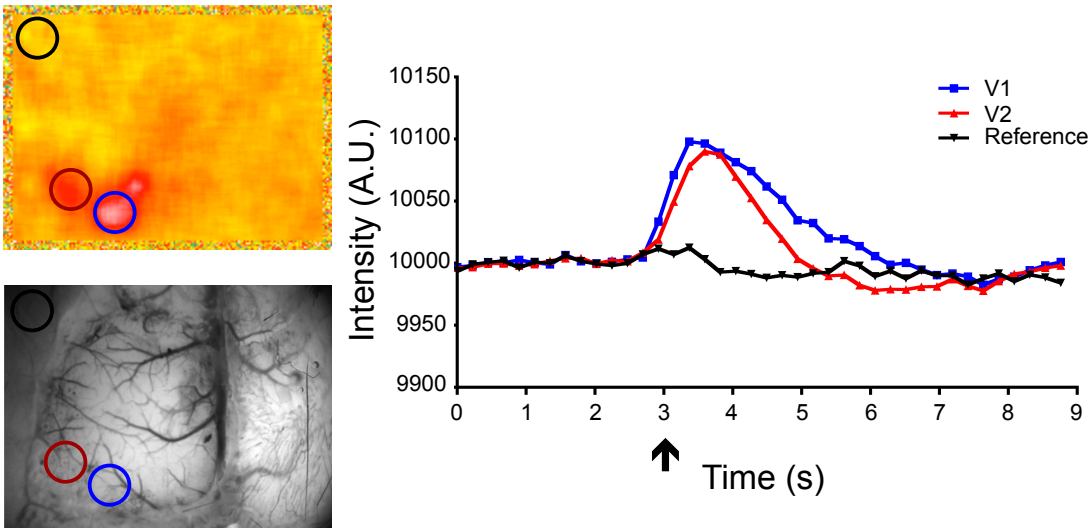

b.

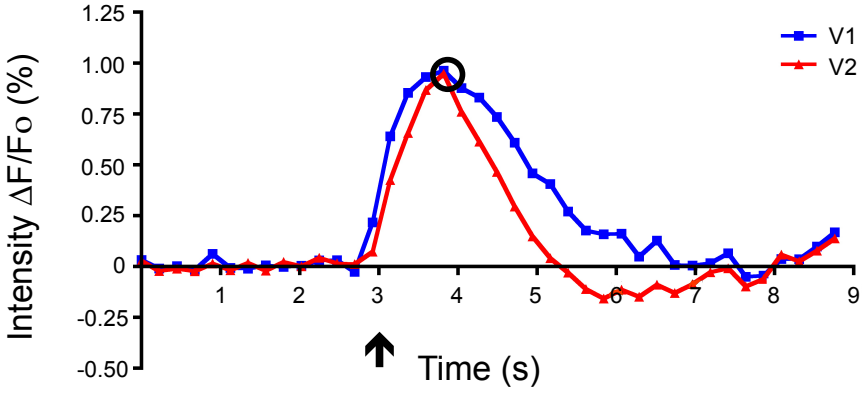

Peak Response = Max (± .5 s) - Avg(0 to 3 s)

V1 = .869 V2 = .760

Figure 2.3 (Continued)

Single-Unit Recording and Analysis

A silicon Neuronexus Technologies® probe (linear probe with 16 sites spaced at 50 μm intervals, model a1x16-3mm50-177) was inserted at multiple sites along visual cortex to a depth of >800 μm below the pial surface to record cells from all layers. Recordings began in the binocular zone of V1 (to ensure a functioning visual system) and progressed laterally and anteriorly through V2L to the borders of auditory cortex. At all recording sites, each stimulus condition (visual, auditory, visual + auditory, blank) was presented 20 times. Mice had between two to eight penetrations during a session, with each penetration lasting about 30 minutes. The signal was amplified, thresholded, band-pass filtered, and discriminated (SciWorks, DataWave or SortClient from Plexon Technologies®). To ensure single unit isolation, the waveforms of recorded units were further examined offline (Offline Sorter from Plexon Technologies®) and discriminated on the basis of their waveforms.

Single-Unit Analysis

Data from individual cells were processed with customized software designed in Matlab® (from MathWorks®). First, a raster plot was constructed (Fig. 2.4a). A peristimulus time histogram (PSTH) was generated by plotting the number of spikes in a sliding 25 ms bin with a 2 ms step (Fig. 2.4b). The peak latency was the time to the peak amplitude in the PSTH. Firing rates were calculated as the average number of spikes during the presentation of the stimulus (Fig. 2.4c). Multisensory interaction (M.I.) and multisensory facilitation

Figure 2.4 | Example neuron from extracellular single-unit recording

(a) Raster plot for an example cell recorded in V1 of an adult LR mouse. Trials are divided into the different stimulus conditions: visual (yellow), auditory (blue), visual + auditory (red), and blank (white). Bold and dotted black lines indicate when the stimulus turned on and off respectively.

(b) PSTH of the neuron in part (a).

(c) A plot of the visual (grey), auditory (blue), visual + auditory (red), and blank (black) firing rates of the neuron in part (a) to different stimuli with increasing window bins (0-100ms, 0-200ms, etc.). Ultimately, we used the firing rates for the largest bin (0-1000ms, the entire duration of the stimulus) for further analysis.

(d) A plot of multisensory interaction (blue, MI = (CM-SM)/SM*100) and multisensory facilitation (red, MI = CM/(A + V)*100) with increasing window bins for the neuron in part (a). We used the largest window bin for further analysis (CM – combined stimuli FR, SM – stronger single stimulus FR, A – auditory FR, V – visual FR).

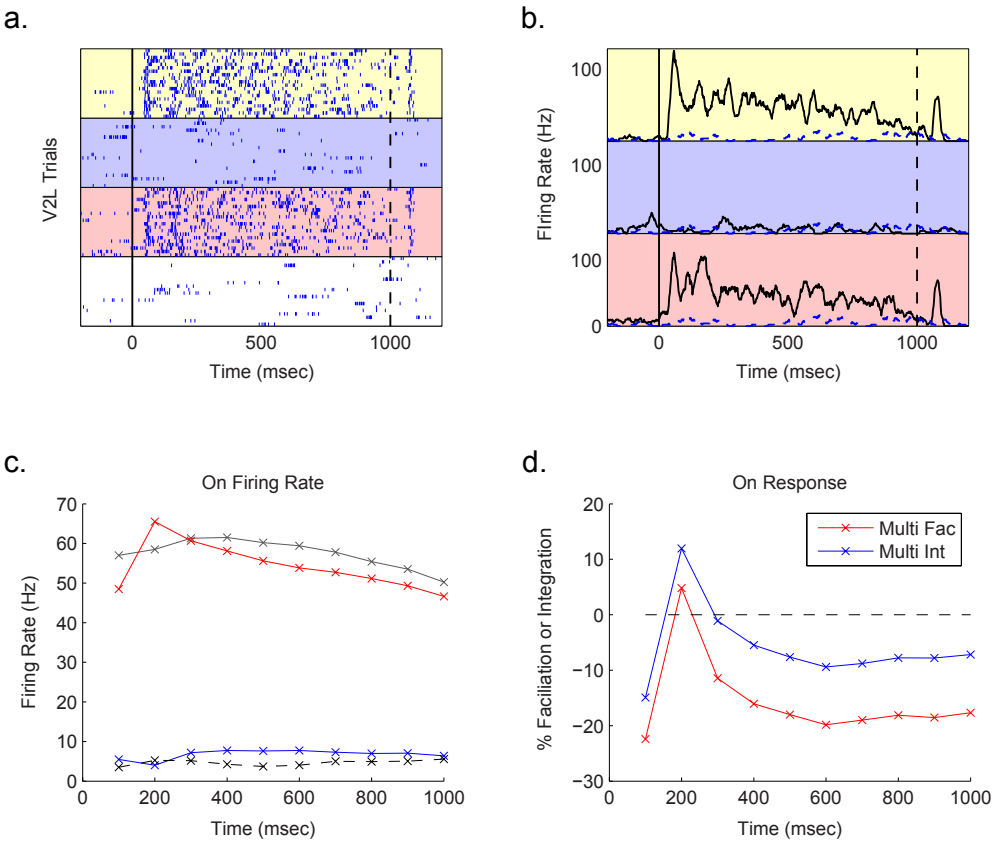

Figure 2.4 (Continued)

(M.F.) were calculated by the following formulas (Fig 2.4d):

$$M.I. = (CM – SM)/SM*100$$

CM = combined stimuli firing rate

SM = stronger single stimulus firing rate

$$M.F. = CM/(A+V)*100$$

A = auditory only firing rate

V = visual only firing rate

Cells were classified by comparing their stimulus evoked firing rate to the blank firing rate using one-way analysis of variance (ANOVA) and Tukey's HSD post-hoc comparisons (Fig. 2.5). If only visual or auditory stimulation was significant, the cell would be classified as visual or auditory accordingly. 'Both' cells responded significantly above spontaneous activity to visual and auditory stimuli individually or only when presented together.

c-Fos **Immunohistochemistry (by Lia Min)**

Exposure Protocol

Mice were adapted to a sound- and light-proof box for >6 hours before exposure to ambient fluorescent light or a series of 5 kHz tones (1 second duration, 0.2 Hz frequency) for 1 hour.

Figure 2.5 | Categorization of cell type by ANOVA

(a) ANOVA was performed on the example cell in figure 2.4 and box plots comparing firing rates between the different stimuli conditions were constructed (red line - median, blue box – interquartile range, dotted black line – range, red pluses – outliers).

(b) A post-hoc multiple comparison's test (Tukey's HSD) was performed on part (a) and an interactive plot of mean firing rates with 95% confidence intervals was constructed. Clicking on column 4 showed what groups were significantly different from the blank response (only visual alone and visual + auditory). This cell was classified as visual.

a.

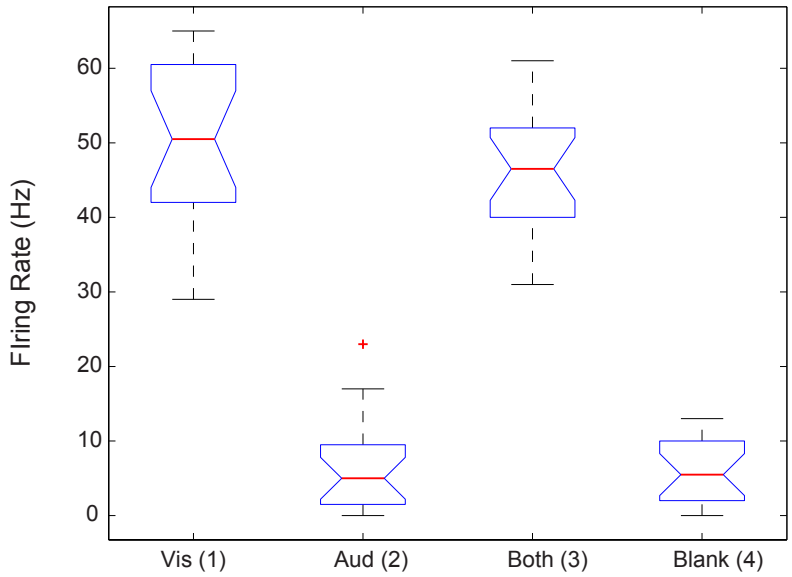

b.

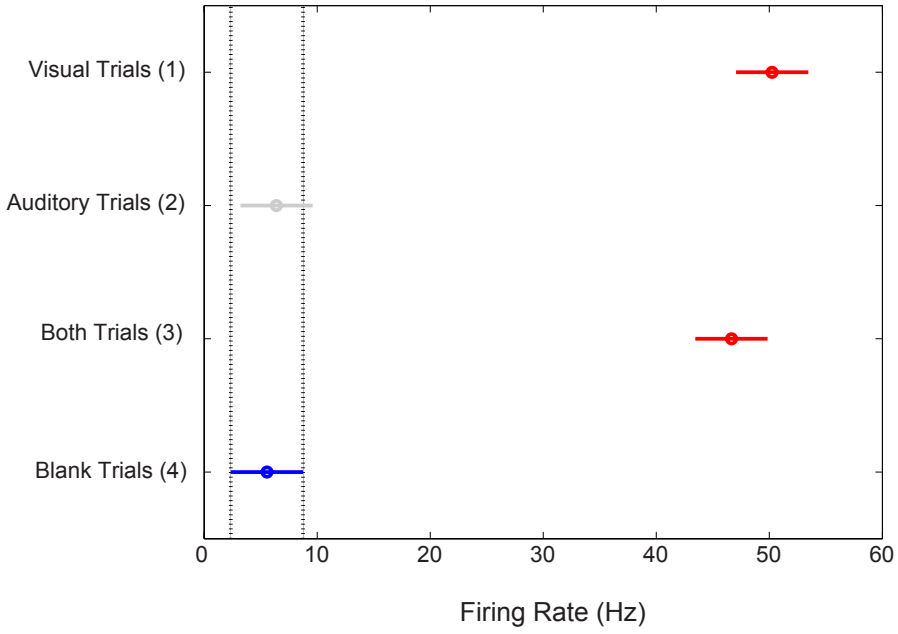

2 groups have means significantly different from Group 4

Figure 2.5 (Continued)

Perfusion

To avoid c-fos induction due to stress, mice were anesthetized with 2.5% isoflurane with O_2. They received an overdose of Nembutal (5mg/ml, i.p.) and were perfused transcardially with 0.9% saline followed by 4% paraformaldehyde (PFA). Brains were post-fixed in PFA for 2 hours and then cryoprotected in a 30% sucrose solution overnight.

Immunohistochemistry

40 µm thick sections were cut from perfused brains on the cryostat. Every 4th section was collected and washed in phosphate buffered saline (PBS) for 30 minutes followed by 4°C overnight incubation in blocking solution (0.3% Triton X-100 and 10% normal goat serum in 0.1M PBS-Triton) and primary antibody rabbit anti-*c-Fos* (Sigma-Aldrich®, diluted at 1:1000 in 0.3% Triton X-100 and 3% NGS in 0.1M PBS-Triton). After three 10 minute washings in PBS-Triton, sections were incubated overnight in the secondary antibody, goat anti-rabbit IgG Alexa 488 (Invitrogen®), diluted at 1:500 in PBS-Triton. Sections were washed three times in PBS-Triton for 10 min prior to being mounting on glass slides.

Counting Procedure for c-Fos (Object Count)

In order to compare the activity within ROIs, the number of *c-Fos* immunoreactive nuclei was estimated using Object Count (NIS-Elements®, Nikon®). Every fourth coronal section (40 µm thick) was analyzed for *c-Fos* expression on a Nikon® Eclipse 80i microscope. Each ROI was identified based on structural morphology. The user defined thresholds for luminance, roundness, and size.

Alternative Counting Procedure for c-Fos (Stereo Investigator®)

We used an additional counting method in a subset of sections to confirm the results from Object Count. Twelve to fifteen sections from each brain were analyzed using the image analysis program Stereo Investigator® (Version 8.10, Microbrightfield®, Colchester, VT, USA). ROIs were identified in each section based on the Mouse Brain Atlas (Paxinos and Watson, 2001). Cortical layers were identified by DAPI and VGlut2 staining. *c-Fos*-positive nuclei within each ROI were counted using the optical fractionator method. Counting frames (30 x 30 µm or 50 x 50 µm) were placed in a virtual grid (150 x 150 µm) randomly generated by the software. Counting was performed with a 40x objective (n.a. 0.75). Cell density was calculated by dividing the estimated number of cells by the total area.

Retrograde Tracing (by Lia Min)

Surgical Preparation

Mice were anesthetized with 2.0% isoflurane with O_2 and body temperature maintained through a heating pad. A small hole was made through the skull 3.8 mm lateral to the midline and 1.5 mm anterior to the lambda point. A 28-gauge Hamilton® syringe connected to a motorized microinjector was inserted into the hole to reach secondary visual cortex and 300 nl of tracer solution (1.0mg/ml Cholera toxin subunit B conjugated to Alexa 488 in PBS, Invitrogen®) was slowly injected. After injection, the area was cleaned and skin sutured. Mice

were given Meloxicam (to reduce pain) every 24 hours for two days after the surgery and then perfused.

Counting Procedure for Tracer Injections (Confocal virtual stacks)

In order to compare the degree of connectivity between auditory regions and secondary visual cortex in LR and DR mice, the number of cell bodies labeled with tracer in each ROI was estimated. Only coronal sections (40 μm thick) from brains with successful injections were used. Criteria for successful injection included no tracer in the white matter tract, a halo diameter of injection site between 200 and 400μm, no tracer overspill on the surface of cortex, and minimum tissue damage during injection. Digital stacks from each ROI identified through structural morphology were collected using a Fluoview FV1000™ scanning microscope (Olympus®) at 20x from three to five sections for each brain. Fluorescent cell bodies were manually counted using the Cell Counter Plugin program in ImageJ.

Computational Modeling

To examine the influence of firing rate, trial number, number of neurons, and degree of possible modulation on our metric of multisensory interaction, I designed a four-parameter spike count model based on the *poissrnd* command in MATLAB®. First, numbers to serve as modulation values were pulled randomly from a uniform distribution bounded by the 'degree of possible modulation' parameter specified by the user. For calculating 'actual' M.I., the firing rate, trial number, and number of neurons were entered into *poissrnd* to generate a two

dimensional matrix simulating a set of neurons responding to a single stimulus. This matrix was averaged along the dimension of trial to create average firing rates (SM) and multiplied by the modulation values to calculate combined modal responses (CM). M.I. was calculated with the formula described earlier. To calculate the 'measured' M.I., the firing rate was multiplied by the modulation values *before* being entered into *poissrnd*. This matrix was processed in a similar way to the 'actual' M.I. 'Neurons' given the same modulation values in each condition were matched and their firing rates compared and stored in a 'differences' matrix (Fig. 2.6).

The entire process from entering values in *poissrnd* to creating a 'differences' matrix was repeated a thousand times for statistical comparisons. In V2L (Chapter 3), differences in M.I. were found between groups using a two-sample Kolmogorov-Smirnoff test (KS test) and by comparing the median values for the positively modulated cells, a measure of multisensory enhancement. In V1 (Chapter 4), differences were found by bootstrapping both interquartile ranges of cumulative distribution functions, a measure of the range of multisensory interaction, and the ratios of positively to negatively modulated cells (+/- ratio). These statistics were examined in the model by using a bootstrap procedure to create and compare 95% confidence intervals (95% CI).

To ensure that our model worked properly, we searched for conditions where identical modulation (or identically shaped distributions of modulation) could lead to biased multisensory interactions. Three values over a wide range were chosen for each condition (firing rate: 1, 10, and 100 Hz; range of

Figure 2.6 | Example simulation illustrating how low firing rates can lead to biased multisensory interactions

(a) With low firing rates (1 Hz), many neurons (500), a large dynamic range of modulation (0-10x), and a low number of trials (10), many cells' measured M.I. deviate greatly from their expected values (should lie along solid black line) (top left panel). A plot of differences versus modulation values suggests that greater modulation leads to larger deviations (top middle panel). The cumulative distribution function of differences illustrates a right-tailed distribution with greater M.I. than expected (top right panel).

(b) Under similar conditions to part (a) but with a higher firing rate (10 Hz), deviations from expected M.I. are much smaller.

(c) The same simulation in part (a) and (b) but with a firing rate of 100 Hz leads to almost no deviations from actual M.I. The differences in deviations between the three conditions could lead to the erroneous conclusion that there is a greater bias in multisensory interactions due to some condition of interest (such as rearing, genotype, etc.) when it really is a reflection of different firing rates.

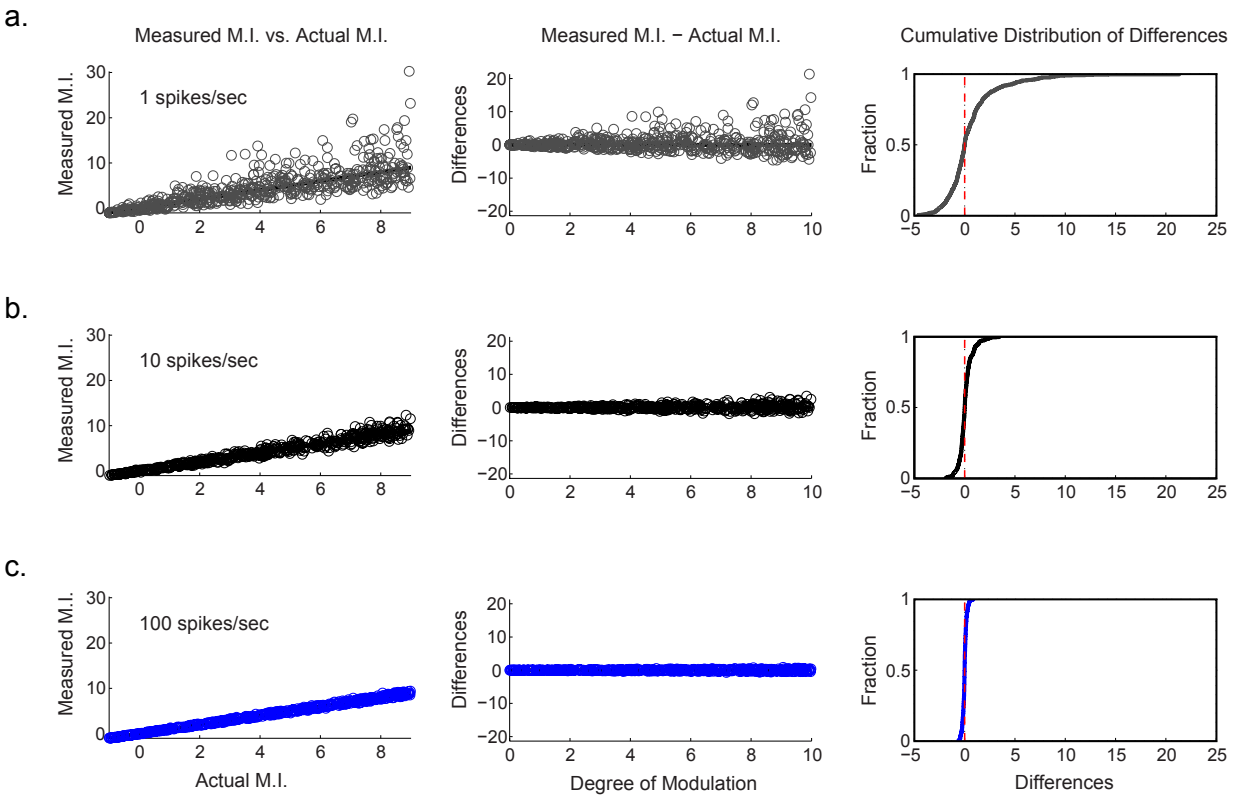

Figure 2.6 (Continued)

modulation: 2x, 6x, and 10x; number of trials: 10, 20, and 50; number of neurons: 50, 100, and 500). While examining a specific parameter, all others were held at the value that would produce the largest amount of bias (firing rate: 1 Hz, modulation: 10x, number of trials: 10, number of neurons: 500).

Increasing the firing rate decreased the difference between measured and actual multisensory interaction. Cumulative distribution functions of differences (CDFs, Fig. 2.7a), the medians of positively modulated cells (Fig. 2.7a inset), and interquartile ranges (Fig. 2.9a) were smaller at lower firing rates.

A large range of modulation can also increase the noise in most M.I. measurements. Distributions of differences (Fig. 2.7b), medians of positively modulated cells (Fig. 2.7b inset), and interquartile ranges (Fig. 2.9b) became progressively larger as modulation increased.

Since the sum of two independent Poisson random variables is itself a Poisson process, doubling the number of trials should be exactly the same as doubling the firing rate. We show this to be true (Fig. 2.8a; Fig. 2.9c).

Increasing the number of neurons could not bias M.I measurements, but did reduce 95% CI. Distributions of differences, medians of positively modulated cells, and interquartile ranges were similar across conditions (Fig 2.8; Fig 2.9d).

Unsurprisingly, the +/- ratio was unaffected by most parameters examined: firing rate, range of modulation, and number of trials were similar between conditions. Changing the number of neurons altered the size of 95% CI (Fig. 2.10a-d respectively).

Figure 2.7 | Low firing rates and a large range of modulation increase noise in multisensory interaction measurements

(a) By running the simulation in figure 2.6 one thousand times we used a bootstrap procedure to test the influence of firing rate on certain statistics of interest. The CDFs of the differences between measured and actual M.I. are significantly different from each other by KS tests (95% CI, 1 vs. 100 Hz: $1x10^{-24}$ to $7x10^{-24}$, 10 vs. 100 Hz: $1x10^{-7}$ to $3x10^{-7}$, $P<0.05$ is significant). The medians of positively modulated cells, a measure of multisensory enhancement, are also significantly different from each other (inset, 95% CI, 1 Hz: 0.96 to 1.4, 10 Hz: 0.26 to 0.38, 100 Hz: 0.077 to 0.11). Large changes in firing rates could lead to differences in the distribution of multisensory interactions and degree of multisensory enhancement despite identical underlying modulation.

(b) Increasing the dynamic range of modulation (while keeping firing rates, number of neurons, and number of trials constant) also increases the noise when measuring multisensory interactions. KS tests are significantly different from each other across all conditions (95% CI, 2 vs. 10x: $1x10^{-11}$ to $9x10^{-11}$, 6 vs. 10x: $1x10^{-5}$ to $7x10^{-5}$). Multisensory enhancement is also significantly different (inset, 95% CI, 2x: 0.25 to 0.37, 6x: 0.63 to 0.93, 10x: 1.0 to 1.5).

a.

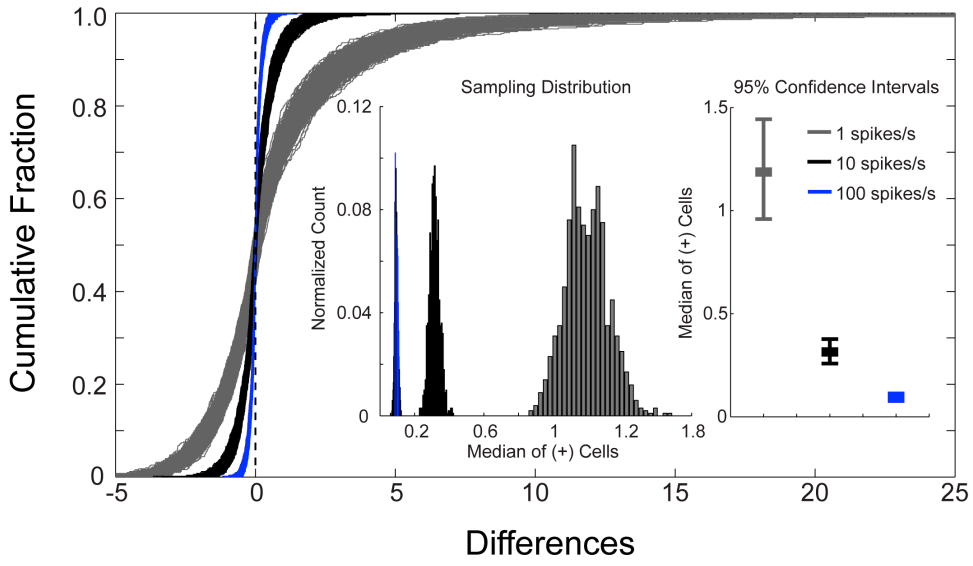

b.

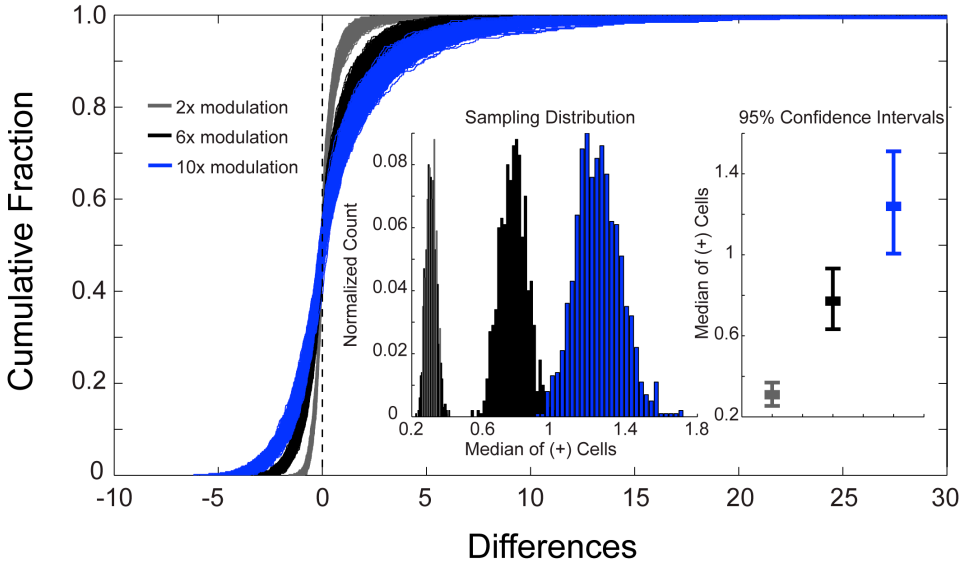

Figure 2.7 (Continued)

Figure 2.8 | Increasing the number of trials reduces noise while increasing the number of neurons reduces the size of 95% confidence intervals when measuring multisensory interactions

(a) An increase of 20 trials reduces noise in multisensory interactions as measured by KS-tests and multisensory enhancement (95% CI of KS test p value, 10 vs. 50 trials: $1x10^{-4}$ to $8x10^{-4}$, 30 vs. 50 trials: $1x10^{-3}$ to $1x10^{-2}$; 95% CI of multisensory enhancement, 10 trials: 0.97 to 1.5, 30 trials: 0.49 to 0.73, 50 trials: 0.37 to 0.54).

(b) The number of neurons does not change any bias in multisensory interactions (95% CI of KS test p value, 50 vs. 100 neurons: 0.025 to 0.98, 50 vs. 500 neurons: 0.018 to 0.99). However, it does influence the size of 95% CI. Any bias acquired by other means (e.g. different firing rates) can become significantly different by increasing the number of neurons (inset, 95% CI of multisensory enhancement, 50 neurons: 0.55 to 2.0, 100 neurons: 0.77 to 1.9, 500 neurons: 1.0 to 1.5).

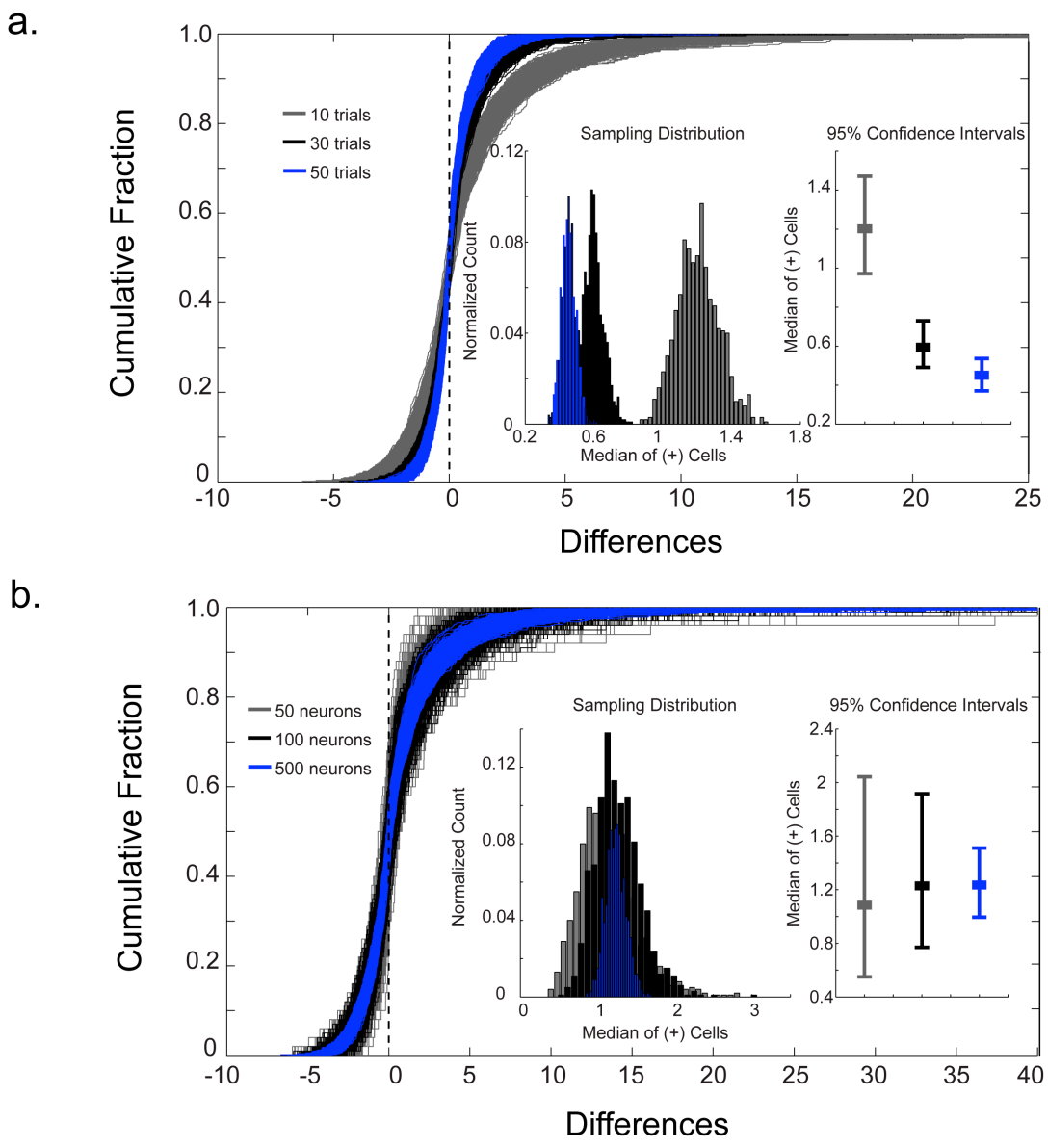

Figure 2.8 (Continued)

In summary, differences in firing rates can affect many measurements of multisensory interaction. At low firing rates, an aberrant spike during a trial can greatly influence M.I. One could erroneously conclude that animals had biased multisensory interaction due to some other condition of interest (rearing, genotype, etc.) when the difference is really a reflection of firing rates. The degree of modulation can also affect measurements. Brain areas under the influence of weak cross-modal input are less likely to have biased measurements. One way to reduce noise in M.I. measurements is to increase the number of trials. This averages out aberrant spikes that occur on a small number of trials.

Finally it is important to note that not all metrics involving M.I. are biased. Classifying a cell as either being suppressed or enhanced by adding another stimulus is impervious to differences in firing rates, range of modulation, or number of trials.

This exercise proved that our model is capable of detecting differences in M.I. despite identical distributions of modulation. By plugging in relevant values from recorded brain regions, our model can serve as a control for claims we make about differences in multisensory interaction between groups of animals. Although I have designed this model for examining M.I., modified versions can be used to control for differences found measuring ocular dominance (Smith & Bear, 2010), orientation selectivity (Kuhlman et al. 2011), or any other measure based on comparing firing rates.

Figure 2.9 | The dynamic range of multisensory interaction is affected by the same factors as multisensory enhancement

(a) The interquartile range of the cumulative distribution function of the differences, a measure of the range of multisensory interactions, is significantly reduced as firing rates increase (95% CI, 1 Hz: 1.9 to 2.9, 10 Hz: 0.48 to 0.68, 100 Hz: 0.14 to 0.20).

(b) The range of multisensory interactions significantly increases as the range of modulation increases (95% CI, 2x: 0.45 to 0.69, 6x: 1.2 to 1.9, 10x: 2.0 to 3.0).

(c) Increasing the number of trials significantly reduces noise in measuring the range of multisensory interactions (95% CI, 10 trials: 2.0 to 2.9, 30 trials: 0.93 to 1.4, 50 trials: 0.68 to 1.0).

(d) The number of neurons does not change any bias in the dynamic range of multisensory interactions but does influence the size of 95% CI. Any bias acquired by other means (e.g. different firing rates) can become significantly different by increasing the number of neurons (95% CI, 50 neurons: 1.1 to 4.3, 100 neurons: 1.5 to 3.9, 500 neurons: 2.0 to 3.0).

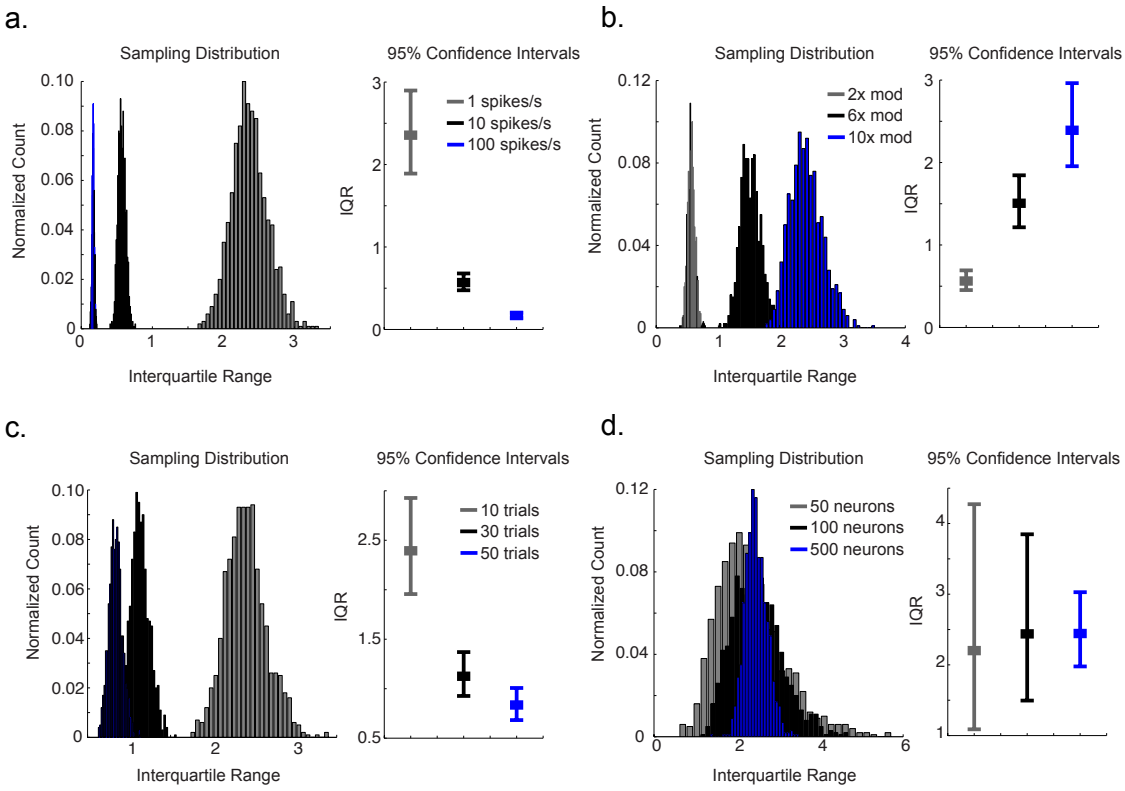

Figure 2.9 (Continued)

Figure 2.10 | The +/- ratio is unaffected by firing rate, range of modulation, or number of trials

(a) The ratio of positively to negatively modulated cells is not affected by differences in firing rate (95% CI, 1 Hz: 0.87 to 1.3, 10 Hz: 0.87 to 1.2, 100 Hz: 0.85 to 1.2).

(b) Degree of modulation does not affect +/- ratio (95% CI, 2x: 0.79 to 1.1, 6x: 0.87 to 1.3, 10x: 0.87 to 1.2).

(c) Number of trials does not affect +/- ratio (95% CI, 10 trials: 0.87 to 1.2, 30 trials: 0.85 to 1.2, 50 trials: 0.85 to 1.2).

(d) Increasing the number of neurons reduces the size of 95% CI when measuring the +/- ratio (95% CI, 50 neurons: 0.61 to 1.9, 100 neurons: 0.70 to 1.7, 500 neurons: 0.87 to 1.2).

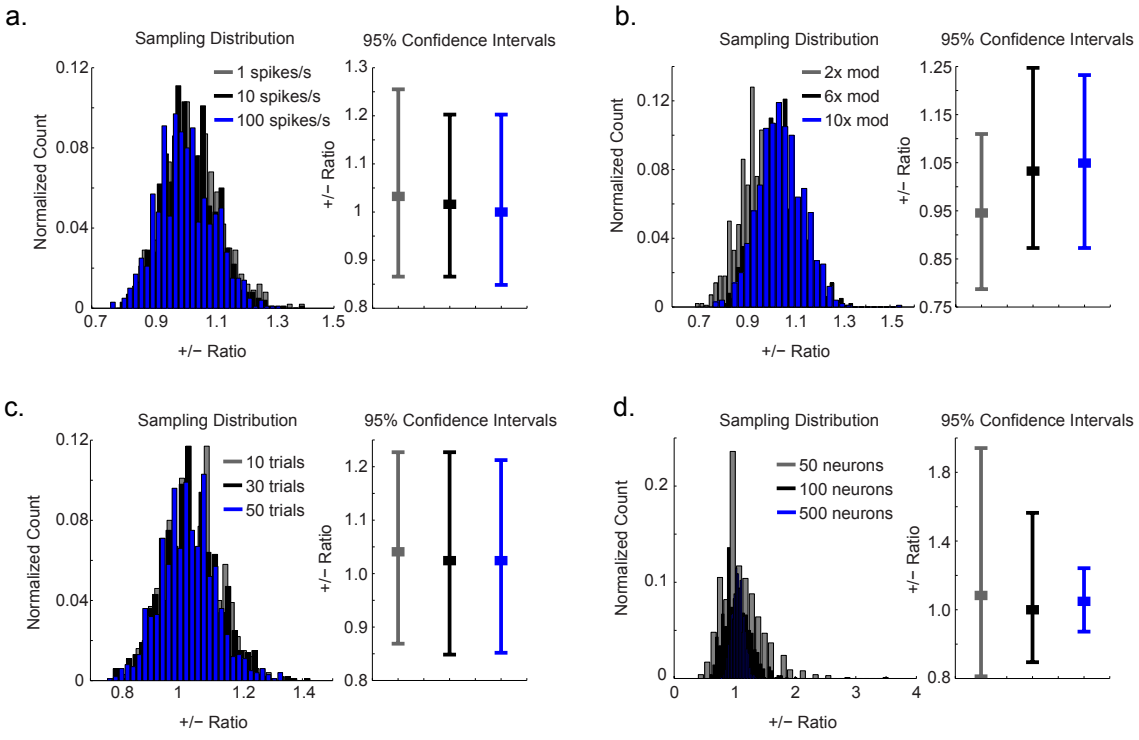

Figure 2.10 (Continued)

Chapter 3

Loss of Cortical Cross-Modal Activity by Vision

Author Contributions

Daniel Brady, Lia Min, Michela Fagiolini, and Takao Hensch designed the experiments; DB performed the neurophysiology; LM performed the tracing and *c-Fos* experiments; DB, LM, MF, and TH analyzed the data and wrote the paper.

Summary

Loss of a sensory system early in life leads to a large-scale reorganization of the remaining modalities. While this phenomenon has been studied for some time, the underlying mechanisms remain largely unknown. To address these issues, we have established the mouse as a model system for studying cross-modal plasticity. First, we describe a sensitive period for cross-modal responses in secondary visual cortex (V2L). Second, we provide evidence that the majority of neurons in this region respond to sound possibly due to input from auditory cortex and auditory thalamus. Third, we show that V2L is initially multimodal, and provide both pre- and postsynaptic mechanisms responsible for diminishing cross-modal responses. Finally, we explore how maintenance of cross-modal connections leads to increased multisensory enhancement in visual cortex, which might explain deficits in multisensory integration in people with restored vision.

Introduction

The brain has a remarkable capacity for being shaped by the environment (Hensch, 2005; Kuhl, 2010). Alteration of one sensory system can have striking effects on the processing and organization of the remaining senses, a phenomenon known as cross-modal plasticity (Bavelier & Neville, 2002). In blind humans and animals, areas of the brain that normally process vision can respond to other senses, such as touch (Sadato et al., 1996) or sound (Burton et al., 2002a). This is not confined to occipital cortex; auditory areas in the deaf can also respond to touch (Levänen et al.,1998) or vision (Finney et al., 2001). Moreover, this process appears to be age dependent. Only those who have lost a sensory modality early in life exhibit this form of plasticity (Sadato et al., 2002).

Cross-modal reorganization is functional and believed to underlie the enhanced perceptual abilities seen in the deaf or blind (Merabet & Pascual-Leone, 2010). Blind subjects are better at peripheral sound localization than sighted controls, an enhancement that is reduced after disrupting neuronal activity by transcranial magnetic stimulation (TMS) over visual cortex (Collingnon et al., 2009). Occipital TMS has also been shown to reduce tactile discriminability (Cohen et al., 1997) and induce phantom Braille percepts (Ptito et al., 2008). Furthermore, an early blind woman suffered alexia for braille after bilateral occipital stroke (Hamilton et al., 2000). In deaf humans, there is a shift toward heightened attention in the peripheral visual field allowing for improved object localization (Neville & Lawson, 1987). Similarly, congenitally deaf cats have superior peripheral visual localization and lower movement detection thresholds

over non-deaf animals. These enhancements can be reduced to normal levels by cooling specific regions of auditory cortex (Lomber et al., 2010). Thus, converging lines of evidence suggest that deprived cortex can be recruited by the remaining sensory systems for attention demanding tasks (Bavelier et al., 2006).

While there have been many studies documenting cross-modal plasticity, the cellular and molecular mechanisms remain largely unknown. Previous studies involved humans or large mammals and were therefore fundamentally limited in their ability to perform the physiological, anatomical, and genetic manipulations necessary to elucidate the mechanisms underlying this process.

To address these issues, we have established the mouse as a model system for studying cross-modal plasticity. First, we identified a region of visual cortex that responds to sound in an experience-dependent manner. Second, we examined the neuronal and anatomical substrates that underlie this response. Third, we found that multimodal activity is a feature of an immature brain, and is therefore present early in life. Fourth, we provide evidence for several molecular mechanisms mediating cross-modal input. Finally, we compared multisensory interactions between visually deprived, sighted, and genetically engineered animals to provide insight into the functional consequences of cross-modal reorganization. We believe that these experiments lay a foundation for understanding what mechanisms are responsible for cortical reorganization after loss of a sensory system and provide novel therapeutic targets that can inform sensory rehabilitation strategies.

Results

A sensitive period for cross-modal plasticity in the mouse

To establish whether cross-modal plasticity occurs in C57BL/6 mice, we compared intrinsic riboflavin fluorescence responses, a measure of neuronal activity (Reinert et al., 2004), over the entire surface of visual cortex in anesthetized adult mice reared in complete darkness from birth (DR) or in a normal 12-hour light/dark cycle (LR). We found a small region adjacent to primary visual cortex (V1) that responded much more strongly to sound in DR than in LR (Fig. 3.1a; time course in Fig. 3.1c bottom panel; videos in Fig. 3.2). Tracer injections identified this area as secondary visual cortex (V2L) (Fig. 3.1b). This cross-modal response was stable in DR adults, as there was no correlation between age at imaging and peak intensity (Fig. 3.3a).

We next examined the influence of age at visual deprivation on cross-modal plasticity by comparing animals placed in the darkness at different points in their lives. Auditory responses in visual cortex were strongest in mice deprived of vision within the first month of life (P0 and P25) and gradually became weaker at later deprivations (P45). By adulthood (P60), the window of plasticity had closed (Fig. 3.1d); animals placed in the darkness after this point had stable weak responses (Fig. 3.3b). Thus, consistent with human imaging studies (Sadato et al., 2002; Burton et al., 2002b), there is a sensitive period for cross-modal plasticity in mouse visual cortex that begins one week after onset of vision and ends in early adulthood.

Figure 3.1 | A sensitive period for cross-modal activity in secondary visual cortex (V2L)

(a) Original riboflavin fluorescence and pseudocolor images ($\Delta F/F_0$) after auditory stimulation in the primary (black circle) and secondary (blue circle) visual cortices of anesthetized C57BL/6 adult mice (>P60) raised in either a normal 12hr light/dark cycle (LR) or 24hr of darkness (DR).

(b) Alignment of retrograde tracer injection (Cholera toxin subunit B conjugated to Alexa 488) over the auditory responsive region in part (a) with the Mouse Brain Atlas (Paxinos and Watson, 2001) confirms area is V2L.

(c) Average time course of riboflavin fluorescence changes for all LR (light gray) and DR (black) animals in V1 (top) show a similar response profile to visual stimulation. However, DR have stronger responses to sound in V2L (bottom). Grey bars indicate stimulus onset and duration.

(d) The amplitude of V2L auditory responses (mean ± s.e.m.) is significantly higher in mice dark-reared from birth (P0, n=16) or within the first month of life (P25, n=7) compared to light-reared adults (LR, n=18). Mice placed into the dark during early adulthood (P45, n=7) show an intermediate response, neither significantly different from early dark-reared nor light-reared mice. Adults placed in the darkness for at least two months (>P60, n=13) do not show an enhanced response. This evidence suggests that there is a sensitive period for strong cross-modal activity in V2L ($\%\Delta F/F_0$, LR: 0.26 ± 0.046, DR P0: 0.46 ± 0.041, DR P25: 0.54 ± 0.10, DR P45: 0.36 ± 0.050, DR >P60: 0.15 ± 0.030, *P<0.05, ANOVA, Dunnett's multiple comparison test, error bars indicate ± s.e.m unless otherwise noted).

(e) *c-Fos* staining after auditory stimulation in awake behaving animals confirms stronger V2L activity in DR (n=7) compared to LR (n=6, *P=0.01, unpaired t-test) (top panel). This cross-modal plasticity is specific to visual cortex; visual stimulation does not activate auditory cortex in DR (n=6) or LR animals (n=4, P>0.05, unpaired t-test) (bottom panel).

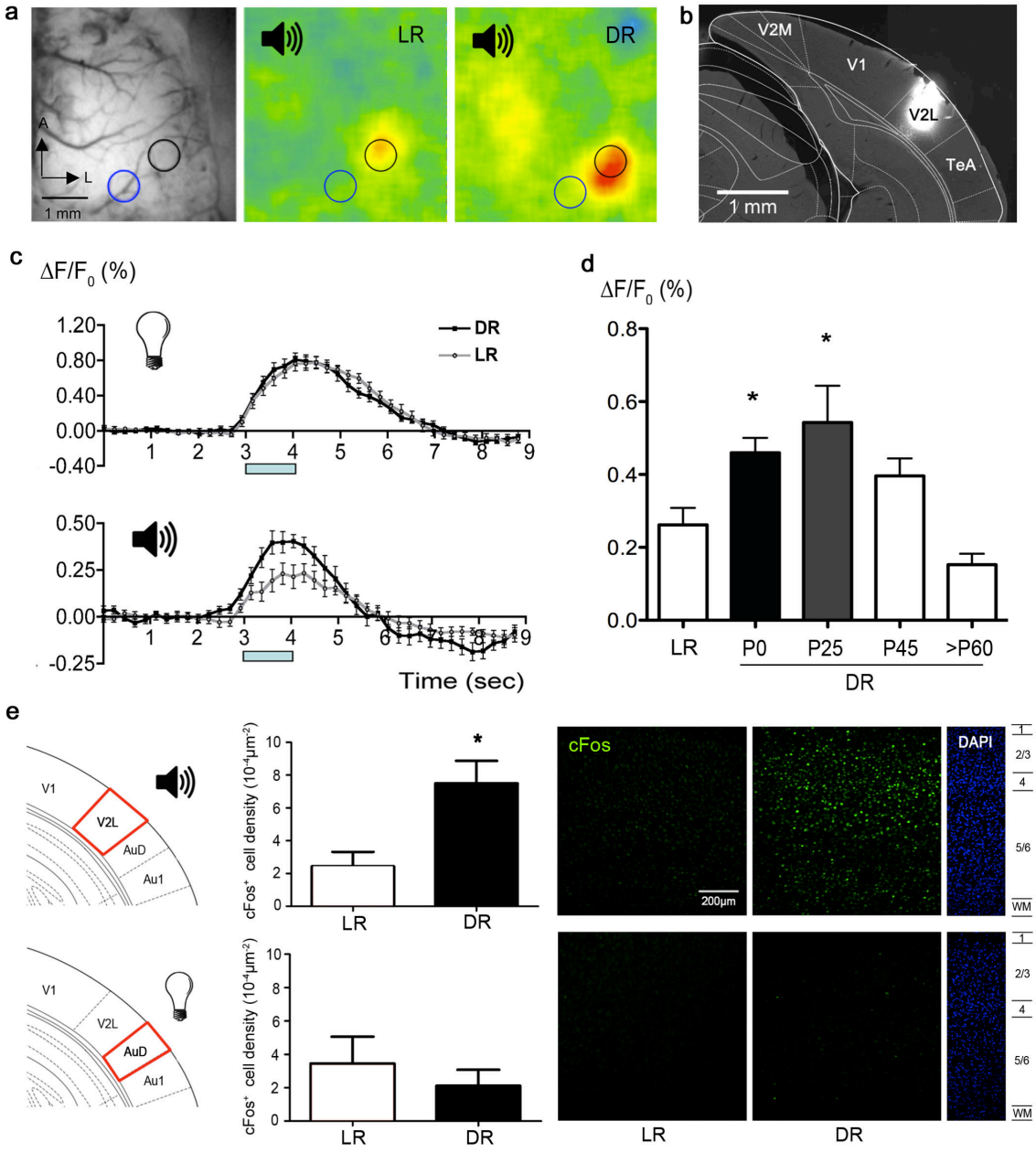

Figure 3.1 (Continued)

Figure 3.2 | Videos of riboflavin fluorescence responses to visual or auditory stimulation in mouse visual cortex

Original fluorescence and pseudocolor movies of representative LR and DR mice after visual or auditory stimulation show similar V1 visual responses but stronger V2L auditory responses in DR (see attached disc for videos).

Figure 3.3 | No correlation between age and V2L auditory responses in mice dark-reared from birth or placed into darkness as adults

(a) After reaching adulthood, age at riboflavin imaging is not correlated with peak amplitude for V2L auditory responses of mice dark-reared from birth (P0 DR, n=16 pairs, P=0.89, Pearson r 95% confidence interval: -0.47 to 0.52).

(b) Age at riboflavin imaging is not correlated with peak amplitude for V2L auditory responses of mice placed into darkness as adults (>P60 DR, n=13 pairs, P=0.79, Pearson r 95% confidence interval: -0.61 to 0.49).

a.

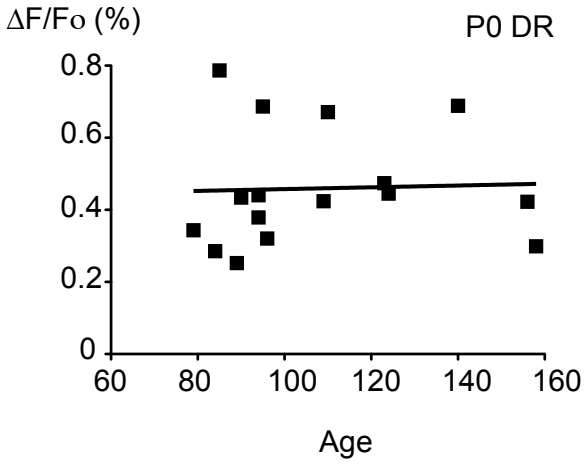

b.

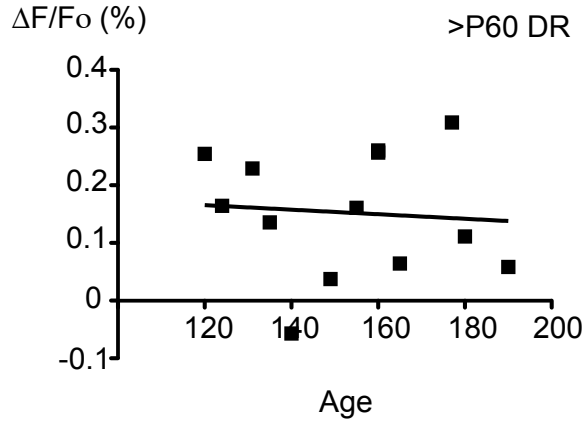

Figure 3.3 (Continued)

An advantage of dark-rearing over other forms of visual deprivation (such as enucleation) is that the visual pathway remains undamaged. Indeed, the time course (Fig. 3.1c top panel; videos in Fig. 3.2) and peak intensities (Fig. 3.4) of V1 visual responses were similar in LR and DR. We therefore could ask whether strong cross-modal responses were still present after exposure to a normal light environment. Dark rearing from birth is believed to maintain the visual cortex in an immature state and subsequent light exposure for 2-3 weeks in adulthood rapidly matures visual receptive field properties (Fagiolini et al., 2003; Iwai et al., 2003; Miyamoto et al., 2003). Along these lines, we found that adult mice dark-reared from birth but later re-exposed to a light environment for 2-3 weeks had a reduction in V2L auditory responses to typical LR levels, implying that cross-modal reorganization is not permanent (Fig. 3.5).

Majority of DR V2L neurons respond to sound

Riboflavin imaging only measures population activity in superficial layers (Tohmi et al., 2006). To evaluate whether individual neurons throughout all layers of visual cortex respond to sound, we first compared *c-Fos* activity (Sheng & Greenberg, 1990) in awake behaving LR and DR animals. Similar to our imaging results in anesthetized animals, V2L auditory responses were stronger in DR (Fig. 3.1e top panel). This activity was higher across all cortical layers (Fig 3.6a), with both excitatory and inhibitory cells being labeled (Fig 3.6b). Furthermore, we found this form of cross-modal plasticity to be specific to visual cortex; auditory cortex was not responsive to light in DR or LR animals (Fig. 3.1e bottom panel).

Figure 3.4 | No significant differences in V1 visual responses between LR and DR mice

The peak amplitude for V1 visual responses (mean ± s.e.m.) by riboflavin imaging is similar between LR and DR mice (%$\Delta F/F_0$, LR: 0.86 ± 0.060, DR: 0.84 ± 0.058, P=0.96, Mann-Whitney, n.s., not significant).

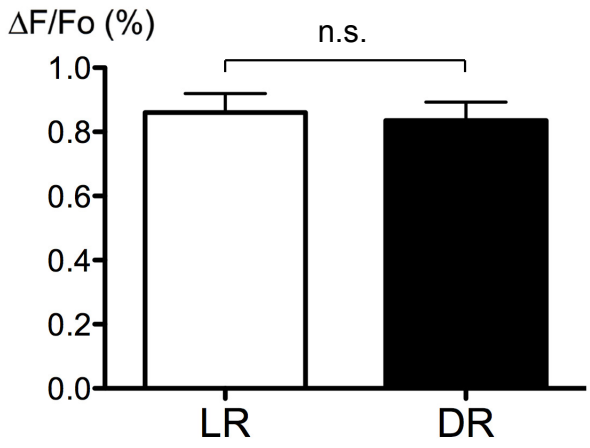

Figure 3.4 (Continued)

Figure 3.5 | Cross-modal responses decrease after 2-3 weeks of light exposure

(a) Original riboflavin fluorescence and pseudocolor images ($\Delta F/F_0$) after auditory stimulation in LR, DR, and DR exposed to a normal light/dark cycle (DR + Light).

(d) Typically strong V2L auditory responses (mean of peak amplitude ± s.e.m.) in DR mice (n=16) are restored to LR levels (n=18) following 2-3 weeks of normal visual experience (DR + Light, n=14) (%$\Delta F/F_0$, LR: 0.26 ± 0.046, DR: 0.46 ± 0.041, DR + Light: 0.28 ± 0.046, *P<0.05, ANOVA, Tukey's HSD).

a.

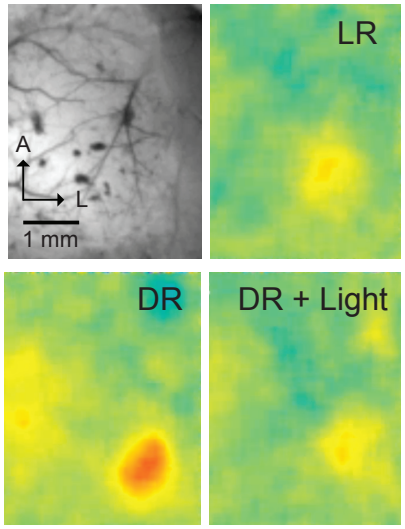

b.

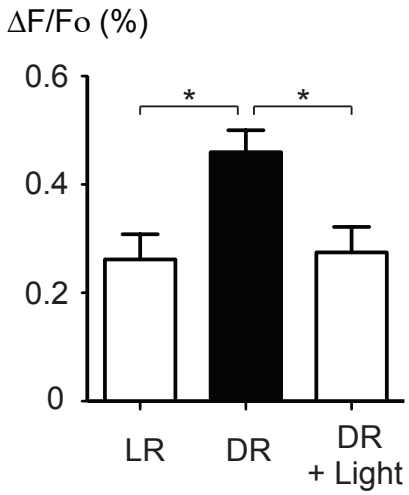

Figure 3.5 (Continued)

Figure 3.6 | GABAergic and non-GABAergic neurons in all layers respond to cross-modal input in DR V2L

(a) *c-Fos* expression is higher across all cortical layers of DR V2L (n=5) compared to LR (n=5, *P<0.05, unpaired t-test with Welch's correction)

(b) 10~20% of neurons with *c-Fos* activity after auditory stimulation in DR V2L (n=6) are GABAergic. $GABA^+$ cells are distributed across all layers.

a.

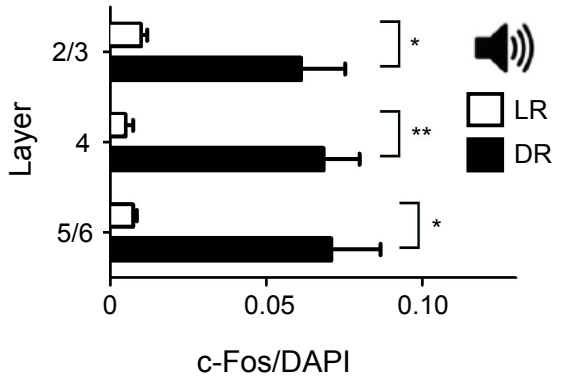

b.

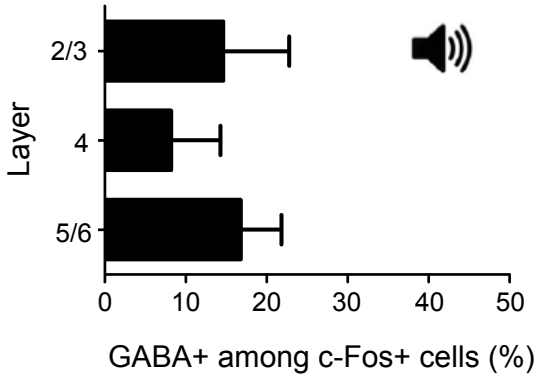

Figure 3.6 (Continued)

To determine whether cross-modal activity arose from a distinct population of auditory neurons in DR V2L or if cells were multimodal, we recorded from individual neurons with extracellular single-unit electrodes. We found that the majority of cells responded to both light and sound (Fig. 3.7a). 33% of all cells recorded were multimodal, with 36% classified as visual only, 10% auditory only, and 21% unresponsive. This percentage of auditory responsive neurons was significantly higher than in LR, where 5% of cells were multimodal, 73% visual only, >>1% auditory only, and 22% unresponsive (Fig. 3.7b). Furthermore, auditory responsive neurons were not evenly distributed throughout DR visual cortex; the density of multimodal and auditory cells increased as the recordings moved laterally and anteriorly away from V1 through V2L to the border of visual and auditory cortex (Fig. 3.8). This discrepancy between the distribution of cell types in LR and DR animals may underlie the differences in riboflavin imaging and *c-Fos* activity measured earlier.

Ectopic cross-modal input in DR

It is unclear how auditory signals reach occipital cortex in the visually deprived. Dynamic causal modeling of human cross-modal responses suggests intracortical connections as the primary pathway (Klinge et al., 2010). Non-human anatomical experiments have led to conflicting results (Laemle et al., 2006; Chabot et al., 2008), and often involve anophthalmic animal models (Doron & Wollberg, 1994) or binocular enucleation (Laramee et al., 2011). Severing afferent inputs at such early ages could lead to gross subcortical reorganization (Pallas et al., 1990; Zeng et al., 2009), which might apply to only a subset of blind

Figure 3.7 | Majority of dark-reared V2L neurons respond to cross-modal input

(a) Raster plot and peristimulus time histogram (PSTH, 25 ms bins) for a multimodal cell in DR V2L. Trials are divided into the different stimulus conditions: visual (yellow), auditory (blue), visual + auditory (red), and blank (white). Bold and dotted black lines indicate when the stimulus turned on and off respectively. The blue dotted line in the PSTH is the blank response.

(b) The distribution of visual (yellow), auditory (blue), multimodal (red), and unresponsive (white) cells in DR V2L (n=147) indicate a significantly larger portion of cells that respond to auditory stimuli than in LR (n=131, *P<0.0001, χ^2 test).

(c) Cumulative distribution function of peak latencies in DR V2L show faster auditory (blue, n=50) than visual (black, n=88) responses (**P=0.004, two-sample Kolmogorov-Smirnov test).

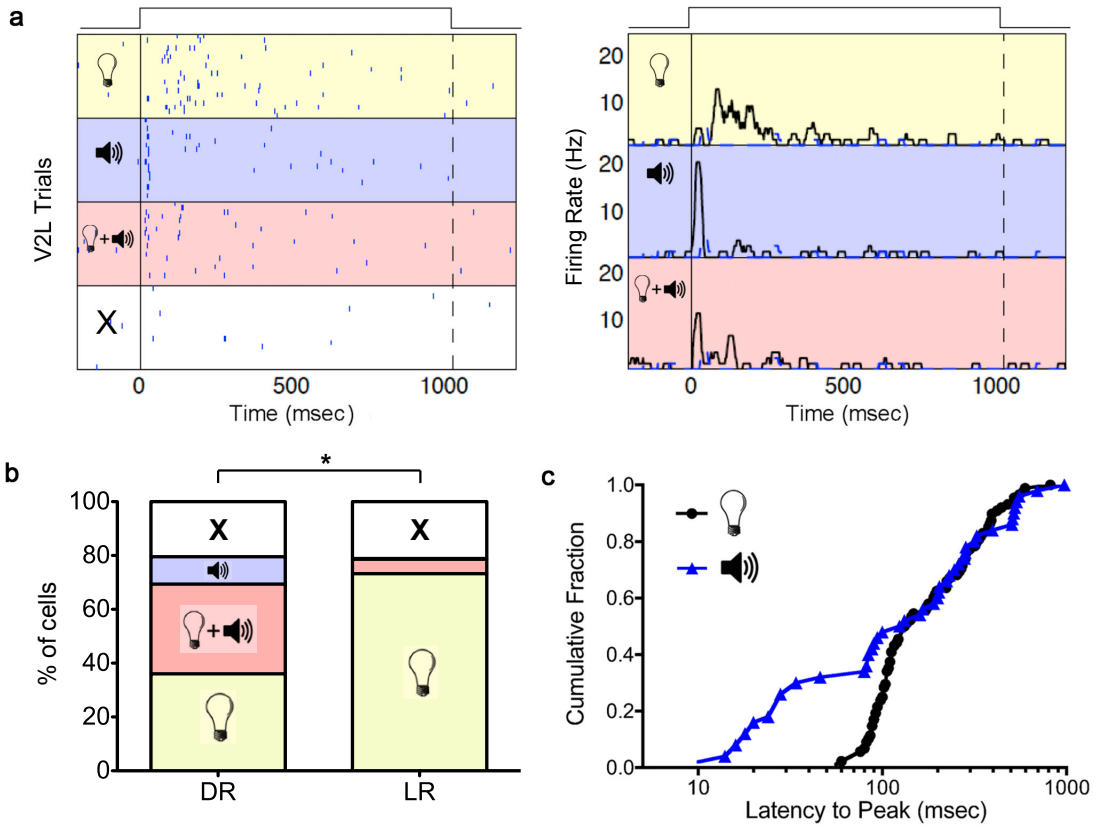

Figure 3.7 (Continued)

Figure 3.8 | Map of cell types in the visual cortex of DR

A map of stereotactic coordinates and cortical depths of all recorded cells in DR animals (n=105) illustrates a gradual increase of auditory and multimodal cells as the electrode progresses laterally and anteriorly from V1 through V2L to the borders of auditory cortex. The origin in the x-y plane (0,2) represents 2 mm lateral from lambda, the point at which the lambdoid and sagittal sutures intersect. Note that visual, auditory, and multimodal cells are distributed throughout all layers.

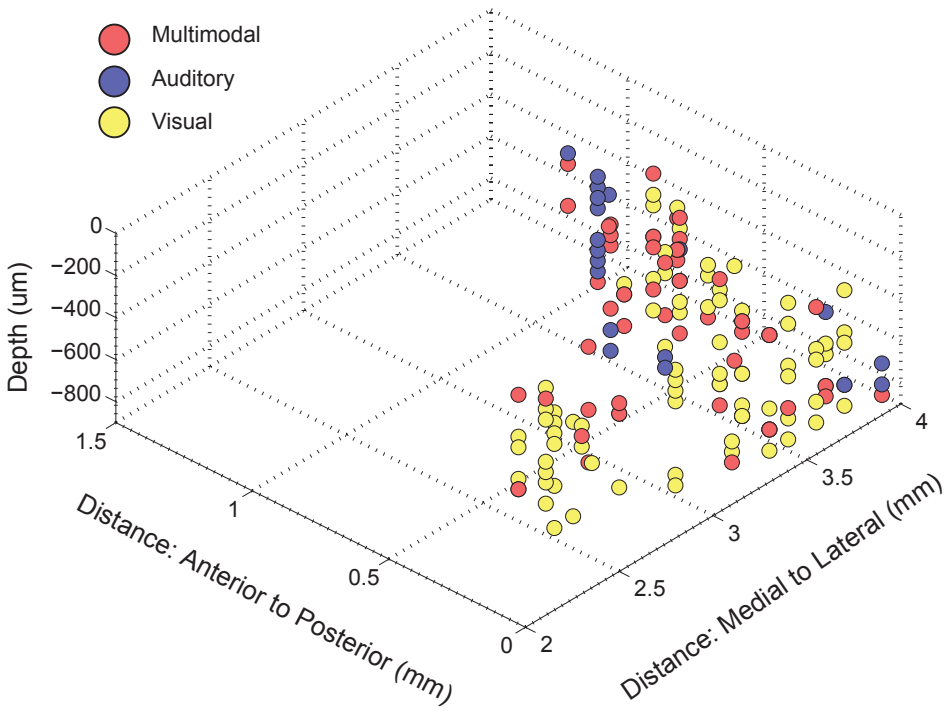

Figure 3.8 (Continued)

Figure 3.9 | Single unit peak latencies are not dependent on firing rate in DR V2L

(a) Peak latency is not correlated with firing rate for visual responses in DR V2L (n=88 pairs, P=0.18, Spearman r 95% confidence interval: -0.38 to 0.078).

(b) Peak latency is not correlated with firing rate for auditory responses in DR V2L (n=50 pairs, P=0.55, Spearman r 95% confidence interval: -0.21 to 0.38).

a.

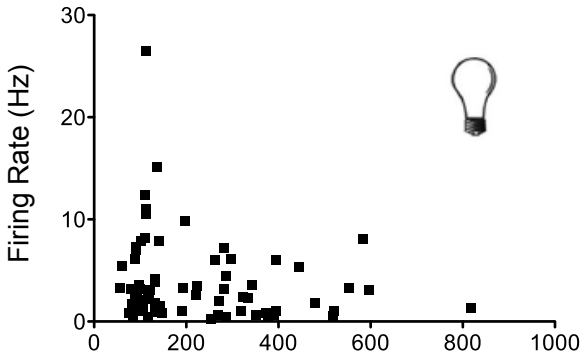

b.

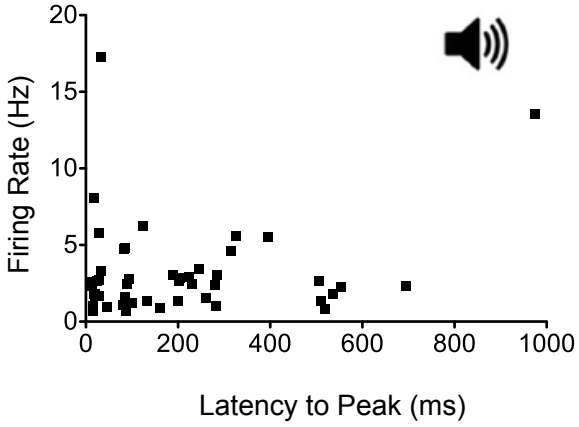

Figure 3.9 (Continued)

individuals. Given the strong emphasis in the scientific literature on intracortical connections, we were surprised to find cells that exhibited a short response latency to auditory stimuli compared with a much slower and sustained visual response (example in Fig. 3.7a). In fact, auditory peak latencies at the population level were faster than visual ones (Fig. 3.7c). Fast cells comprised around 30% of the total auditory responsive population, with some latencies reaching V2L at the same timescale as been recorded in primary auditory cortex (Linden et al., 2003). These differences in response latencies were not due to differences in firing rates. No correlation between firing rates and visual (Fig. 3.9a) or auditory latencies was found (Fig. 3.9b).

To determine how auditory information reaches visual cortex, we injected retrograde tracers into V2L (Fig. 3.10a). We found labeled cell bodies in the auditory cortex of both LR and DR animals. However, there were many more labeled cells in DR (Fig. 3.10b). More importantly, we also provide the first evidence for direct projections between auditory thalamus and V2L in DR. These connections were absent in LR (Fig. 3.10c). This thalamocortical projection may underlie the fast auditory responses in Fig. 3.7c while multisynaptic connections are responsible for the slower latencies. These results extend previous studies by suggesting two possible pathways for auditory signals to reach visual cortex in the blind.

Early, strong cross-modal activity is retained in NgR -/- mice

Increased cross-modal activity and connectivity in the DR may occur in one of two ways. One possible explanation is that ectopic axonal outgrowth from

Figure 3.10 | Ectopic cross-modal connections in DR V2L

(a) Schematic of tracing experiments. Retrograde tracers (CTB-488) were injected into V2L of DR and LR animals and labeled cell bodies were counted in auditory cortex and thalamus.

(b) Representative images and quantification of CTB-488^{+} cell bodies illustrate greater connectivity between V2L and auditory cortex in DR (n=6) than in LR mice (n=5, *P=0.004, unpaired t-test).

(c) Representative images, *camera lucida* reconstructions, and quantification show projections from auditory thalamus to V2L in DR mice (n=6). This connection is absent in LR (n=6, *P=0.01, unpaired t-test).

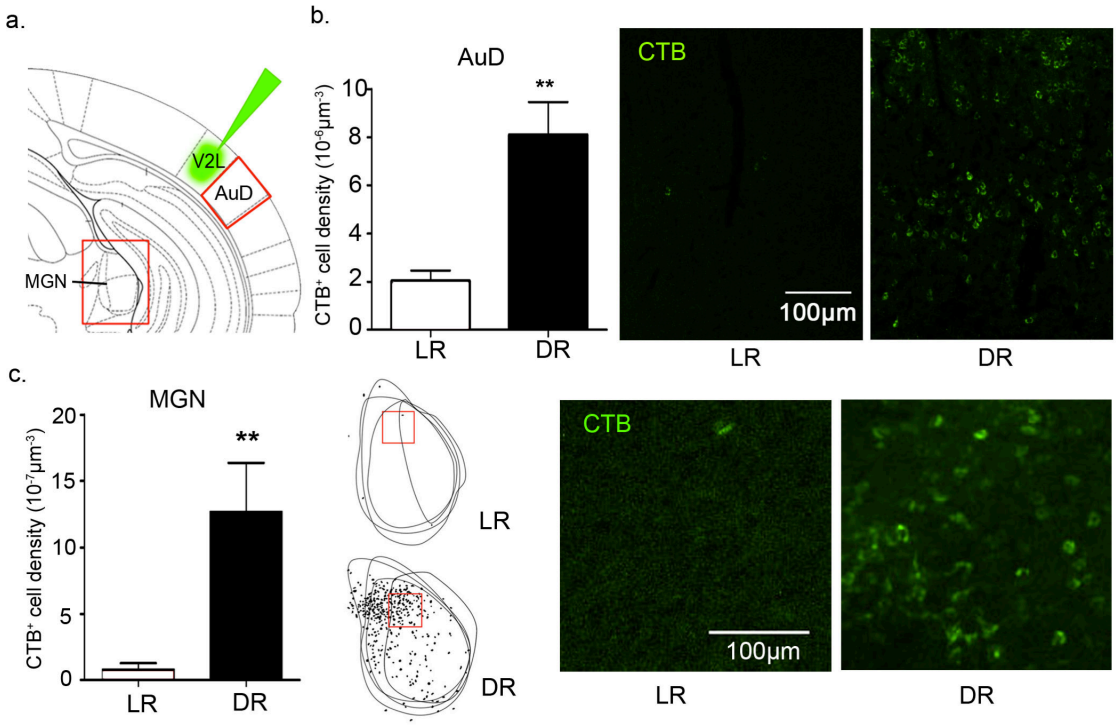

Figure 3.10 (Continued)

auditory cortex and auditory thalamus invades the deprived visual cortex. An alternative possibility is that V2L is initially innervated by auditory inputs but becomes less so with normal visual experience. To discriminate between these two hypotheses, we imaged juvenile mice raised in a normal light/dark cycle. We found that young LR mice exhibit significant V2L auditory activity compared to LR adults and similar to DR (Fig. 3.11a). This multimodal activity steadily decreases with age (Fig 3.11b).

Since auditory activity in V2L is a hallmark of a juvenile brain, we examined several circuit and signaling pathways that are kept immature in DR animals. Previous work has shown that the maturation of excitatory circuits (Carmignoto & Vicini, 1992; Quinlan et al., 1999), inhibitory circuits (Katagiri et al., 2007; Sugiyama et al., 2008), and myelination (Morishita et al., in preparation) are all experience-dependent and delayed by dark-rearing. We found no difference in V2L auditory activity in adult LR animals with immature excitatory (NR2A -/-) or inhibitory (Gad65 -/-) circuits. However, mice with disrupted Nogo receptor signaling retained a juvenile response (Fig. 3.11a & b). Furthermore, single-unit recordings found a similar distribution of cell types between NgR -/- and DR (Fig. 3.11c).

Nogo receptor signaling is crucial for myelin-based inhibition of axonal sprouting (Schwab, 2010) and is therefore a possible mediator of cross-modal refinement. With normal light experience, coherent visual input selectively strengthens within modality connections at the expense of cross-modal ones. As myelination and NgR signaling increase across development, this weak input is

Figure 3.11 | Strong, early cross-modal response persists in adult NgR -/- mice

(a) Pseudocolor riboflavin fluorescence images ($\Delta F/F_0$) after auditory stimulation for light-reared adult +/+, juvenile +/+, adult NR2A -/-, adult GAD65 -/-, and adult NgR -/- mice.

(b) Peak V2L auditory responses (mean ± s.e.m.) are strong in light-reared juvenile mice (P25, n=13), suggesting that V2L is initially multimodal. Cross-modal responses decrease with age (P45, n=7; >P60, n=18). Signaling through the Nogo receptor is important in diminishing this activity; auditory responses in adult NgR -/- mice (n=10) are similar to wild-type juveniles. This is not the case for adult NR2A -/- (n=7) or GAD65 -/- mice (n=8) ($\%\Delta F/F_0$, P25 +/+: 0.55 ± 0.091, P45 +/+: 0.43 ± 0.058, >P60 +/+: 0.26 ± 0.046, NR2A -/-: 0.27 ± 0.063, Gad65 -/-: 0.33 ± 0.058, NgR -/-: 0.57 ± 0.059, **P<0.01, ANOVA, Dunnett's multiple comparison test).

(c) NgR -/- (n=101) have a similar distribution of visual, auditory, multi-modal, and unresponsive cells in V2L to DR mice (n=147, P=0.67, χ^2 test) as measured by single-unit recordings.

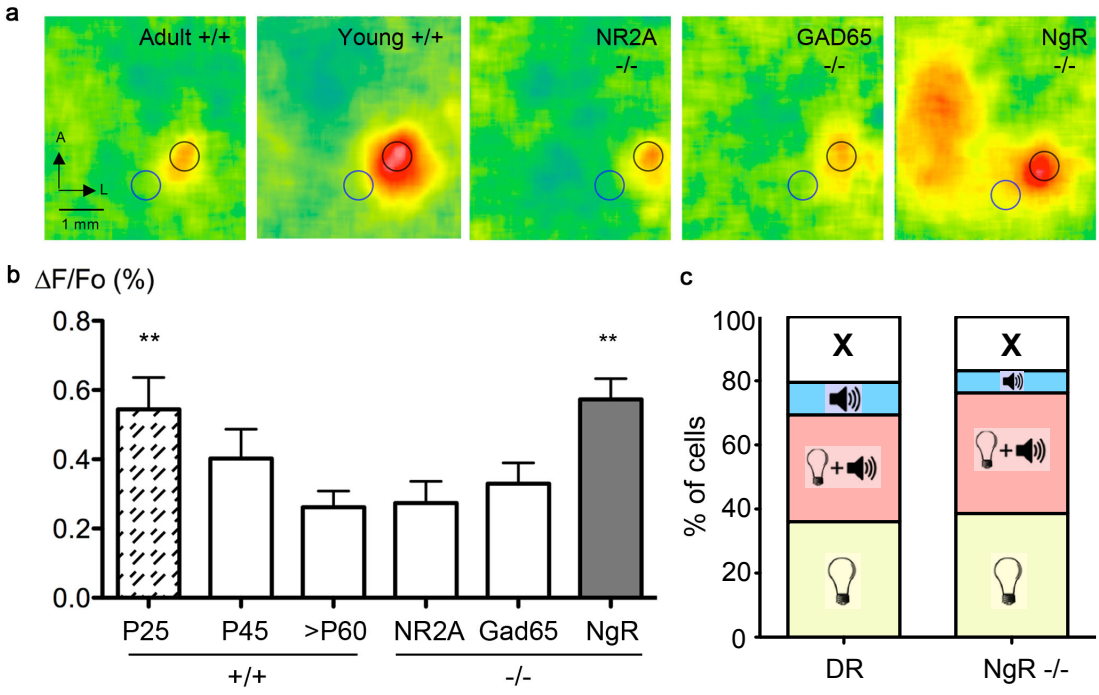

Figure 3.11 (Continued)

Figure 3.12 | Auditory responses in V2L decrease with age in light-reared mice

Age at riboflavin imaging is negatively correlated with peak amplitude of V2L auditory responses in light-reared mice (n=38 pairs, *P=0.021, Pearson r = -0.33).

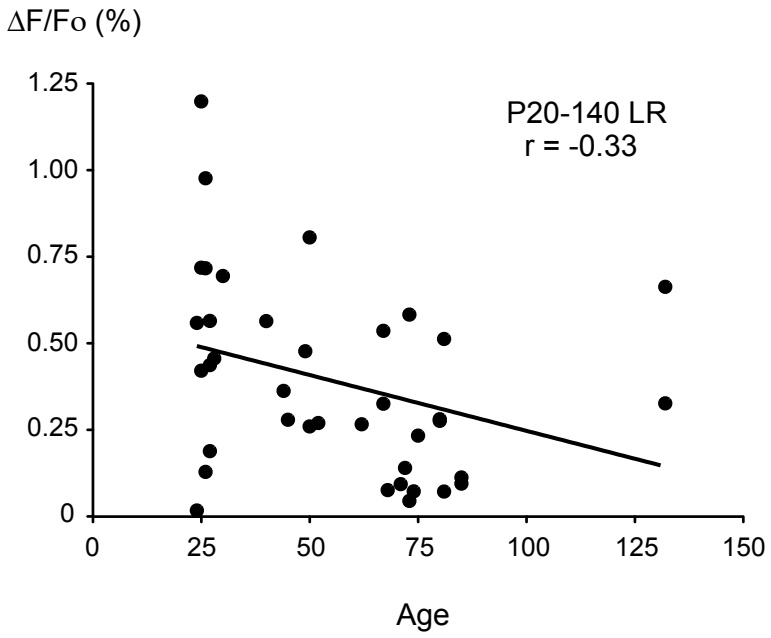

Figure 3.12 (Continued)

Figure 3.13 | NgR signaling selectively prunes intracortical over thalamocortical cross-modal input

(a) Raster plot and peristimulus time histogram (PSTH, 25 ms bins) for a multimodal cell in DR V2L with a fast auditory response (different from figure 3.5). Trials are divided into the different stimulus conditions: visual (yellow), auditory (blue), visual + auditory (red), and blank (white). Bold and dotted black lines indicate when the stimulus turned on and off respectively. The blue dotted line in the PSTH is the blank response.

(b) Raster plot and PSTH for a multimodal cell in NgR -/- V2L. The auditory peak latency is considerably slower than in part (a).

(c) Cumulative distribution function of auditory latencies in V2L show faster responses in DR (n=50) than NgR -/- mice (n=34, **P<0.01, two-sample Kolmogorov-Smirnoff test). The fast auditory component is nearly absent in NgR -/- mice because the ratio of intracortical to thalamocortical projections is much higher.

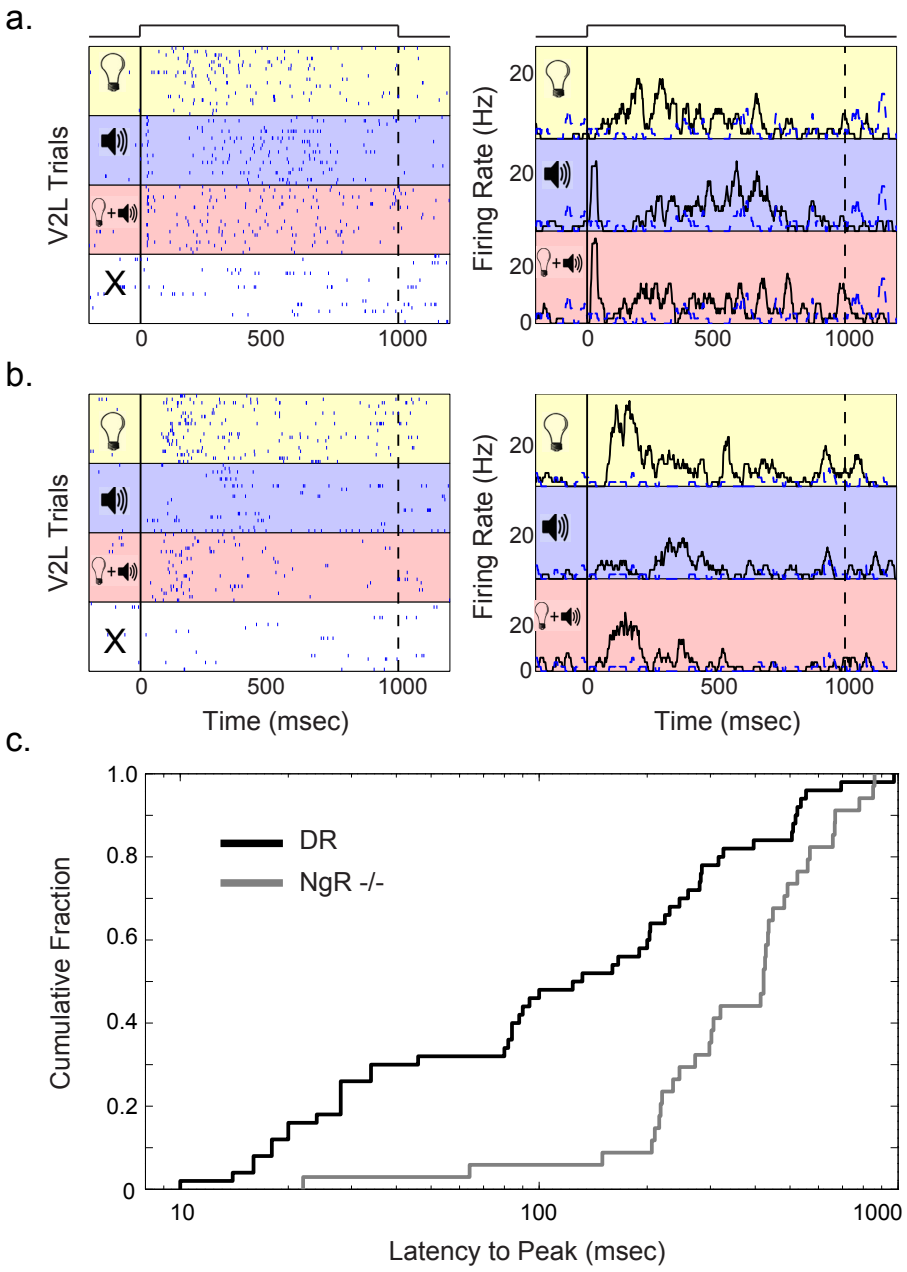

Figure 3.13 (Continued)

selectively pruned (Min et al., in preparation). Interestingly, we found that NgR signaling has a much larger effect on intracortical connections compared to thalamocortical ones. V2L auditory responses were much slower in NgR -/- animals (Fig. 3.13) due to a higher ratio of intracortical to thalamocortical connections (DR: 4 to 1, NgR -/-: 11 to 1, Min et al., in preparation).

Cholinergic modulation through the nucleus basalis is critical in regulating the attentional and arousal state of an animal (Gu, 2002). Stimulation of the basal forebrain can enhance cortical encoding (Goard & Dan, 2009) and lead to experience-dependent plasticity (Theil et al., 2002). Lynx1 is neuronal membrane molecule whose expression increases over development. It binds to and reduces the sensitivity of nicotinic acetylcholine receptors (Ibañez-Tallon et al., 2002), acting as a brake on cortical plasticity. Lynx1 -/- mice remain plastic for ocular dominance throughout their lives (Morishita et al., 2010). Similarly, we found that adult LR Lynx -/- retain cross-modal activity in V2L similar to DR (Fig. 3.14). We have thus found that V2L is initially multimodal and that there are at least two mechanisms by which cross-modal responses are reduced. Both NgR and Lynx1 signaling increase with normal sensory experience, with one leading to the pruning of weak connections between sensory regions and the other dampening the efficacy of cross-modal input.

Experience-independent maturation of cross-modal plasticity in Icam5 -/- mice

Since NgR signaling (Li & Strittmatter, 2003) and Lynx1 expression (Lucas-Meunier et al., 2006) affect presynaptic function, we wanted to examine

Figure 3.14 | Cross-modal response persists in adult light-reared Lynx1 -/- mice

Adult Lynx1 -/- (n=6) raised in a normal light environment maintain an enhanced cross-modal response in V2L similar to DR (n=16) and stronger than wild-type LR mice (n=18) (%$\Delta F/F_0$, LR: 0.26 ± 0.046, DR: 0.46 ± 0.041, Lynx -/-: 0.47 ± 0.032, *P<0.05, ANOVA, Dunnett's multiple comparison test).

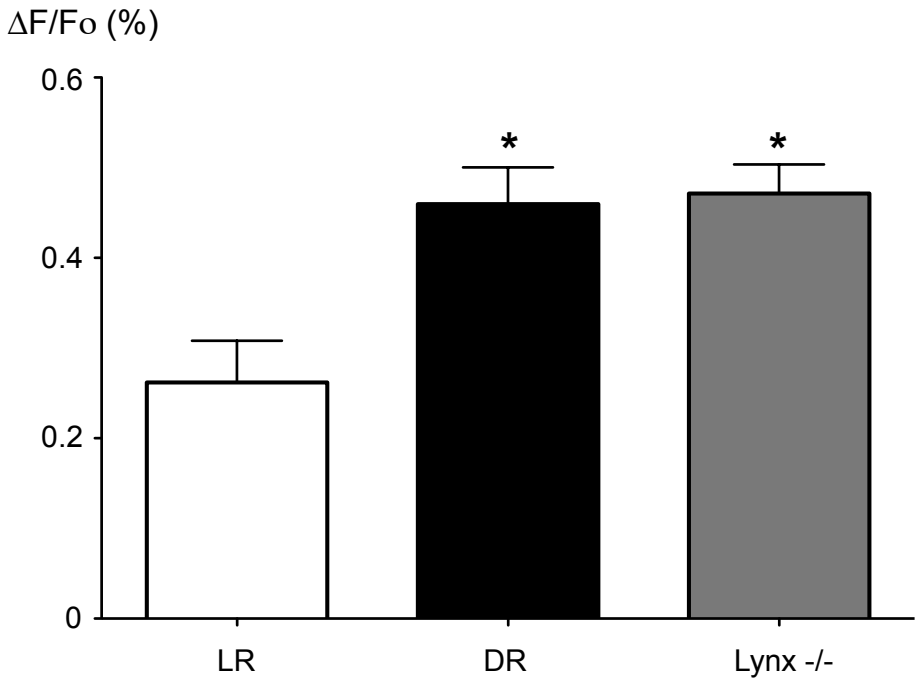

Figure 3.14 (Continued)

Figure 3.15 | Experience-independent maturation of cross-modal plasticity in Icam5 -/- mice

In wild-type animals, V2L is initially multimodal (Young +/+, n=13) and becomes less so with age (LR +/+, n=18). This phenomenon is experience-dependent; mice dark-reared from birth maintain this multimodality (DR +/+, n=16) (left panel, $\%\Delta F/F_0$, Young +/+: 0.55 ± 0.091 LR +/+: 0.26 ± 0.046, DR +/+: 0.46 ± 0.041, *P<0.05, ANOVA, Dunnett's multiple comparison test). In Icam5 -/- mice, V2L undergoes a similar maturation during development (Young -/-, n=8). However, this process is experience-independent. Adult Icam5 -/- mice dark-reared from birth (DR -/-, n=8) are no different from light-reared (LR -/-, n=9) (right panel, $\%\Delta F/F_0$, Young -/-: 0.69 ± 0.06, LR -/-: 0.44 ± 0.044, DR -/-: 0.38 ± 0.050, *P<0.05, one-way analysis of variance, Dunnett's multiple comparison test; n.s., not significant).

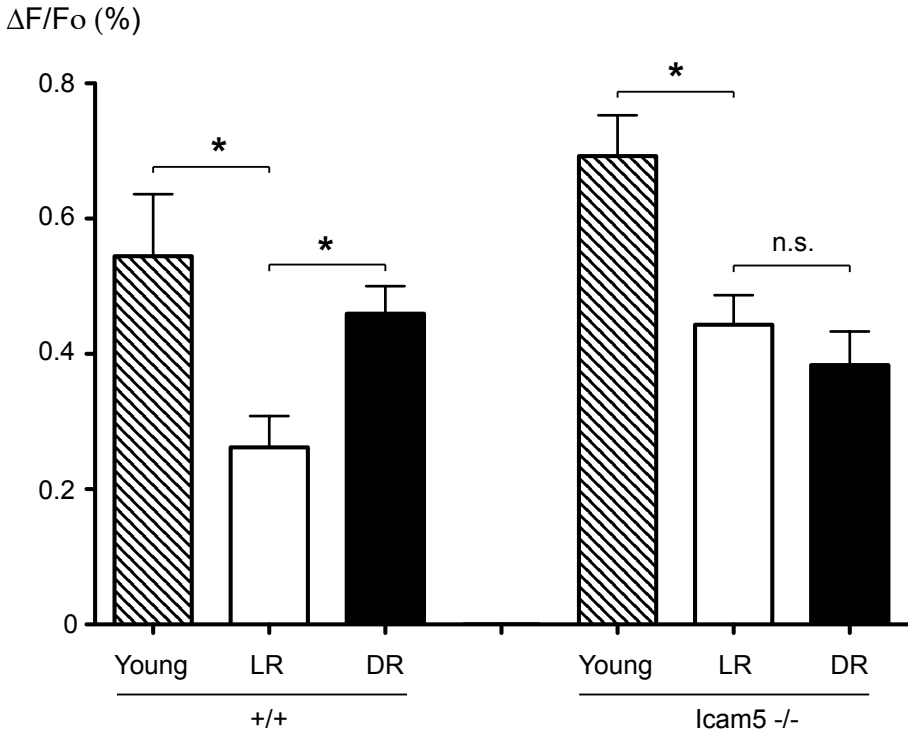

Figure 3.15 (Continued)

how postsynaptic maturation affects cross-modal reorganization. The motility, retraction, and stabilization of dendritic spines have been shown to play a role in coupling functional to structural changes in experience-dependent plasticity (Mataga et al., 2002; Mataga et al., 2004). Intracellular adhesion molecule 5 (Icam5), a forebrain-specific molecule expressed in the dendrites of pyramidal cells, is responsible for slowing spine maturation (Matsuno et al., 2006) and controls the duration of critical period plasticity for auditory thalamocortical connectivity (Barkat et al., 2011). We found that although cross-modal responses mature in an age-dependent manner, V2L auditory responses were similar between adult LR and DR Icam5 -/- mice. This suggests that shortening the window of cross-modal plasticity favors the consolidation of within modality connections (Fig. 3.15).

Biased multisensory interactions in DR and NgR -/- mice

Previous studies have shown that visual deprivation early in life can lead to permanent impairments in multisensory integration. People with restored vision are less distracted in a multisensory interference task and have impaired audio-visual speech perception (Putzar et al., 2007; Putzar et al., 2010). While the exact loci of these deficits are unknown, a recent study in rodents showed that inactivation of secondary visual cortex selectively impairs auditory-visual multisensory facilitation (Hirokawa et al., 2008).

To probe the functional consequences of cross-modal plasticity in our model system, we compared multisensory interactions (M.I.) in animals with strong cross-modal responses (DR and NgR -/-) to those with weak ones (LR).

Figure 3.16 | Biased multisensory interactions in DR and NgR -/- mice

(a) Raster plot and PSTH of a visual cell in DR V2L with an enhanced response to visual + auditory stimuli (red) compared to visual only (yellow).

(b) Cumulative distribution function of multisensory interactions suggests a greater range of modulation in DR (n=117) and NgR -/- (n=84) compared to LR (n=104, *P<0.05, Kolmogorov-Smirnov test). This difference is explained by an increase in multisensory facilitation (inset, LR n=57, DR n=66, NgR -/- n=48; %M.I., LR: 26 ± 4.9, DR: 55 ± 7.0, NgR -/-: 73 ± 13, **P<0.01, Kruskal-Wallis test, Dunn's multiple comparison test).

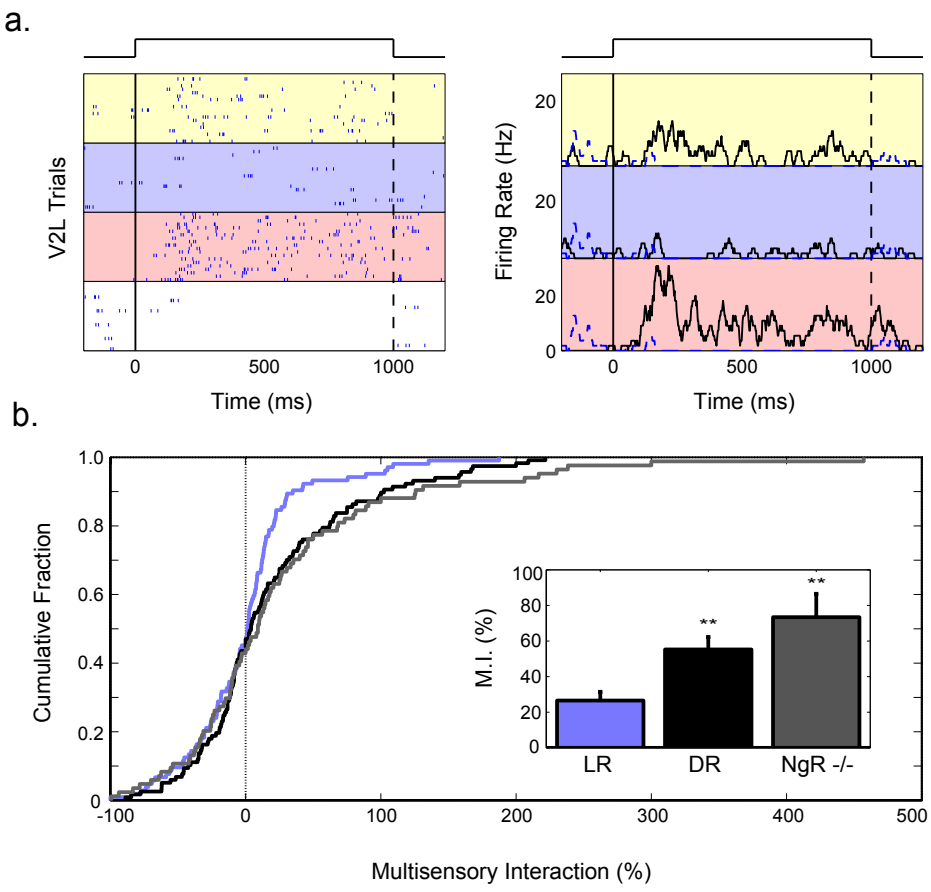

Figure 3.16 (Continued)

Figure 3.17 | Multisensory suppression and the ratio of enhanced to suppressed cells is the same in DR, LR, and NgR -/- mice

(a) The magnitude (inset) and distribution (P>0.05, Kolmogorov-Smirnov test) of negatively modulated cells in V2L is similar among LR (n=47), DR (n=51), and NgR -/- mice (n=36) (%MI, LR: -32 ± 3.6, DR: -27 ± 3.1, NgR -/-: -34 ± 4.5, P=0.51, Kruskal-Wallis test).

(b) The ratio of enhanced to suppressed cells is similar across LR (n=104), DR (n=117) and NgR -/- (n=84) mice (+/- ratio 95% CI, LR: 0.79 to 1.7, DR: 0.84 to 1.8, NgR -/-: 0.84 to 2.0, bootstrap procedure, 100,000 iterations, error bars indicate ± s.d.).

a.

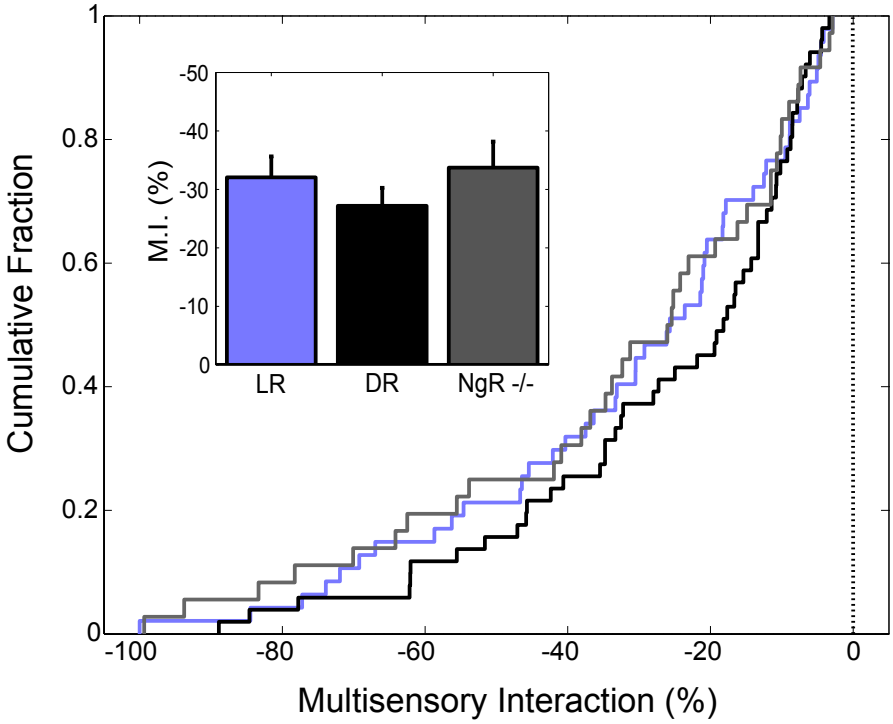

b.

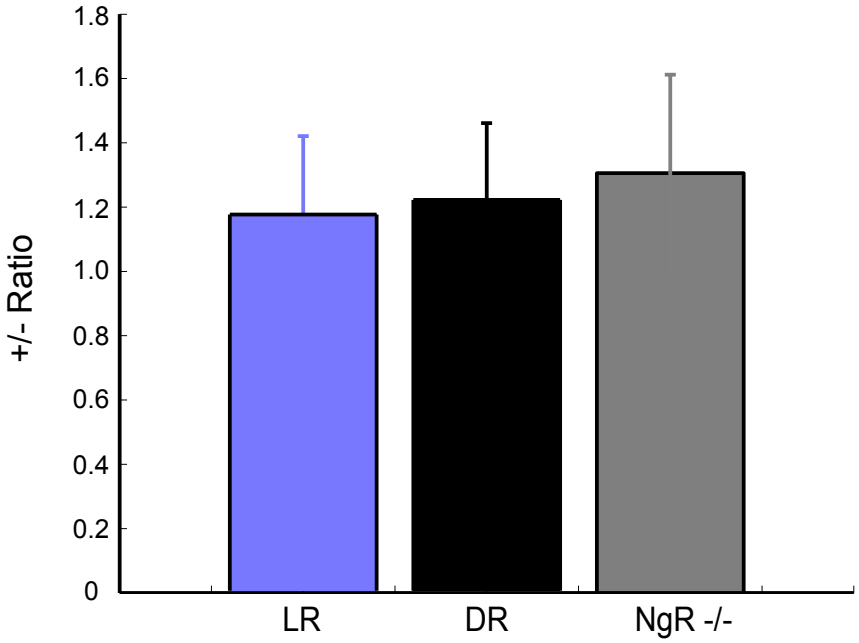

Figure 3.17 (Continued)

We measured the degree to which a neuron's firing rate is either suppressed (Fig. 3.7a) or enhanced (Fig. 3.16a) when exposed to a cross-modal stimulus. We found biased multisensory interactions in DR and NgR -/- mice (Fig. 3.16b) due to a specific strengthening of multisensory enhancement (Fig. 3.16b inset); neither multisensory suppression (Fig. 3.17a inset) nor the ratio of enhanced to suppressed cells (Fig. 3.17b) were different between the three groups.

To ensure that the differences in multisensory enhancement we found were not due to relative firing rates (Ponce et al., 2008; Kuhlman et al., 2011), we created a four-parameter bootstrap model that could predict the amount of M.I. bias we should expect given the firing rates, number of trials, number of neurons, and dynamic range of modulation recorded in V2L (Fig. 3.19). Our model assumed that V2L neurons were Poisson processes. We calculated the 95% confidence intervals within which a neuron can be deemed a Poisson process given that the expected distribution of the Fano factor is a gamma distribution whose shape is dependent on the number of trials (Eden & Kramer, 2010) (Fig. 3.18a). We found that the majority of V2L neurons in all animals examined fell within these limits (Fig. 3.18b-d), and that this did not change with the introduction of a cross-modal stimulus (Fig. 3.18b-d inset). By running our model through 1000 iterations to create 95% confidence intervals for the statistics that were significantly different between groups, we found that the bias in multisensory interactions measured could not be explained by relative firing rates alone (Fig. 3.20). Thus, mice with strong cross-modal responses have disrupted multisensory interactions due to a strengthening of multisensory enhancement.

Figure 3.18 | Majority of V2L neurons in LR, DR, and NgR -/- mice are Poisson processes.

(a) Gamma function of the expected distribution of Fano factors for a Poisson process with 20 trials. Blue dotted lines indicate the upper (1.729) and lower (0.4688) limits of the 95% confidence interval of the distribution. Cells with a Fano factor outside of these limits are not Poisson processes.

(b) Cumulative distribution function of Fano factors for all cells recorded in LR V2L (n=104) to the strongest single modality stimulus (SM, blue) or combined stimuli (CM, red). The majority of neurons behave in a Poisson manner whether responding to one (74%) or multiple stimuli (75%, light grey bar). Fano factors (mean ± s.e.m.) are not significantly different between SM and CM conditions (P=0.56, Mann Whitney test).

(c) Cumulative distribution function of Fano factors for all cells recorded in DR V2L (n=105). The majority of neurons behave in a Poisson manner whether responding to one (75%) or multiple stimuli (82%, light grey bar). Fano factors (mean ± s.e.m.) are not significantly different between SM and CM conditions (P=0.36, Mann Whitney test).

(d) Cumulative distribution function of Fano factors for all cells recorded in NgR -/- V2L (n=84). The majority of neurons behave in a Poisson manner whether responding to one (70%) or multiple stimuli (63%, light grey bar). Fano factors (mean ± s.e.m.) are not significantly different between SM and CM conditions (P=0.48, Mann Whitney test).

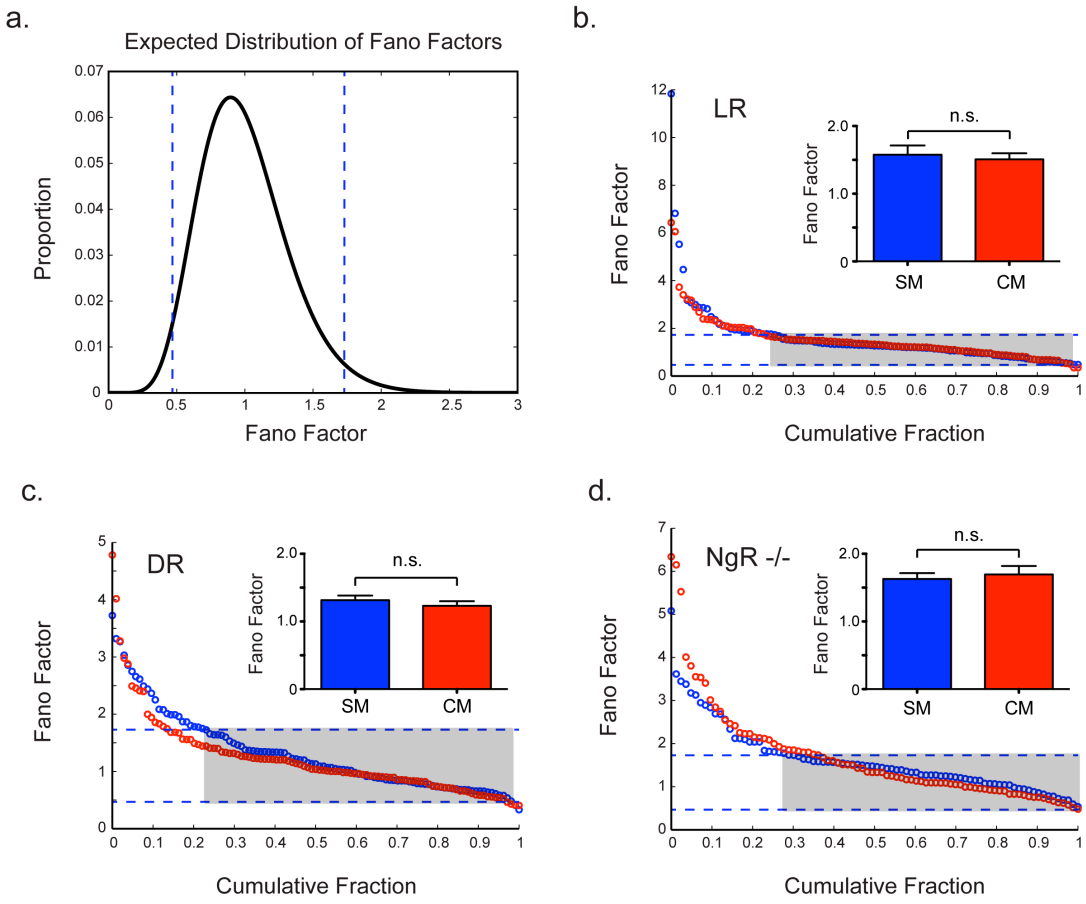

Figure 3.18 (Continued)

Figure 3.19 | Example simulation of multisensory interaction model using measured values from V2L

(a) Example run of the four-parameter model (see methods) with measured values from NgR -/- (median firing rate = 3.06 Hz, range of modulation: -100% to 500%, number of trials = 20, number of neurons = 84).

(b) Example run of model with measured values from DR (median firing rate = 3.35 Hz, range of modulation: -100% to 500%, number of trials = 20, number of neurons = 105).

(c) Example run of model with measured values from LR (median firing rate = 6.24 Hz, range of modulation: -100% to 500%, number of trials = 20, number of neurons = 104). Despite differences in firing rates, the distributions of the residuals are similar across groups (compare left panels).

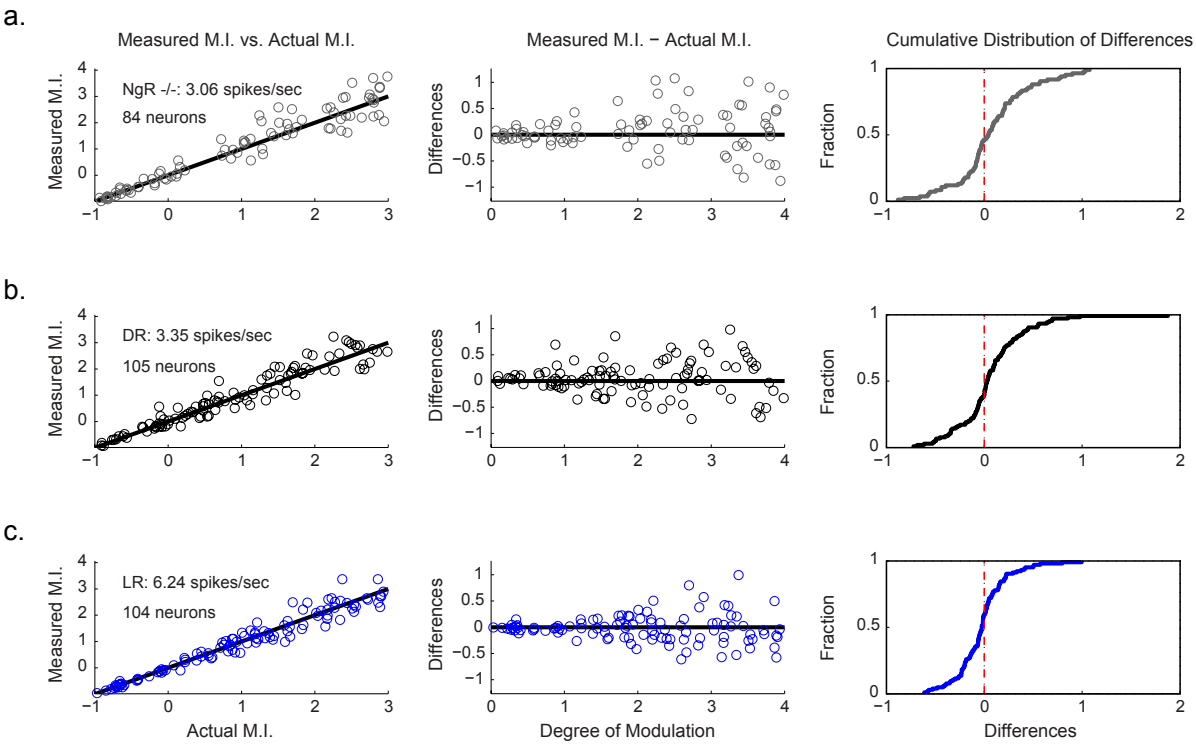

Figure 3.19 (Continued)

Figure 3.20 | Biased multisensory interactions in DR and NgR -/- mice is not due to differences in firing rates

Distributions of the error are not different from each other after running the simulation in figure 3.19 one thousand times (KS test p value 95% CI, DR vs. LR: 0.028 to 0.98, NgR -/- vs. LR: 0.014 to 0.86, $P<0.05$ significant). Similarly, multisensory enhancement is not significantly different between groups (95% CI of medians of positively modulated cells, LR: 0.099 to 0.22, DR: 0.15 to 0.34, NgR -/-: 0.14 to 0.39). Biased multisensory interactions in DR and NgR -/- mice cannot be explained by firing rates alone, their underlying modulation must also be different.

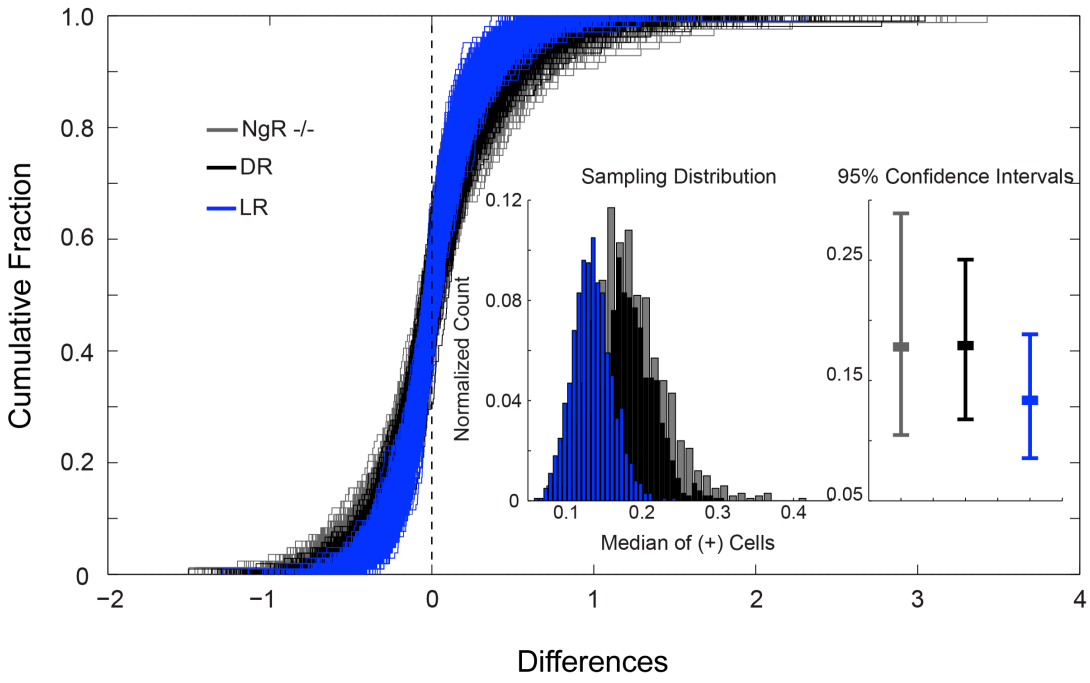

Figure 3.20 (Continued)

Discussion

Here we have established the mouse as a model system for studying cross-modal plasticity. We show that early in development V2L responds strongly to auditory stimuli in an age- and experience-dependent manner. Our anatomical evidence suggests that this phenomenon might be mediated by ectopic input from auditory cortex and auditory thalamus. Interestingly, previous work has suggested a similar transient connection between auditory thalamus and primary somatosensory cortex that is stabilized by whisker removal in rats (Nicolelis et al., 1991).

In synesthesia, stimulation of one sensory system leads to automatic, involuntary experiences in a secondary sensory pathway. One of the leading theories behind this phenomenon is that all juvenile animals go through a normal developmental phase of sensory fusion (Mauer, 2003). We are the first to provide physiological evidence in support of it. Failure to prune low level cross-modal connections despite normal sensory experience might underlie at least one subtype of adult synesthesia where experiences are associated with the outside world (‘projectors’) as opposed to those whose experiences are associated in the ‘mind’s eye’ (‘associators’). Along these lines, studies using diffusion tensor imaging and fMRI have shown increased structural and functional connectivity in people with grapheme-color synesthesia. Hyperconnectivity among early sensory areas was strongest among ‘projectors’ whereas ‘associators’ had increased connectivity in the hippocampus and parahippocampal gyrus (Rouw & Scholte, 2007; Rouw & Scholte, 2010).

This hyperconnectivity early in life provides the basis for a sensitive period of cross-modal plasticity in animals deprived of a sensory system. At the cellular level, we found three distinct mechanisms that control the closure and duration of this period. Myelin based inhibition of axonal sprouting through Nogo receptor signaling and Lynx1-dependent regulation of cholinergic modulation play a role in destabilizing weak cross-modal presynaptic inputs. Postsynaptically, maturation of dendritic spines consolidates the strongest connections, a process that heavily favors intramodal input. Even in the absence of vision, accelerating the sensitive period by targeted disruption of Icam5, a molecule responsible for slowing spinogenesis, reduces cross-modal responses. Together, these signaling pathways bridge functional to structural changes induced by early life experience, consolidating the degree of multimodality in early sensory areas (Fig. 3.21).

Although we focused on hyperconnectivity in lower levels of visual cortex, higher areas can be as well (Saenz et al., 2007; Bedny et al., 2010). Interestingly, patients with Williams Syndrome, a rare genetic form of mental retardation, exhibit visual cortical activity in response to music (Thorton-Wells et al., 2010) and have aberrant levels of white and grey matter in the temporal and frontal cortices (Campbell et al., 2009). Disruption of connectivity in higher brain regions is thought to underlie some neurodevelopmental disorders such as schizophrenia (Zikopoulos & Barbas, 2007) and autism (Müller et al., 2011). Bridging these studies with our current findings, there is increasing evidence of disrupted Nogo receptor signaling in schizophrenia (Schwab, 2010). The Nogo receptor gene is located in a key genetic locus associated with schizophrenia

(Hsu et al., 2007), and several rare sequence variants of NgR in patients with schizophrenia fail to transduce myelin signals of axonal inhibition (Budel et al., 2008).

Both schizophrenics and people with restored vision have disruptions in multisensory integration. They exhibit impairments in lip reading and audio-visual speech tasks (De Gelder et al., 2003; Putzar et al., 2010). Schizophrenics were also found to have reduced multisensory facilitation compared to controls, a deficit that was particularly pronounced in those suffering both auditory and visual hallucinations (Williams et al., 2010). However, a more recent study found the opposite effect. Furthermore, they also found an increase in multisensory facilitation along the temporal and occipital cortices as measured by EEG (Stone et al., 2011). The most likely explanation for this discrepancy is that there were differences in unisensory processing between the two groups. In accordance with these studies, we found differences in multisensory interactions between DR, NgR -/-, and LR mice. Both DR and NgR -/- have a similar facilitation of multisensory enhancement compared to LR. Further studies are necessary to see if this specific strengthening leads to similar alterations in multisensory integration behavior seen in schizophrenics or people with restored vision.

Our work provides a model of how cross-modal inputs into early sensory areas are pruned or retained dependent on normal sensory experience and neurological function. We provide molecular targets that can facilitate or suppress this process with the hope that they will shape future rehabilitation strategies in sensory restoration or cognitive impairment.

Figure 3.21 | Summary schematic of cross-modal refinement by visual experience in V2L

Secondary visual cortex is initially multimodal, receiving projections from primary visual cortex, auditory cortex, and auditory thalamus (top panel). With normal visual experience, there is an increase in Nogo receptor and Lynx1 signaling that leads to a destabilization of weak presynaptic cross-modal input. Around the same time, Icam5 signaling is regulated, promoting the maturation of spines receiving strong within modality input (middle panel). In adulthood, thalamocortical cross-modal connections are absent and only weak intracortical ones remain (bottom panel).

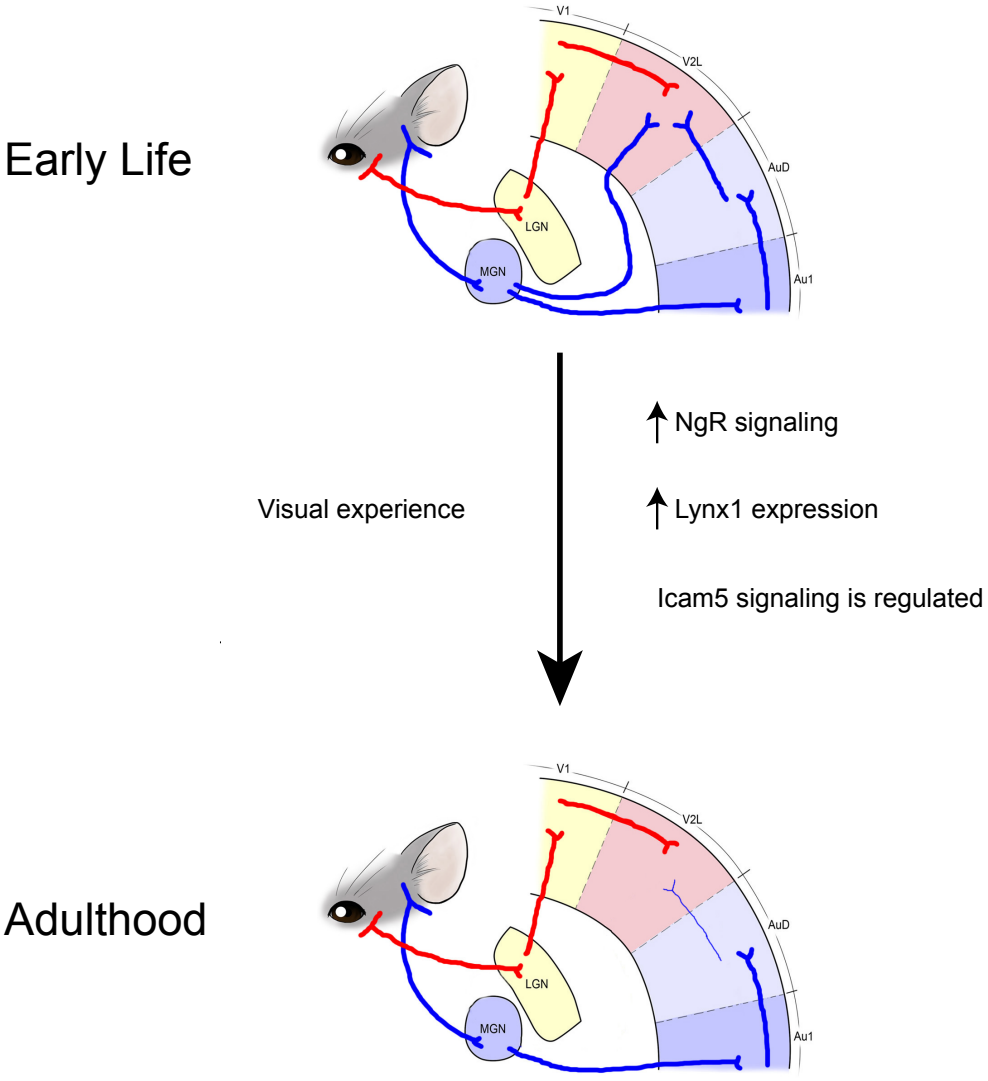

Figure 3.21 (Continued)

Chapter 4

Two Mechanisms Affecting Cross-Modal Influence in Primary Visual Cortex

Author Contributions

Daniel Brady, Michela Fagiolini, and Takao Hensch designed the experiments; DB performed the experiments; DB, MF, and TH analyzed the data and wrote the paper.

Summary

Recent work suggests that regions of the brain traditionally thought of as unisensory can be influenced by other modalities. The degree of this 'cross-modal' modulation is dependent on early life experience. Until now, the mechanisms underlying this process were unknown. During experiments to record multisensory interactions in V2L by extracellular single-unit electrodes, we first measured cross-modal influence in primary visual cortex (V1). We describe two circuit and signaling pathways responsible for experience dependent auditory influence in V1. We show that Nogo receptor (NgR) signaling affects the range of modulation and the distribution of unimodal and multimodal cells. The maturation of inhibitory circuits affects whether this input is facilitative or suppressive. In conclusion, we provide the first evidence of molecular mechanisms involved in cross-modal influence of primary sensory areas.

Introduction

It is rare in normal everyday experience that we rely exclusively on one sensory modality. Combining visual and auditory stimuli can drastically alter spatial and categorical perception, leading to well-known illusions such as ventriloquism (Alais & Burr, 2004) and the McGurk effect (McGurk & MacDonald, 1976). Furthermore, information from two or more sensory modalities can improve an animal's perceptually guided behavior, facilitating object localization and reducing reaction times (Stein & Meredith, 1990).

For many years, sensory information was believed to be processed in the cortex in dedicated unisensory regions first and only later combined at higher multimodal centers. Much recent work has suggested that this is not the case; even early 'unisensory' areas can be modulated by cross-modal stimuli (Kayser & Logothetis, 2007; Musacchia & Schroeder, 2009). For example, somatosensory stimuli have been shown to elicit single and multiunit responses in early auditory cortices (Brosch et al., 2005) and bimodal stimuli can reset oscillations in primary auditory cortex (Lakatos et al., 2007). Along similar lines, neurons in somatosensory cortex can respond to visual stimuli during a haptic task (Zhou & Fuster, 2000) and rodent primary visual cortex (V1) can participate in information processing during whisker-based exploration of objects (Vasconcelos et al., 2011). These studies comprise part of a growing body of work suggesting that most of the neocortex might be multisensory (Ghazanfar & Schroeder, 2006).

The role of developmental experience in the processing of early cortical multisensory interactions remains poorly understood. The first and only study of this topic showed that the facilitation of auditory-tactile stimulation in primary somatosensory cortex is indeed dependent on the rearing environment, with the strongest effects occurring for animals both whisker-deprived and click-reared (Ghoshal et al., 2011). Whether similar differences in multisensory interactions occur in V1 is unclear. Furthermore, the circuit and molecular mechanisms that underlie this process are unknown. To address these issues, we compared multisensory interactions in mice raised in a normal light environment to those that were visually deprived from birth. We followed this with the use of genetically modified animals to probe the contribution of several signaling pathways responsible for these differences. Altogether, our results provide evidence for some of the molecular mechanisms that underlie cross-modal influence in primary visual cortex and provide a framework for understanding how early cortical areas process multisensory information.

Results

Range and sign of cross-modal modulation is dependent on visual experience

To see if V1 is modulated by other sensory modalities in an experience-dependent manner, we used single-unit extracellular recordings to compare multisensory interactions (M.I.) in anesthetized adult C57BL/6 mice reared in complete darkness from birth (DR) or a normal 12-hour light/dark cycle (LR). M.I. was measured as the percent change in the visually evoked firing rate after introducing a cross-modal stimulus. We found that while V1 visual responses in LR were relatively static, they could be greatly modulated by sound in DR (Fig. 4.1a & b). Thus, the range of modulation differed between the two groups (Fig. 4.1c; Fig. 4.2c).

In addition to the range of modulation, we found that the ratio of enhanced to suppressed cells was different between LR and DR (Fig. 4.1c; Fig. 4.3d). In LR, most cells were suppressed by sound ($P = 0.0063$, one-tailed binomial test); in DR, the opposite was true ($P = 0.00059$, one-tailed binomial test). Thus, visual experience affects cross-modal influence of V1 in two ways: it dramatically reduces the range of modulation by auditory stimuli and inverts the sign of input from excitatory to inhibitory.

NgR signaling affects the range of cross-modal modulation and the maturation of inhibitory circuits affects its sign

To understand what mechanisms underlie these two properties, we examined several circuit and signaling pathways that are affected by dark-

Figure 4.1 | Greater range and +/- ratio of multisensory interactions in primary visual cortex (V1) of dark-reared mice

(a) Raster plot and peristimulus time histogram (PSTH, 25 ms bins) for a V1 visual cell in an anesthetized C57BL/6 adult mouse (>P60) reared in a normal 12hr light/dark cycle (LR). Trials are divided into the different stimulus conditions: visual (yellow), auditory (blue), visual + auditory (red), and blank (white). Responses to visual and combined stimuli are nearly identical. Bold and dotted black lines indicate when the stimulus turned on and off respectively. The blue dotted line in the PSTH is the blank response.

(b) Raster plot and PSTH for a V1 visual cell in an adult mouse reared in 24hr of darkness (DR). The visual + auditory response is much stronger than to just visual alone.

(c) The cumulative distribution functions (CDFs) of multisensory interaction are significantly different in LR (n=127) and DR (n=118) animals (LR: -65.0 to 66.7%, DR: -95.2 to 350%; *P<0.001 KS test). Fitting the two distributions with Gaussian functions (inset) highlights the differences in both range (spread) and ratio of positively to negatively modulated cells (centers, dotted lines).

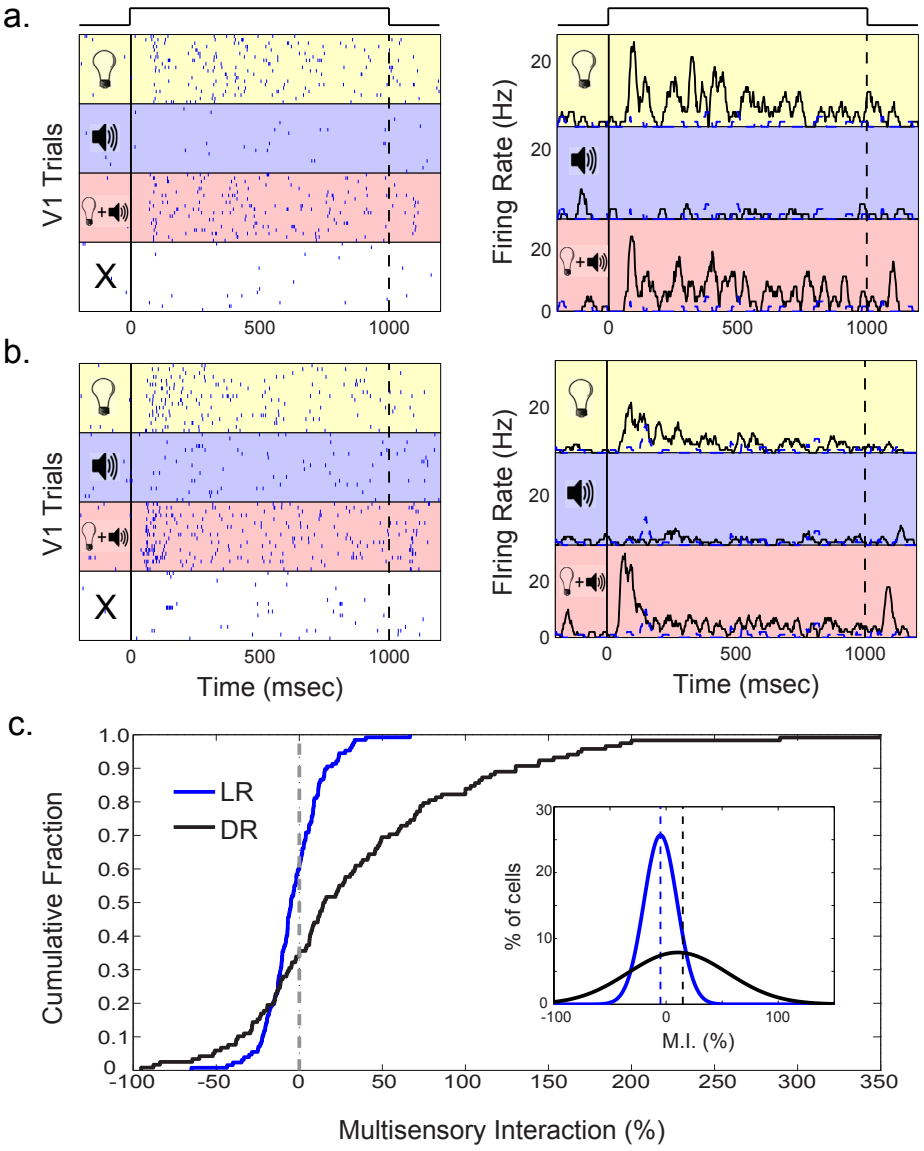

Figure 4.1 (Continued)

Figure 4.2 | NgR signaling affects the range and inhibitory circuits affects the +/- ratio of multisensory interactions in V1

(a) CDFs are significantly different from each other in adult LR wild-type (n=127) and NgR -/- (n=71) mice (*P<0.001, two-sample Kolmogorov-Smirnoff test). Fitted Gaussian functions (inset) illustrate similar +/- ratios (centers, dotted lines), but different ranges of modulation (spread).

(b) CDFs are significantly different from each other in adult LR wild-type (n=127) and Gad65 -/- (n=66) mice (*P=0.003, two-sample Kolmogorov-Smirnoff test). Fitted Gaussian functions (inset) illustrate similar ranges of modulation (spread), but different +/- ratios (centers, dotted lines).

(c) The range of modulation (mean ± s.d.) of DR and NgR -/- mice is significantly higher than LR and Gad65 -/- as measured by bootstrapping (interquartile range 95% confidence intervals, LR: 16.2 to 25.2, DR: 63.8 to 113, NgR -/-: 41.1 to 73.4, Gad65 -/-: 16.8 to 38.5, NR2A -/-: 23.5 to 44.4, 100,000 iterations).

(d) The +/- ratio (mean ± s.d.) of DR and Gad65 -/- mice is significantly higher than LR as measured by bootstrapping (+/- ratio 95% confidence intervals, LR: 0.448 to 0.923, DR: 1.29 to 2.83, NgR -/-: 0.628 to 1.59, Gad65 -/-: 1.03 to 2.88, NR2A -/-: 0.396 to 1.06, 100,000 iterations).

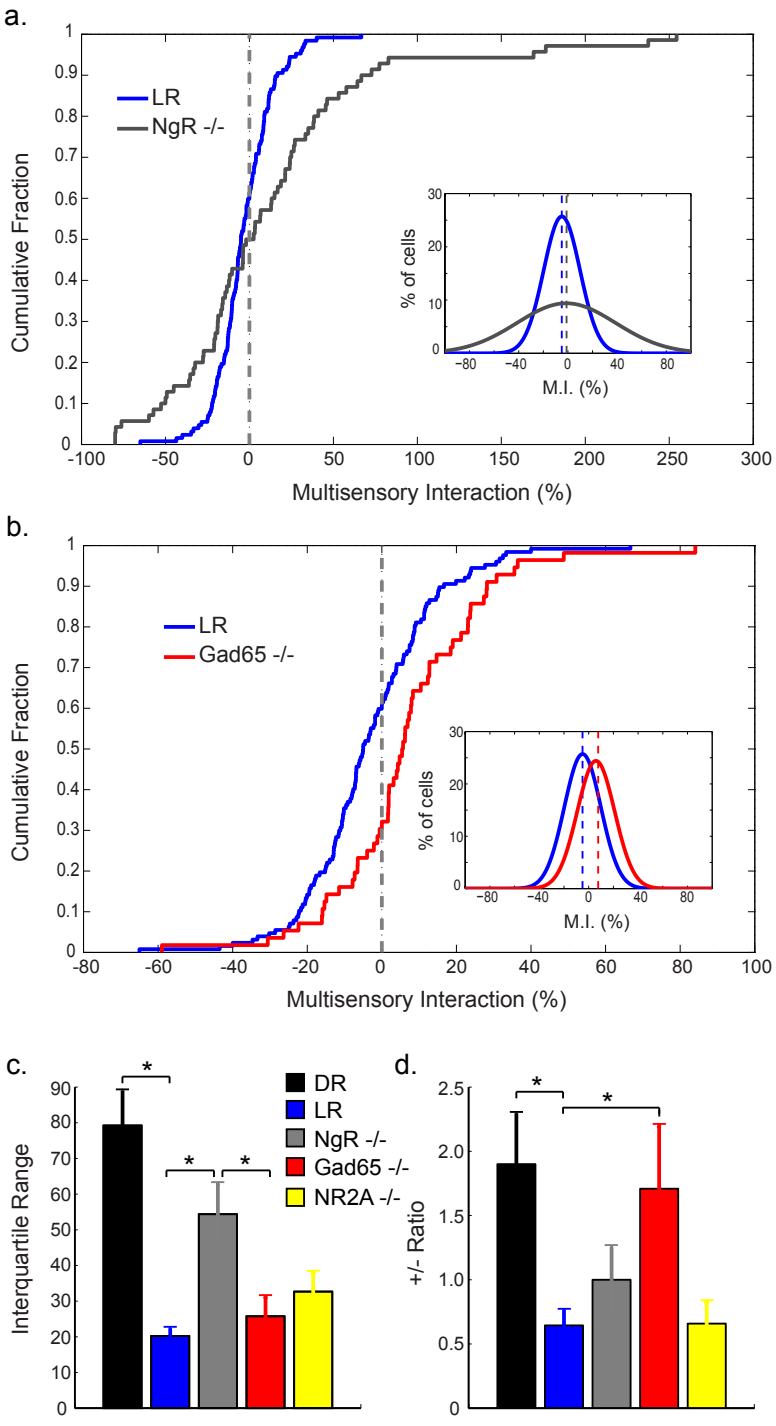

Figure 4.2 (Continued)

rearing. Previous work has shown that inhibitory circuits (Katagiri et al., 2007; Sugiyama et al., 2008) and myelination (Morishita et al., in preparation) is experience-dependent and delayed by dark-rearing. Furthermore, myelination can inhibit axonal sprouting through Nogo receptor signaling (Schwab 2010), a signaling cascade that is crucial in closing the window of ocular dominance plasticity (McGee et al., 2005). Interestingly, we found that cross-modal influence in V1 is affected in light-reared mice with either disrupted Nogo receptor signaling (NgR -/-) or immature inhibitory circuits (Gad65 -/-).

In NgR -/- mice, the range of modulation was much greater than LR and Gad65 -/- despite normal visual experience (Fig. 4.2a; Fig. 4.2c). The ratio of enhanced to suppressed cells, however, was similar to LR (Fig. 4.2a; Fig. 4.2d). In contrast, Gad65 -/- had a similar range of modulation to LR (Fig. 4.2b; Fig. 4.2c) but a larger ratio of enhanced to suppressed cells (Fig. 4.2b; Fig. 4.2d). Thus, NgR signaling affects the range of cross-modal influence in V1 and the maturation of inhibitory circuits affects whether this input will be excitatory or inhibitory.

To determine the specificity of these two signaling pathways in controlling multisensory interactions in V1, we looked at another group of genetically engineered mice with properties similar to DR animals. NR2A, a subunit of the N-methyl D-aspartate receptor (NMDA), increases in expression relative to NR2B over development in an experience-dependent manner. Visually deprived mice maintain low expression of NR2A, which enhances excitation (Carmignoto &

Vicini, 1992; Quinlan et al., 1999). We found that NR2A -/- raised in a normal light environment have a similar range of modulation and ratio of enhanced to suppressed cells to LR (Fig. 4.2c & d).

To ensure that the differences in multisensory interactions we found were not due to relative firing rates (Ponce et al. 2008; Kuhlman et al. 2011), we created a four-parameter bootstrap model (for further explanation refer to Chapter 2) that could predict the amount of M.I. bias we should expect given the firing rates, number of trials, number of neurons, and range of modulation recorded in V1 (Fig. 4.4). Our model assumed that V1 neurons were Poisson processes. We calculated the 95% confidence intervals within which a neuron can be deemed a Poisson process given that the expected distribution of the Fano factor is a gamma distribution whose shape is dependent on the number of trials (Eden & Kramer, 2010) (Fig. 4.3a). We found that the majority of V1 neurons in all animals examined fell within these limits (Fig. 4.3b-e), and that this did not change with the introduction of a cross-modal stimulus (Fig. 4.3b-e inset). By running our model through 1000 iterations to create 95% confidence intervals for the statistics that were significantly different between groups, we found that the bias in multisensory interactions measured could not be explained by relative firing rates alone (Fig. 4.5a & b). Thus, the experience dependent maturation of myelination and inhibitory circuits affects cross-modal influence in V1.

Figure 4.3 | Majority of V1 neurons in LR, DR, NgR -/-, and Gad65 -/- mice are Poisson processes.

(a) Gamma function of the expected distribution of Fano factors for a Poisson process with 20 trials. Blue dotted lines indicate the upper (1.729) and lower (0.4688) limits of the 95% confidence interval of the distribution. Cells with a Fano factor outside of these limits are not Poisson processes.

(b) CDF of Fano factors for all cells recorded in LR V1 (n=127) to the strongest single modality stimulus (SM, blue) or combined stimuli (CM, red). The majority of neurons behave in a Poisson manner whether responding to one (84%) or multiple stimuli (79%, light grey bar). Fano factors (mean ± s.e.m.) are not significantly different between SM and CM conditions (P=0.16, Mann-Whitney test).

(c) CDF of Fano factors for all cells recorded in DR V1 (n=118). The majority of neurons behave in a Poisson manner whether responding to one (61%) or multiple stimuli (68%, light grey bar). Fano factors (mean ± s.e.m.) are not significantly different between SM and CM conditions (P=0.070, Mann-Whitney test).

(d) CDF of Fano factors for all cells recorded in NgR -/- V1 (n=71). The majority of neurons behave in a Poisson manner whether responding to one (72%) or multiple stimuli (76%, light grey bar). Fano factors (mean ± s.e.m.) are not significantly different between SM and CM conditions (P=0.34, Mann-Whitney test).

(d) CDF of Fano factors for all cells recorded in Gad65 -/- V1 (n=66). The majority of neurons behave in a Poisson manner whether responding to one (70%) or multiple stimuli (79%, light grey bar). Fano factors (mean ± s.e.m.) are not significantly different between SM and CM conditions (P=0.23, Mann-Whitney test).

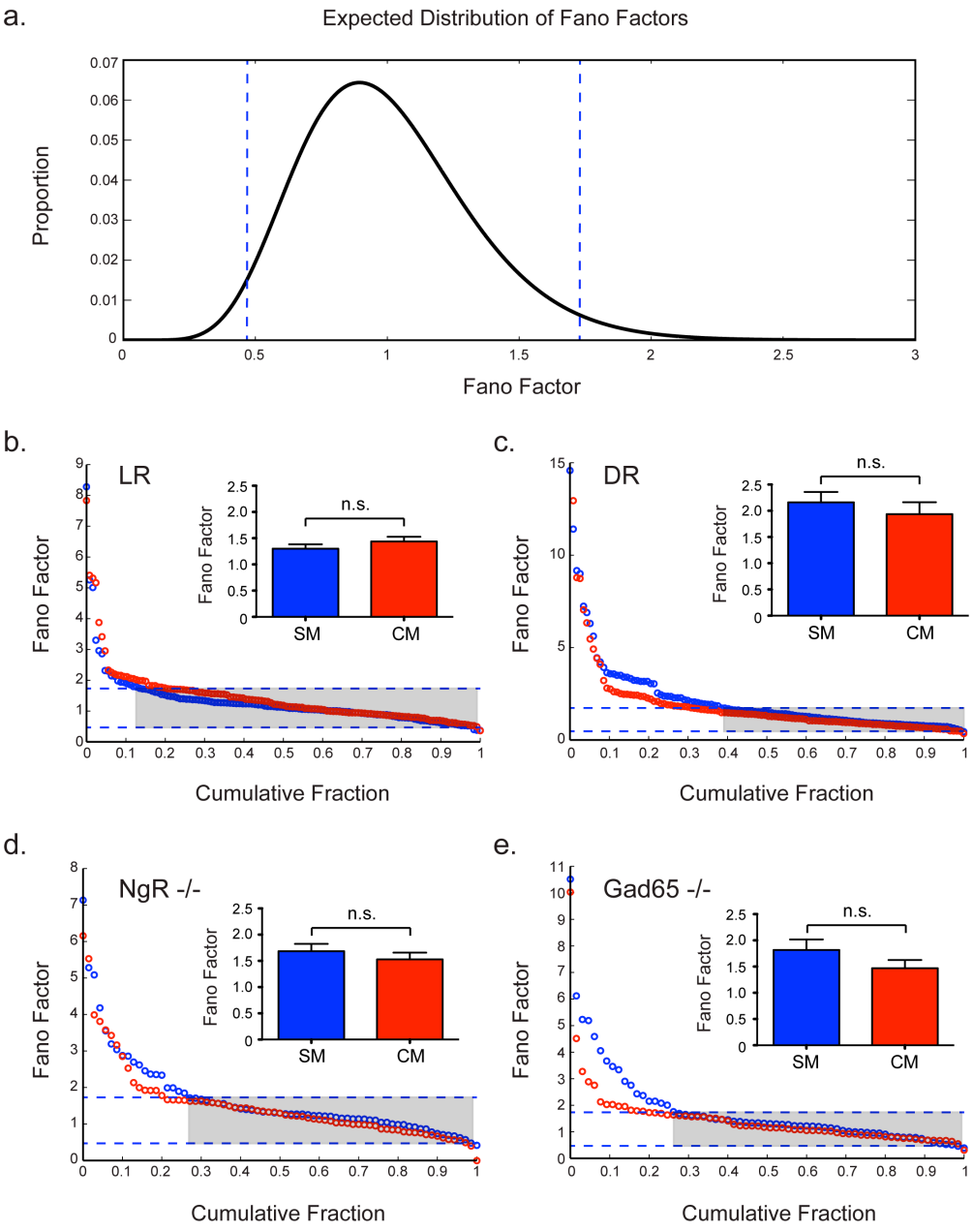

Figure 4.3 (Continued)

Figure 4.4 | Example simulation of multisensory interaction model using measured values from V1

(a) Example run of the four-parameter model (see methods) with measured values from NgR -/- (median firing rate = 3.02 Hz, range of modulation: -100% to 300%, number of trials = 20, number of neurons = 71).

(b) Example run of model with measured values from DR (median firing rate = 5.62 Hz, range of modulation: -100% to 300%, number of trials = 20, number of neurons = 118).

(c) Example run of model with measured values from LR (median firing rate = 9.95 Hz, range of modulation: -100% to 300%, number of trials = 20, number of neurons = 127).

(d) Example run of model with measured values from Gad65 -/- (median firing rate = 10.2 Hz, range of modulation: -100% to 300%, number of trials = 20, number of neurons = 66). Despite differences in firing rates, the distributions of the residuals are similar across groups (compare left panels).

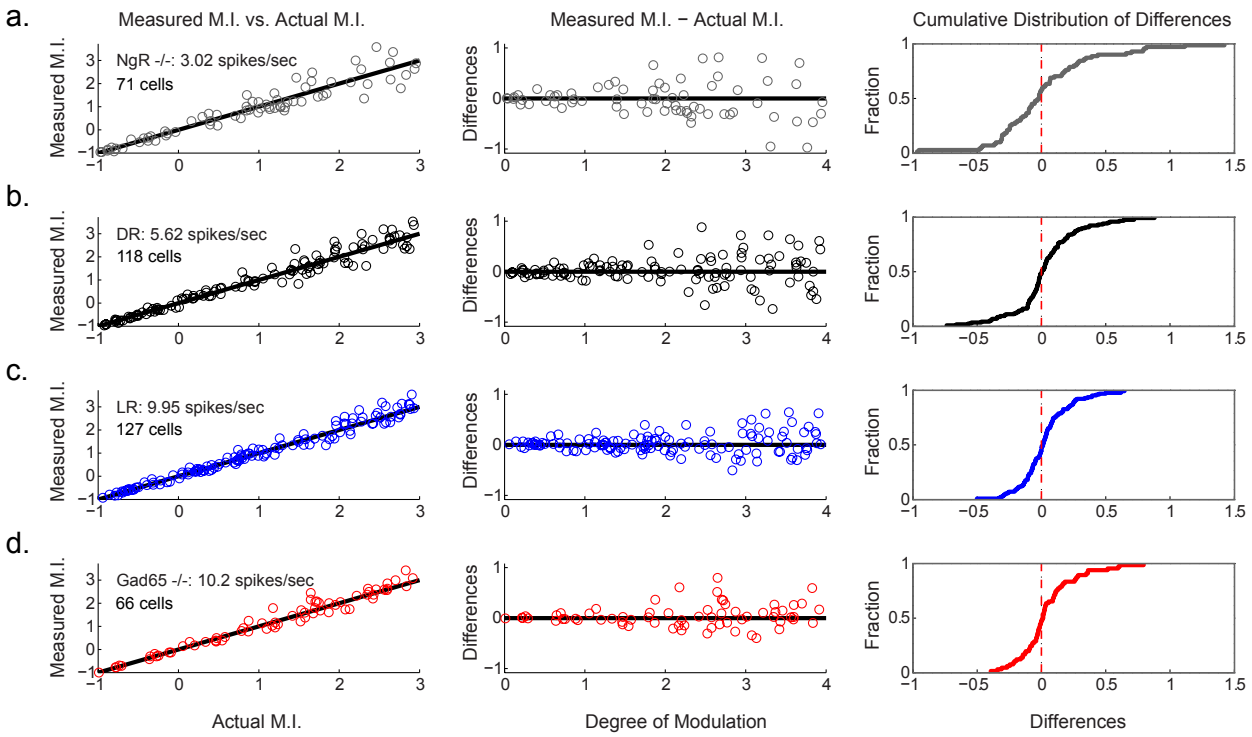

Figure 4.4 (Continued)

Figure 4.5 | Differences in multisensory interactions between DR, LR, NgR -/-, and Gad65 -/- mice are not due to relative firing rates

(a) Distributions of the differences are not different from each other after running the simulation in figure 4.4 one thousand times (KS test p value 95% CI, NgR -/- vs. LR: 0.0023 to 0.52, DR vs. LR: 0.0067 to 0.72, Gad65 -/- vs. LR: 0.018 to 0.97, $P<0.05$ significant). Similarly, the interquartile ranges are not significantly different between groups (95% CI, NgR -/-: 0.34 to 0.90, DR: 0.28 to 0.61, LR: 0.20 to 0.40, Gad65 -/-: 0.16 to 0.46). Differences in the range of modulation cannot be explained by firing rates alone.

(b) The +/- ratio is similar across all groups (95% CI, NgR -/-: 0.65 to 1.6, DR: 0.69 to 1.4, LR: 0.71 to 1.4, Gad65 -/-: 0.61 to 1.6). Differences in the +/- ratio cannot be explained by firing rates alone.

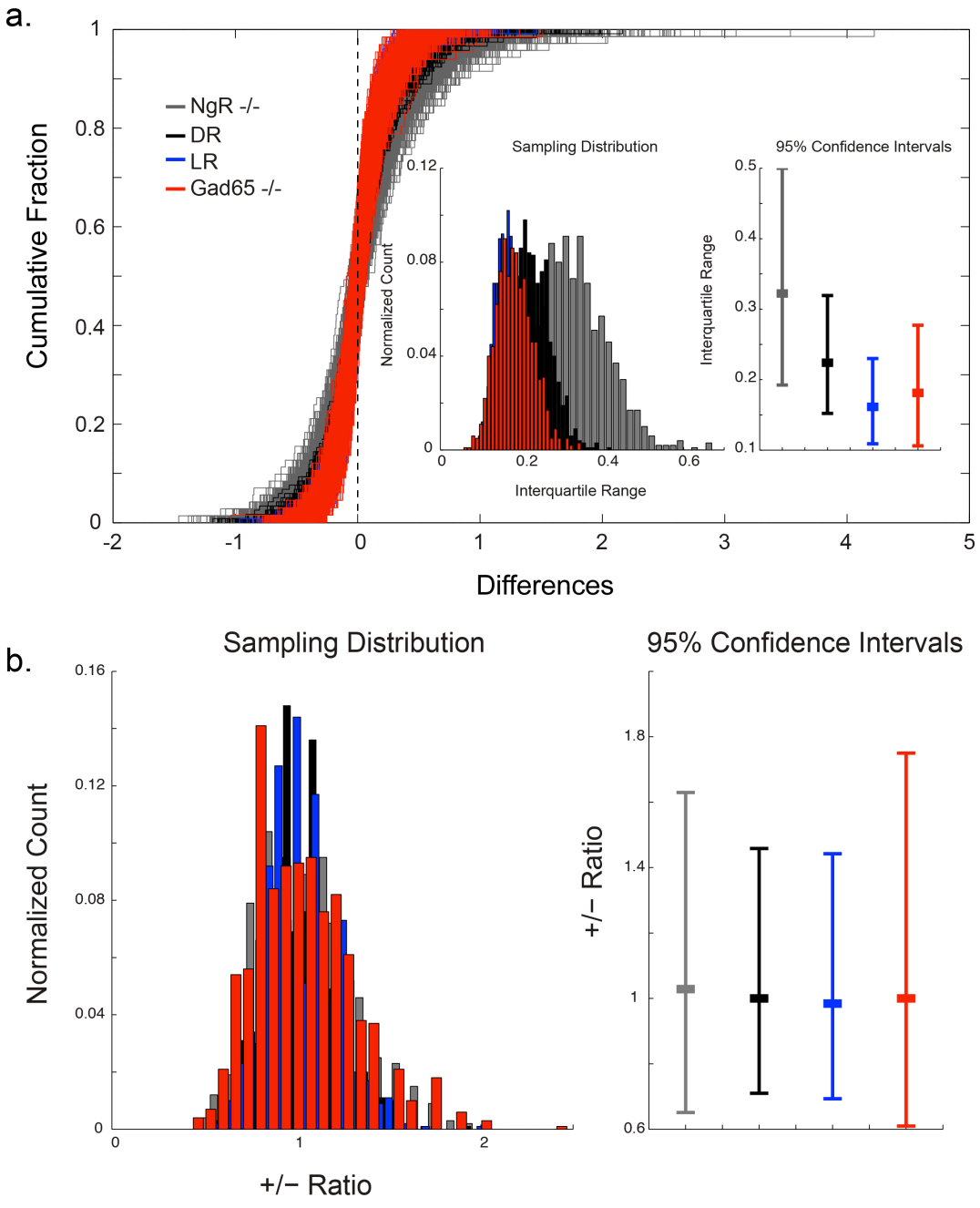

Figure 4.5 (Continued)

NgR signaling affects the distribution of uni- and multimodal cells

In addition to differences in multisensory interactions, we found that there were significantly more auditory responsive cells in DR than LR. The vast majority of neurons in LR V1 were visual (85%), with a few multimodal (6%), no auditory, and a small number of unresponsive cells (9%). In the DR, there were fewer visual cells (64%), with more multimodal (21%), auditory (2%), and unresponsive (13%) ones. To see what circuit or signaling pathway was responsible for this difference, we compared the distribution of cell types in NgR -/- and Gad65 -/-. We found that NgR signaling affected cell type, as NgR -/- had a similar distribution (visual: 53%, multimodal: 29%, auditory: 4%, unresponsive: 14%) to DR while Gad65 -/- had a similar distribution (visual: 90%, multimodal: 2%, auditory: 0%, unresponsive: 8%) to LR despite both being reared in a normal light environment (Fig. 4.6). Thus, similar to secondary visual cortex (see Chapter 3), NgR signaling affects the distribution of unimodal and multimodal cells in primary visual cortex.

Figure 4.6 | Higher percentages of auditory responsive cells in DR and NgR -/- mice

The distribution of visual (yellow), auditory (blue), multimodal (red), and unresponsive (white) cells in V1 of DR (n=137) and NgR -/- (n=83) indicate a significantly larger proportion of cells that respond to auditory stimuli than in LR (n=139) or Gad65 -/- (n=70, *P<0.0001, χ^2 test).

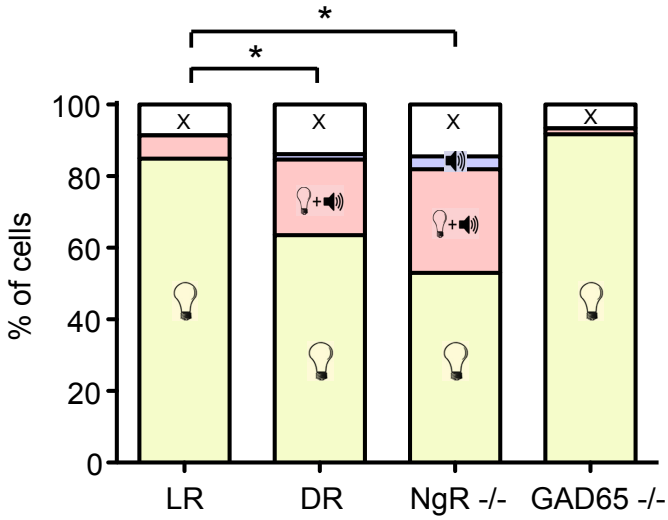

Figure 4.6 (Continued)

Discussion

Our results show that cross-modal influence in primary visual cortex can be modulated by early life experience. We found that multisensory interactions were significantly different between LR and DR in two ways: the range of modulation and the ratio of enhanced to suppressed cells. In DR, cells could be strongly negatively or positively modulated after the addition of a cross-modal stimulus; overall, there were twice as many cells that underwent multisensory enhancement. In contrast, neurons in LR had a much smaller range of modulation and the majority of them were suppressed by sound. In addition, we found that there were significantly more cells that responded to auditory stimuli in DR.

We provide evidence for two circuit and signaling pathways that underlie these differences. NgR signaling affects the distribution of visual, multimodal, and auditory cell types and the range of cross-modal influence in primary visual cortex. In contrast, the maturation of inhibitory circuits affects whether this input is excitatory or inhibitory. NgR signaling is involved in the myelin-based inhibition of axonal sprouting (Schwab, 2010) and evidence from our lab suggests that NgR -/- exhibit hyperconnectivity both within and across sensory domains (Min et al., in preparation). Much work has shown that inhibition gradually increases throughout development in an experience-dependent manner (Hensch, 2005). With these two features in mind, we propose a model in which V1 receives a large amount of cross-modal input early in life. Individual neurons can be innervated by a large or small amount (in terms of strength or number) of cross-

modal connections. In the absence of vision, these connections are not pruned by NgR signaling, giving rise to a large range of modulation and diversity of cell types. Normal visual experience also gradual strengthens inhibition, ultimately inverting cross-modal influence from being largely facilitative to suppressive (Fig. 4.7).

Although the precise nature of multisensory processing in early sensory cortices is unclear, disrupting cross-modal input into primary and secondary areas can dramatically alter perceptually guided behavior (Romei et al., 2007; Hirokawa et al., 2008). Abnormal multisensory integration has been reported in several neurodevelopmental disorders, such as schizophrenia and autism. Schizophrenics exhibit reduced multisensory integration compared to controls (De Gelder et al., 2003; Williams et al., 2010), although some studies have found the opposite (Stone et al., 2011). There is increasing evidence that NgR signaling is disrupted in schizophrenia (Budel et al., 2008), which might contribute to the abnormal structural connectivity seen in patients suffering from the disorder (Kubicki et al., 2007; Konrad & Winterer, 2008). Similarly, autistic children have impaired multisensory integration (Magnee et al., 2011) and connectivity within and across brain regions (Minshew & Williams, 2007; Wass, 2011). In addition to structural differences, an imbalance between excitation and inhibition in prefrontal cortex is believed to contribute to social dysfunction in both disorders (Yizhar et al., 2011). It is possible that similar disruptions in NgR signaling and E/I balance restricted to early sensory areas might underlie the deficits seen in multisensory integration of people with restored vision (Putzar et al., 2007) or

hearing later in life (Schorr et al., 2005). Future experiments are necessary to determine how the mechanisms we found shape multisensory behavior. Overall, our results provide a model of how cross-modal influence into primary sensory areas is regulated by early life experience.

Figure 4.7 | Summary model of mechanisms underlying cross-modal influence in V1

In DR, there are a large number of cross-modal inputs into V1. The diversity in strength and number of connections gives rise to a large range of modulation and a higher proportion of auditory responsive cells. Most of this input is excitatory. Increasing NgR signaling reduces the number of cross-modal inputs, clamping down the range of modulation. The maturation of inhibitory circuits shifts the E/I balance of inputs towards inhibition. Together, these two signaling pathways give rise to the narrow range of modulation slightly favoring suppression seen in LR mice.

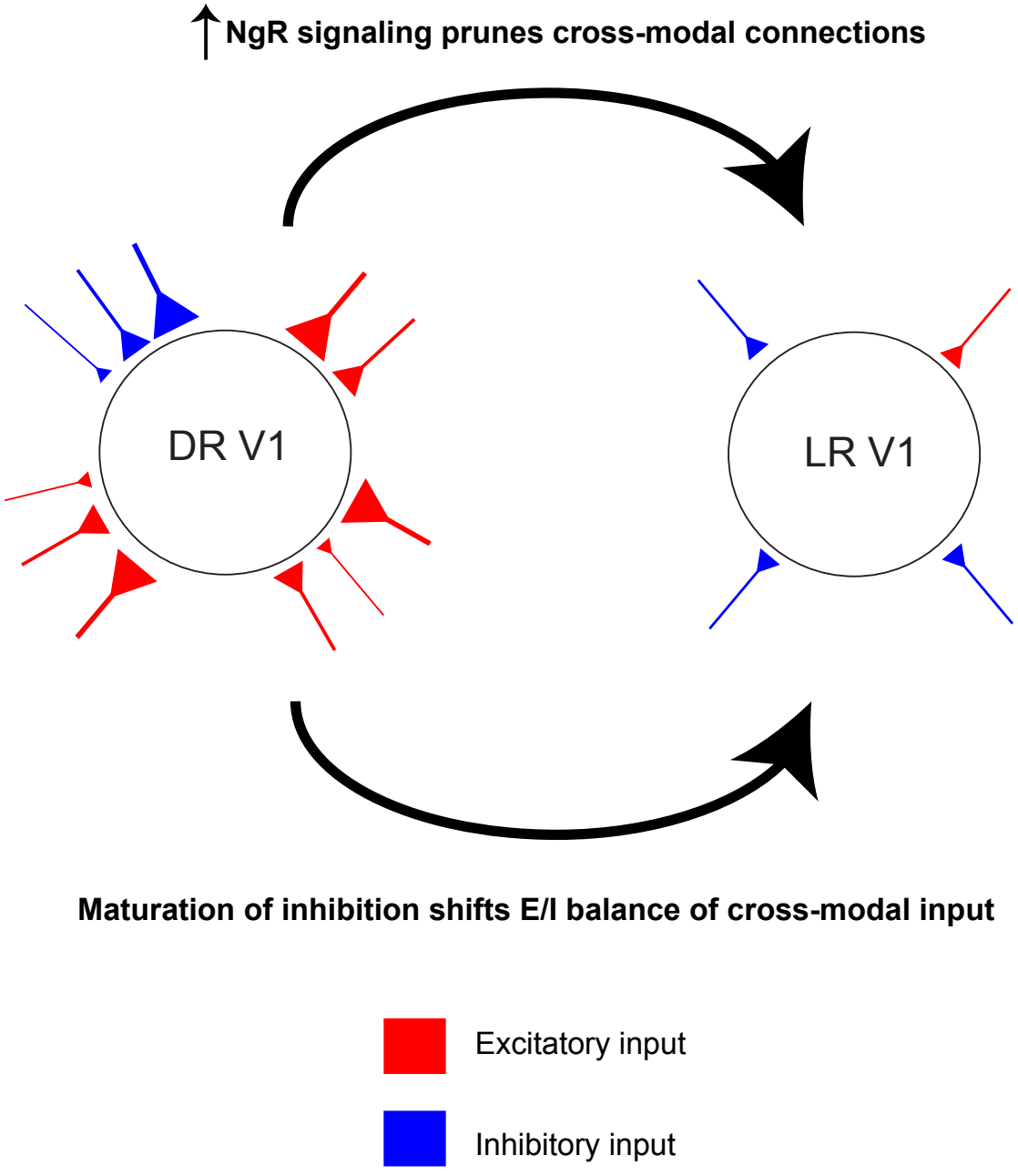

Figure 4.7 (Continued)

Chapter 5

Discussion

Loss of a sensory system early in life has a profound effect on the organization and processing in the remaining modalities. It was the goal of this thesis to understand the anatomical, circuit, and molecular mechanisms underlying this form of 'cross-modal' plasticity. My work has led to two main findings. First, occipital cortex is initially multimodal early in life. Second, many of the circuit and signaling pathways involved in other forms of plasticity control cross-modal influence in primary and secondary visual cortices.

Reorganization after loss of vision in secondary visual cortex

Our first goal was to establish the C57BL/6 strain of the mouse as a model system for studying cross-modal plasticity. Previous mouse models were engineered to be anophthalmic (Chabot et al., 2008) or congenitally deaf (Hunt et al., 2005), so vision or hearing could not be restored in these animals. To determine whether cross-modal plasticity occurs in our strain, we compared intrinsic riboflavin fluorescence responses over the entire surface of visual cortex in anesthetized adults reared in complete darkness from birth (DR) or in a normal 12-hour light/dark cycle (LR). We found that secondary visual cortex (V2L) responded strongly to sound in DR but not in LR.

We next examined the influence of age at visual deprivation and showed that there is a sensitive period for cross-modal plasticity in mouse visual cortex that begins one week after eye opening and gradually weakens until adulthood. This is considerably later than plasticity within a sensory domain. Acuity, orientation selectivity, and ocular dominance become functionally mature between P20 and P30. Auditory cortex matures even earlier, with a critical period for thalamocortical connectivity between P12 and P15. A late cross-modal sensitive period may be advantageous, as it would allow early visual and auditory cortices to become fully functional before losing their multimodality.

It is interesting to note that cross-modal responses can be induced after long-term blindfolding in adult humans (Merabet et al., 2008). The main difference between this study and ours is that the human subjects were intensively trained in tactile discrimination tasks while being visually deprived. It is likely that weak cross-modal connections in sighted humans were temporarily strengthened. It would be interesting to see if immersion in an enriched auditory or somatosensory environment could facilitate cross-modal responses in mice placed into the darkness as adults. Previous work has suggested that the degree of cross-modal takeover of visual cortex can be influenced by rearing conditions (Piché et al., 2004).

Almost all previous studies used a permanent form of deprivation (Karlen et al., 2006; Meredith & Lomber, 2011). The few that did not failed to examine cortical responses after exposure to a normal sensory environment (Rauschecker & Korte, 1993; Yaka et al., 1999). This work is the first to show

that adult mice dark-reared from birth but later exposed to a normal light environment for 2-3 weeks had a reduction in V2L auditory responses to typical LR levels, implying that cross-modal reorganization is not permanent. This has profound implications for sensory restoration later in life. Interestingly, auditory inputs to visual cortex remain in dark-reared animals even after exposure to a normal light environment for over a month (Min et al., in preparation).

Similar to previous findings (Yaka et al., 2000), individual neurons in DR V2L responded to sound. We found that auditory responses were faster than visual ones, leading us to wonder about the origin of this cross-modal input. To determine how auditory information reaches visual cortex, we injected retrograde tracers into V2L. We found many more labeled cell bodies in the auditory cortex of DR animals. We also provide the first evidence for direct projections between auditory thalamus and V2L in DR. These connections were absent in LR adults. Our results support previous theories about increased intracortical connectivity after sensory deprivation (Klinge et al., 2010) and extend them by adding a thalamocortical component. In the future, we are planning experiments to temporally inactivate auditory thalamus and auditory cortex while monitoring V2L responses to establish a causal link between hyperconnectivity and multimodality in visual cortex.

Riboflavin imaging (Chapter 3) and anatomical experiments (Min et al., in preparation) show that juvenile occipital cortex is multimodal from birth. Taken together, we report the first physiological and anatomical evidence to support the hypothesis that early sensory areas are hyperconnected, and that with normal

experience, sensory regions become dedicated to processing mainly one modality. This idea, termed the neonatal synethesia hypothesis, is based upon human studies suggesting that there is increased cross-modal transfer in infants (Maurer, 2002).

Since auditory activity in V2L is a hallmark of a juvenile brain, we examined several circuit and signaling pathways that are kept immature in DR animals. We found that mice with disrupted Nogo receptor signaling, which is crucial for myelin-based inhibition of axonal sprouting (Schwab, 2010), retained a juvenile response. We believe that with normal light experience, coherent visual input strengthens within modality connections at the expense of cross-modal ones. As myelination and NgR signaling increase across development, this weak input is selectively pruned. It remains to be seen if disruption of NgR signaling later in life can reactivate cross-modal plasticity by promoting axonal outgrowth from remaining intermodal connections.

Interestingly, the maturation of inhibitory and excitatory circuits did not affect our metrics of cross-modal plasticity in V2L. Previous work has shown that inhibitory circuits, specifically Parvalbumin-postive large basket (PV) cells, control the timing of ocular dominance plasticity (Hensch et al., 1998b; Fagiolini & Hensch, 2000; Fagiolini et al., 2004). Excitatory circuit maturation, on the other hand, is necessary for the development of orientation selectivity (Fagiolini et al., 2003). There are several reasons that might underlie the discrepancy between these results and our current findings. First, it may be that inhibitory and excitatory circuits are responsible for the experience-dependent maturation of

cross-modal receptive field properties different from the ones we measured. Our stimuli explored only a small portion of the possible receptive field space. Future work is necessary to provide a more detailed picture of how these neurons respond to a diverse range of sensory stimuli. Inhibitory and excitatory circuits may control higher properties such as direction selectivity, velocity selectivity, or the precise size and spatial organization of V2L.

A second hypothesis is that cross-modal input into V2L follows fundamentally different connectivity principles than other visual or auditory receptive field properties. PV cells have organized long-range projections that span ocular dominance columns in higher mammals, which is useful for discriminating input between the two eyes (Hensch & Stryker, 2004). In contrast, we found little organization of cross-modal inputs in V2L. Individual neurons responded to sound across all layers as measured by both c-Fos immunoreactivity and extracellular single-unit recordings. Also, retrograde tracer injections labeled cell bodies throughout all layers of auditory cortex. This lack of specificity might explain why we only found an experience-dependent reliance on signaling pathways involved in anatomical reorganization and not local circuit computations in cross-modal plasticity.

We also show that disrupting Lynx1 signaling from birth made animals retain cross-modal responses throughout life. Lynx1, a neuronal membrane molecule whose expression increases over development, binds to and reduces the sensitivity of nicotinic acetylcholine receptors (Ibañez-Tallon et al., 2002). Cholinergic modulation through the nucleus basalis is critical in regulating the

attentional and arousal state of an animal (Gu, 2002), and can alter the balance of excitation and inhibition (Lucas-Meiner et al., 2009). We believe that sustained cholinergic activity in deprived cortices enhances excitation in that region, allowing for the improved processing of information from different modalities.

Finally, we found that while the acceleration of spine maturation by targeted-deletion of Icam5 leads to a similar age-dependent refinement of cross-modal responses to LR wild-types, it is independent of sensory experience. Current experiments are underway to see if the window for plasticity is indeed shorter, as in other sensory systems (Barkat et al., 2011). If so, this would suggest that there is a certain level of auditory activity necessary to maintain cross-modal connections.

These three mechanisms represent prime targets for intervention after sensory loss. By manipulating dendritic spine maturation and motility, cholinergic modulation, and myelination, it should be possible to extend cross-modal plasticity beyond the first few years of life. This could aid people who lose their sensory capabilities as adults, whether through injury or degeneration.

Previous studies have shown that early visual deprivation can permanently disrupt multisensory integration (Putzar et al., 2007; Putzar et al., 2010). While the exact locus of this deficit is unknown, a recent study in rodents showed that inactivation of secondary visual cortex selectively impairs auditory-visual multisensory facilitation (Hirokawa et al., 2008) To probe whether multisensory integration is compromised in our model system, we compared multisensory interactions (M.I.) in animals with strong cross-modal responses

(DR and NgR -/-) to those with weak ones (LR). We found biased M.I. in DR and NgR -/- mice due to a specific strengthening of multisensory enhancement. Thus, in agreement with human and rodent studies, animals with strong cross-modal responses have disrupted multisensory interactions. Future experiments are necessary to see if this specific facilitation shapes behavior. If we do find differences in multisensory integration, cross-modal transfer, or auditory localization in DR, NgR -/-, and LR mice, our mouse model could serve as a powerful tool in understanding exactly how hyperconnectivity early in life contributes to behavioral adaptations after loss of a sensory system.

Cross-modal influence in primary visual cortex

The effects of dark-rearing were much more subtle in primary visual cortex. Although there were more auditory cells in DR than LR, the difference was much smaller than in V2L. We found that similar to V2L, NgR signaling affects the distribution of cell types.

We did find features of multisensory interaction that were different between LR and DR. The majority of cells in LR V1 were suppressed by sound, and the range of modulation was quite small. In DR, the majority of cells were facilitated by sound, and the range was much larger. Furthermore, we found that NgR signaling affects the range of modulation while the maturation of inhibitory circuits affects its sign.

It is unclear why multisensory interactions are different between V1 and V2L, but differences in anatomical connectivity might be a reasonable hypothesis. We have shown that V2L receives a large amount of cross-modal

input in DR animals, and that this is mainly excitatory in nature (hence strengthened multisensory enhancement in DR). Preliminary evidence from our lab suggests that while there are some intracortical connections between V1 and auditory cortex, it is much weaker than in V2L. Furthermore, there seems to be no difference between LR and DR animals (Min et al., unpublished observations). Therefore, the majority of auditory input into V1 may be through V2L. Feedback from V2L is probably more structured than cross-region connectivity, so the circuit dynamics might be fundamentally different.

Although multisensory processing in 'unisensory' cortices has been reported multiple times (Kayser & Logothetis 2007; Lakatos et al., 2007), its behavioral role is largely unknown. It would be interesting to specifically disrupt cross-modal input into V1 and monitor perceptual abilities during multisensory tasks. Perhaps behavioral deficits would be stronger in DR as cross-modal influence is much larger in these animals.

Our work in multisensory integration in both V1 and V2L is preliminary. Over the past three decades, work by Stein, Wallace, and others in the superior colliculus (SC) and anterior ectosylvian sulcus (AES) of cats have led to a set of proposed principles governing multisensory integration. Integration is strongest when stimuli are spatially congruent, are temporally aligned so that their individual spike trains coincide, and the effectiveness of the modality-specific stimulus component is weak to moderate (known as the principle of inverse effectiveness) (for review see Stein & Stanford, 2008). It should be noted that recent evidence has gone against the principle of inverse effectiveness, favoring

a model of linear weighting of the modalities dependent on cue reliability (Morgan et al., 2008). Further exploration of stimulus parameter space is necessary to see how these principles align in mouse V1 and V2L. Ease of various rearing paradigms and the availability of genetically engineered mice should give us tremendous insight into the principles of multisensory integration. Despite this, direct comparisons between V1 and V2L in the mouse and SC and AES in cats (or the tectum in barn owls) should be done cautiously because the age- and experience-dependent nature of their multimodality is very different. AES and SC are well-established multisensory regions that become increasingly integrated given normal visual, auditory, and somatosensory experience. V1 and V2L, if anything, follow the exact opposite trajectory. They are initially influenced by multiple modalities but become increasingly less so with normal visual and auditory experience. They could follow very different mechanisms of multisensory integration and so comparisons between them could be misleading.

Towards a cohesive model of cross-modal plasticity

The work of my thesis combined with an overview of the literature in this field has led me to propose an inclusive model of where, when, and how cross-modal plasticity occurs. I believe that there are two fundamentally different routes that give rise to cross-modal responses in visual cortex. First, enucleation at a very early stage in development (or being born without eyes as in anophthalmic and evolutionary models) fails to establish any meaningful connection between the retina and the visual thalamus (LGN). As a result, auditory subcortical nuclei, such as the inferior colliculus, invade the deprived LGN. This maintains normal

thalamocortical connectivity between LGN and V1, but with auditory information being transferred instead (Fig. 5.1 top panel, 'premature blind'). This is a similar mechanism to how visual information is rerouted to somatosensory or auditory thalamus by the destruction of lower somatosensory or auditory areas (Frost & Metin, 1985; Sur et al., 1988; Pallas et al., 1990; Sharma et al., 2000).

In contrast, enucleation later in life (but still early), binocular deprivation, or dark-rearing allow a minimal connection to be established between retina and LGN that prevents invasion from auditory areas. In line with this, we failed to elicit auditory responses in the LGN of DR mice as measured by c-fos immunoreactivity (Min et al., unpublished observations). Instead, an otherwise transient connection between auditory thalamus (MGN) and V2L is stabilized, making V2L the primary locus for auditory activity in visual cortex (Fig 5.1 middle panel, 'early blind'). This hypothesis is supported by work in rats, where a transient connection between auditory thalamus and primary somatosensory cortex is maintained after early whisker deprivation (Nicolelis et al., 1991).

I believe that these two different modes of early blindness explain why some studies report activity in primary visual cortex (Yaka et al., 2000; Bronchti et al., 2002; Kahn & Krubitzer, 2002) and others do not (Yaka et al., 1999; Chabot et al., 2007). This could lead to different sets of molecular mechanisms controlling the two forms of plasticity. In the 'early blind,' mechanisms stated in this thesis would be the primary method for cross-modal refinement. In the 'premature blind,' there might be more of a reliance on signaling pathways

Figure 5.1 | Age at visual deprivation determines whether V1 or V2L is the primary recipient of cross-modal input

(a) In animals enucleated in a premature state, the lack of retinal input leads to an innervation of visual thalamus (LGN) by the inferior colliculus (IC), an auditory subcortical nucleus. V1 retains its normal connectivity with LGN, so it becomes the primary locus for auditory activity in visual cortex (indicated by red fill).

(b) Animals visually deprived at a more mature (but still early) state by enucleation, binocular sutures, or dark-rearing do not undergo a rewiring of LGN. Instead, typically transient connections between V2L and auditory thalamus (MGN) and cortex (AC) are stabilized, making V2L (red) the primary region for cross-modal plasticity.

(c) Animals with normal sensory experience prune auditory innervation of secondary visual cortex by early adulthood to maintain separate auditory and visual processing streams.

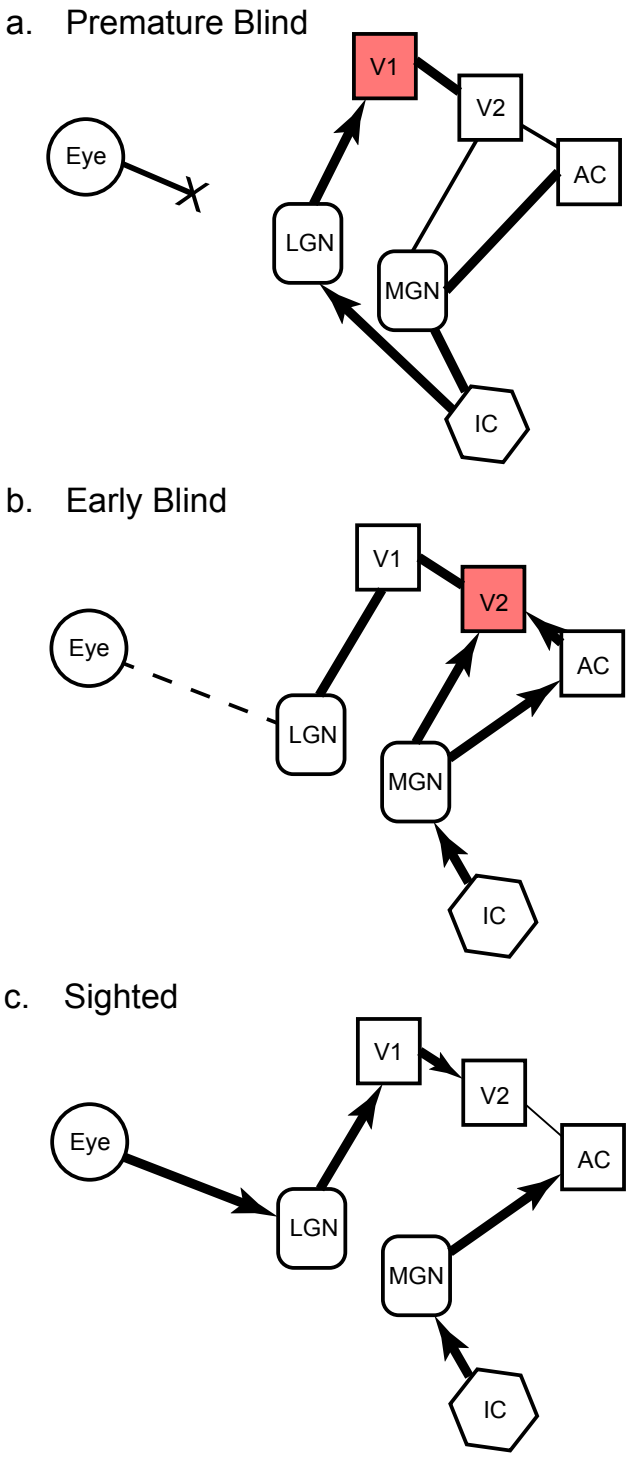

Figure 5.1 (Continued)

involved in axon guidance and patterning, such as ephrin signaling (Cang et al., 2005).

Concurrently to changes in the deprived cortex, functional reorganization also occurs within intact sensory regions. In line with this, visual deprivation has been shown to selectively increase extracellular serotonin in rodent barrel cortex. This upregulation acts on 5HT2A/2C receptors and extracellular signal-related kinases (ERK) to facilitate the synaptic delivery of AMPA-type glutamate receptors at layer 4-2/3 synapses, thereby sharpening whisker-barrel map responses (Jitsuki et al., 2011). Thus, serotonergic modulation might be selectively enhanced in intact sensory regions while cholinergic modulation is enhanced in the deprived cortex. Along with maintained cross-modal connectivity by a reduction in NgR and Icam5 signaling, these pathways would be responsible for enhancing cortical processing in the remaining modalities leading to marked behavioral improvements.

I believe that this thesis has successfully laid a framework in understanding the mechanisms underlying cross-modal plasticity. I hope that by taking advantage of the anatomical and molecular targets outlined in this work, we can further our knowledge of how to rehabilitate neuronal circuits after loss of a sensory system.

References

Alais, D. and Burr, D. (2004). The ventriloquist effect results from near-optimal bimodal integration. Curr. Biol. 14(3): 257-62.

Allman, B.L., Keniston, L.P., Meredith, M.A. (2009). Adult deafness induces somatosensory conversion of ferret auditory cortex. PNAS 106(14): 5925-30.

Amedi, A. et al. (2003). Early 'visual' cortex activation correlates with superior verbal memory performance in the blind. Nat. Neurosci. 6(7): 758-66.

Amedi, A. et al. (2004). Transcranial magnetic stimulation of the occipital pole interferes with verbal processing in blind subjects. Nat. Neurosci. 7(11): 1266-70.

Anderson, V., Spencer-Smith, M., and Wood, A. (2011). Do children really recover better? Neurobehavioural plasticity after early brain insult. Brain 134(Pt 8): 2197-221.

Atwal, J.K. et al. (2008). PirB is a functional receptor for myelin inhibitors of axonal regeneration. Science 322(5903): 967-70.

Barkat, T.R., Polley, D.B., and Hensch, T.K. (2001). A critical period for auditory thalamocortical connectivity. Nat. Neurosci. 14(9): 1189-94.

Bavelier, D. et al. (2000). Visual attention to the periphery is enhanced in congenitally deaf individuals. J. Neurosci. 20(17): RC93.

Bavelier, D. and Neville, H.J. (2002). Cross-modal plasticity: where and how? Nat. Rev. Neurosci. 3(6): 443-52.

Bavelier, D., Dye, M.W.G, and Hauser, P.C. (2006). Do deaf individuals see better? Trends Cogn. Sci. 10(11): 512-8.

Bear, M.F. et al. (1983). Two methods of catecholamine depletion in kitten visual cortex yield different effects on plasticity. Nature 302(5905): 245-7.

Bedny, M. et al. (2010). Sensitive period for a multimodal response in human visual motion area MT/MST. Curr. Biol. 20(21): 1900-6.

Bedny, M. et al. (2011). Language processing in the occipital cortex of congenitally blind adults. PNAS 108(11): 4429-34.

Bronchti, G. et al. (2002). Auditory activation of "visual" cortical areas in the blind mole rat (Spalax ehrenbergi). Eur. J. Neurosci. 16(2): 311-29.

Brosch, M., Selezneva, E., and Scheich, H. (2005). Nonauditory events of a behavioral procedure activate auditory cortex of highly trained monkeys. J. Neurosci. 25(29): 6797-806.

Budel, S. et al. (2008). Genetic variants of Nogo-66 receptor with possible association to schizophrenia block myelin inhibition of axon growth. J. Neurosci. 28(49): 13161-72.

Burton, H. et al. (2002a). Adaptive changes in early and late blind: a fMRI study of Braille reading. J. Neurophysiol. 87:589-611.

Burton, H. et al. (2002b). Adaptive changes in early and late blind: a fMRI study of verb generation to heard nouns. J. Neurophysiol. 88:3359-71.

Campbell, L.E. et al. (2009). Brain structural differences associated with the behavioural phenotype in children with Williams syndrome. Brain Research 1258: 96-107.

Cang, J. et al. (2005). Ephrin-as guide the formation of functional maps in the visual cortex. Neuron 48(4): 577-89.

Carmignoto, G. and Vicini, S. (1992). Activity-dependent decrease in NMDA receptor responses during development of the visual cortex. Science 258(5084): 1007-11.

Chabot, N. et al. (2008). Subcortical auditory input to the primary visual cortex in anophthalmic mice. Neurosci. Lett. 433(2): 129-34.

Cohen, L.G. et al. (1997). Functional relevance of cross-modal plasticity in humans. Nature 389(6647): 180-3.

Collignon, O. et al. (2009). Cross-modal plasticity for the spatial processing of sounds in visually deprived subjects. Exp. Brain Res. 192(3): 343-58.

De Gelder, B. et al. (2003). Audio-visual integration in schizophrenia. Schizophrenia Research 59(2-3): 211-8.

Dehay, C., Kennedy, H., and Bullier, J. (1998). Characterization of transient cortical projections from auditory, somatosensory, and motor cortices to visual areas 17, 18, and 19 in the kitten. J. Comp. Neurol. 272(1): 68-89.

Desai, S., Stickney, G., and Zeng, F. (2008). Auditory-visual speech perception in normal-hearing and cochlear-implant listeners. J. Acoust. Soc. Am. 123(1): 428-40.

Doron, N. and Wollberg, Z. (1994). Cross-modal neuroplasticity in the blind mole rat Spalax ehrenbergi: a WGA-HRP tracing study. Neuroreport 5(18): 2697-701.

Eden, U.T. & Kramer, M.A. (2010). Drawing inferences from Fano factor calculations. J. Neuro. Methods 190(1): 149-52.

Elbert, T. et al. (2002). Expansion of the tonotopic area in the auditory cortex of the blind. J. Neurosci. 22(22): 9941-4.

Fagiolini, M. and Hensch, T.K. (2000). Inhibitory threshold for critical-period activation in primary visual cortex. Nature 404(6774): 183-6.

Fagiolini, M. et al. (2003). Separable features of visual cortical plasticity revealed by N-methyl-D-aspartate receptor 2A signaling. PNAS 100(5): 2854-9.

Fagiolini, M. et al. (2004). Specific GABAA circuits for visual cortical plasticity. Science 303(5664): 1681-3.

Feldman, D.E., Brainard, M.S., and Knudsen, E.I. (1996). Newly learned auditory responses mediated by NMDA receptors in the owl inferior colliculus. Science 271(5248): 525-8.

Felleman, D.J. and Van Essen, D.C. (1991). Distributed hierarchical processing in the primate cerebral cortex. Cereb. Cortex 1: 1-47.

Ffytche, D.H. et al. (1998). The anatomy of conscious vision: an fMRI study of visual hallucinations. Nat. Neurosci. 1(8): 738-42.

Fujii, T. et al. (2009). An investigation of cross-modal plasticity of effective connectivity in the blind by dynamic causal modeling of functional MRI data. Neurosci. Res. 65(2): 175-86.

Fine, I. et al. (2005). Comparing the effects of auditory deprivation and sign language within the auditory and visual cortex. J. Cogn. Neurosci. 17(10): 1621-37.

Finney, E.M., Fine, I., Dobkins, K.R. (2001). Visual stimuli activate auditory cortex in the deaf. Nat. Neurosci. 4(12): 1171-3.

Fish, K.N., Sweet, R.A., and Lewis, D.A. (2011). Differential distribution of proteins regulating GABA synthesis and reuptake in axon boutons of subpopulations of cortical interneurons. Cerebral Cortex 21(11): 2450-60.

Foxe, J.J. et al. (2000). Multisensory auditory-somatosensory interactions in early cortical processing revealed by high-density electrical mapping. Brain Res. Cogn. Brain Res. 10(1-2): 77-83.

Frost, D.O. & Metin, C. (1985). Induction of functional retinal projections to the somatosensory system. Nature 317(6033): 162-4.

Garcia, J.O., Grossman, E.D., and Srinivasan, R. Evoked potentials in large-scale cortical networks elicited by TMS of the visual cortex. J. Neurophysio. 10.1152/jn.00739.2010.

Ghazanfar, A.A. and Schroeder, C.E. (2006). Is neocortex essentially multisensory? Trends Cog. Sci. 10(6): 278-85.

Ghoshal, A., Tomarken, A., and Ebner, F. (2011). Cross-sensory modulation of primary sensory cortex is developmentally regulated by early sensory experience. J. Neurosci. 31(7): 2526-36.

Goard, M. and Dan, Y. (2009). Basal forebrain activation enhances cortical coding of natural scenes. Nat. Neurosci. 12(11): 1444-9.

Goldreich, D. and Kanics, I.M. (2003). Tactile acuity is enhanced in blindness. J. Neurosci. 23(8): 3439-45.

Gu, Q. (2003). Neuromodulatory transmitter systems in the cortex and their role in cortical plasticity. Neuroscience 111(4): 815-35.

Guillem, K. et al. (2011). Nicotinic acetylcholine receptor β2 subunits in the medial prefrontal cortex control attention. Science 333(6044): 888-91.

Hall, A.J. and Lomber, S.G. (2008). Auditory cortex projections target the peripheral field representation of primary visual cortex. Exp. Brain Res. 190(4): 413-30.

Hamilton, R. et al. (2000). Alexia for Braille following bilateral occipital stroke in an early blind woman. Neuroreport 11(2): 237-40.

Hanover, J.L. et al. (1999). Brain-derived neurotrophic factor overexpression induces precocious critical period in mouse visual cortex. J. Neurosci. 19(22): RC40.

Hartline, P.H., Kass, L., Loop, M.S. (1978). Merging of modalities in the optic tectum: infrared and visual integration in rattlesnakes. Science 199(4334): 1225-9.

Held, R. et al. (2011). The newly sighted fail to match seen with felt. Nat Neurosci. 14(5): 551-3.

Hensch, T.K. and Stryker, M.P. (1996). Ocular dominance plasticity under metabotropic glutamate receptor blockade. Science 272(5261): 554-7.

Hensch, T.K. et al. (1998a). Comparison of plasticity in vivo and in vitro in the developing visual cortex of normal and protein kinase A RIbeta-deficient mice. J. Neurosci. 18(6): 2108-17.

Hensch, T.K. et al. (1998b). Local GABA circuit control of experience-dependent plasticity in developing visual cortex. Science 282(5393): 1504-8.

Hensch, T.K. (2004). Critical period regulation. Annu. Rev. Neurosci. 27: 549-79.

Hensch, T.K. and Stryker, M.P. (2004). Columnar architecture sculpted by GABA circuits in developing cat visual cortex. Science 303(5664): 1678-81.

Hensch, T.K. (2005). Critical period plasticity in local cortical circuits. Nat. Rev. Neurosci. 6(11): 877-88.

Hirokawa, J. et al. (2008). Functional role of the secondary visual cortex in multisensory facilitation in rats. Neuroscience 153(4): 1402-17.

Hubel, D.H., Wiesel, T.N., and LeVay, S. (1977). Plasticity of ocular dominance columns in monkey striate cortex. Philos. Trans. R. Soc. Lond. B Biol. Sci. 278(961): 377-409.

Hunt, D.L. et al. (2005). Aberrant retinal projections in congenitally deaf mice: how are phenotypic characteristics specified in development and evolution? Anat. Rec. A Discov. Mol. Cell Evol. Biol. 287(1): 1051-66.

Hsu, R. et al. (2007). Nogo Receptor 1 (RTN4R) as a candidate gene for schizophrenia: analysis using human and mouse genetic approaches. PLoS ONE 2(11): e1234

Ibañez-Tallon, I. et al. (2002). Novel modulation of neuronal nicotinic acetylcholine receptors by association with the endogenous prototoxin lynx1. Neuron 33(6): 893-903.

Innocenti, G.M., Berbel, P., and Clarke, S. (1988). Development of projections from auditory to visual areas in the cat. J. Comp. Neurol. 272(2): 242-59.

Izraeli, R. et al. (2002). Cross-modal neuroplasticity in neonatally enucleated hamsters: structure, electrophysiology and behavior. Eur. J. Neurosci. 15(4): 693-712.

Jiang, H. et al. (1994). Sensory modality distribution in the anterior ectosylvian cortex (AEC) of cats. Exp. Brain. Res. 97(3): 404-14.

Jiang, J. et al. (2009). Thick visual cortex in the early blind. J. Neurosci. 29(7): 2205-11.

Jiang, W. et al. (2001). Two cortical areas mediate multisensory integration in superior colliculus neurons. J. Neurophysiol. 85(2): 506-22.

Kahn, D.M. and Krubitzer, L. (2002). Massive cross-modal cortical plasticity and the emergence of a new cortical area in developmentally blind mammals. PNAS 99(17): 11429-34.

Karlen, S.J., Kahn, D.M, and Krubitzer, L. (2006). Early blindness results in abnormal corticocortical and thalamocortical connections. Neuroscience 142(3): 843-58.

Kasamatsu, T. and Pettigrew, J.D. (1976): Depletion of brain catecholamines: failure of ocular dominance shift after monocular occlusion in kittens. Science 194(4261): 206-9.

Katagiri, H., Fagiolini, M., and Hensch, T.K. (2007). Optimization of somatic inhibition at critical period onset in mouse visual cortex. Neuron 53(6): 805-12.

Kayser, C. and Logothetis, N.K. (2007). Do early sensory cortices integrate cross-modal information? Brain Struct. Funct. 212(2): 121-32.

King, A.J. et al. (1988). Developmental plasticity in the visual and auditory representations in the mammalian superior colliculus. Nature 332(6159): 73-6.

Klinge, C. et al. (2010). Corticocortical connections mediate primary visual Cortex responses to auditory stimulation in the blind. J. Neurosci. 30(38): 12798-805.

Knudsen, E.I. (1983). Early auditory experience aligns the auditory map of space in the optic tectum of the barn owl. Science 222(4626): 939-42.

Knudsen, E.I. (1998). Capacity for plasticity in the adult owl auditory system expanded by juvenile experience. Science 279(5356): 1531-3.

Knudsen, E.I. and Brainard, M.S. (1991). Visual instruction of the neural map of auditory space in the developing optic tectum. Science 253(5015): 85-7.

Knudsen, E.I. and Knudsen, P.F. (1985). Vision guides the adjustment of auditory localization in young barn owls. Science 230(4725): 545-8.

Knudsen, E.I. and Knudsen, P.F. (1989a). Visuomotor adaptation to displacing prisms by adult and baby barn owls. J. Neurosci. 9(9): 3297-305.

Knudsen, E.I. and Knudsen, P.F. (1989b). Vision calibrates sound localization in developing barn owls. J. Neurosci. 9(9): 3306-13.

Knudsen, E.I. and Knudsen, P.F. (1990). Sensitive and critical periods for visual calibration of sound localization by barn owls. J. Neurosci. 10(1): 222-32.

Konrad, A. and Winterer, G. (2008). Disturbed structural connectivity in schizophrenia primary factor in pathology or epiphenomenon? Schizo. Bulletin 34(1): 72-92.

Korte, M. and Rauschecker, J.P. (1993). Auditory spatial tuning of cortical neurons is sharpened in cats with early blindness. J. Neurophysio. 70(4): 1717-21.

Kubicki, M. et al. (2007). A review of diffusion tensor imaging studies in schizophrenia. J. Psychiatr. Res. 41(1-2): 15-30.

Kuhl, P.K. (2004). Early language acquisition: cracking the speech code. Nat. Rev. Neurosci. 5(11): 831-43.

Kuhl, P.K. (2010). Brain mechanisms in early language acquisition. Neuron 67(5): 713-27.

Kuhlman, S.J., Tring, E., Trachtenberg, J.T. (2011). Fast-spiking interneurons have an initial orientation bias that is lost with vision. Nat. Neurosci. 14(9): 1121-3.

Kupers, R. et al. (2011). Neural correlates of olfactory processing in congenital blindness. Neuropsychologia 49(7): 2037-44.

Laemle, L.K., Strominger, N.L., and Carpenter, D.O. (2006). Cross-modal innervation of primary visual cortex by auditory fibers in congenitally anophthalmic mice. Neurosci. Lett. 396(2): 108-12.

Lakatos, P. et al. (2007). Neuronal oscillations and multisensory interaction in primary auditory cortex. Neuron 53(2): 279-92.

Laramee, M.E. et al. (2011). Indirect pathway between the primary auditory and visual cortices through layer V pyramidal neurons in V2L in mouse and the effects of bilateral enucleation. Eur. J. Neurosci. 34(1): 65-78.

Lessard, N. et al. (1998). Early-blind human subjects localize sound sources better than sighted subjects. Nature 395(6699): 278-80.

Levänen, S., Jousmäki, V., and Hari, R. (1998). Vibration-induced auditory-cortex activation in a congenitally deaf adult. Curr. Biol. 8(15): 869-72.

Li, S. and Strittmatter, S.M. (2003). Delayed systemic Nogo-66 receptor antagonist promotes recovery from spinal cord injury. J. Neurosci. 23(10): 4219-27.

Linden, J.F. et al. (2003). Spectrotemporal structure of receptive fields in areas AI and AAF of mouse auditory cortex. J. Neurophysiol. 90(4): 2660-75.

Linkenhoker, B.A., Von Der Ohe, C.G., and Knudsen, E.I. (2005). Anatomical traces of juvenile learning in the auditory system of adult barn owls. Nat. Neurosci. 8(1): 93-8.

Lomber, S.G., Meredith, M.A., and Kral, A. (2010). Cross-modal plasticity in specific auditory cortices underlies visual compensations in the deaf. Nat. Neurosci. 13(11): 1421-7.

Lucas-Meunier, E. et al. (2009). Involvement of nicotinic and muscarinic receptors in the endogenous cholinergic modulation of the balance between excitation and inhibition in the young rat visual cortex. Cerebral Cortex 19(10): 2411-27.

Macaluso, E., Frith, C.D., and Driver, J. (2000). Modulation of human visual cortex by crossmodal spatial attention. Science 289(5482): 1206-8.

Magnee, M.J.C.M. et al. (2011). Multisensory integration and attention in autism spectrum disorder: evidence from event-related potentials. PLoS ONE 6(8): e24196.

Mataga, N., Nagai, N., Hensch, T.K. (2002). Permissive proteolytic activity for visual cortical plasticity. Proc. Natl. Acad. Sci. 99(11): 7717-21/

Mataga, N., Mizuguchi, Y., Hensch, T.K. (2004). Experience-dependent pruning of dendritic spines in visual cortex by tissue plasminogen activator. Neuron 44(6): 1031-41.

Matsuno, H. et al. (2005). Telencephalin slows spine maturation. J. Neurosci. 26(6): 1776-86.

Maurer, D. Neonatal synesthesia: implications for the processing of speech and faces. In de Boysson-Bardies, B. et al. (Eds) *Developmental Neurocognition: Speech and face processing in the first year of life.* Dordrecht: Kluwer Academic Publishers, 2003.

McCullough, S. and Emmorey, K. (1997). Face processing by deaf ASL signers: evidence for expertise in distinguished local features. J. Deaf Stud. Deaf Educ. 2(4): 212-22.

McGee, A.W. et al. (2005). Experience-driven plasticity of visual cortex limited by myelin and Nogo receptor. Science 309(5744): 2222-6.

McGurk, H. and MacDonald, J. (1976). Hearing lips and seeing voices. Nature 264(5588): 746-748.

Mennan, R. and Kim, S. Spatial and temporal limits in cognitive neuroimaging with fMRI. Trends in Cog. Sci. 3(6): 207-216.

Merabet, L.B. et al. (2008). Rapid and reversible recruitment of early visual cortex for touch. PLoS One 3(8): e3046.

Merabet, L.B. and Pascual-Leone, A. (2010). Neural reorganization following sensory loss: the opportunity for change. Nat. Rev. Neurosci. 11(1): 44-52.

Meredith, M.A. and Stein, B.E. (1983). Interactions among converging sensory inputs in the superior colliculus. Science 221(4608): 389-91.

Meredith, M.A. and Lomber, S.G. (2011). Somatosensory and visual crossmodal plasticity in the anterior auditory field of early-deaf cats. Hearing Res. 280(1-2): 38-47.

Minshew, N.J. and Williams, D.L. (2007). The new neurobiology of autism: cortex, connectivity, and neuronal organization. Archives of Neurology 64(7): 945-50.

Miyamoto, H., Katagiri, H., and Hensch, T.K. (2003). Experience-dependent slow-wave sleep development. Nat. Neurosci. 6(6): 553-4.

Morishita, H. et al. (2010). Lynx1, a cholinergic brake, limits plasticity in adult visual cortex. Science 330(6008): 1238-40.

Morgan, M.L., Deangelis, G.C., and Angelaki, D.E. (2008). Multisensory integration in macaque visual cortex depends on cue reliability. Neuron 59(4): 662-73.

Morrell, F. (1972). Visual system's view of acoustic space. Nature 238: 44-46.

Müller, R. et al. (2011). Underconnected, but how? A survey of functional connectivity MRI studies in autism spectrum disorders. Cerebral Cortex 21(10): 2233-43.

Musacchia, G. and Schroeder, C.E. (2009). Neuronal mechanisms, response dynamics and perceptual functions of multisensory interactions in auditory cortex. Hearing Research 258(1-2): 72-9.

Nelson, C.A. et al. (2007). Cognitive recovery in socially deprived young children: the Bucharest Early Intervention Project. Science 318(5858): 1937-40.

Neville, H.J. and Lawson, D. (1987). Attention to central and peripheral visual space in a movement detection task: an event-related potential and behavioral study. II. Congenitally deaf adults. Brain Research 405(2): 258-283.

Newman, L.A. and McGaughy, J. (2008). Cholinergic deafferentation of prefrontal cortex increases sensitivity to cross-modal distractors during a sustained attention task. J. Neurosci. 28(10): 2642-50.

Nicolelis, M.A., Chapin, J.K., and Lin, R.C. (1991). Neonatal whisker removal in rats stabilizes a transient projection from the auditory thalamus to the primary somatosensory cortex. Brain Research 567(1): 133-9.

Nishimura, H. et al. (1999). Sign language 'heard' in the auditory cortex. Nature 397(6715): 116.

Oray, S., Majewska, A., and Sur, M. (2004). Dendritic spine dynamics are regulated by monocular deprivation and extracellular matrix degradation. Neuron 44(6): 1021-30.

Pallas, S.L., Roe, A.W., Sur, M. (1990). Visual projections induced into the auditory pathway of ferrets. I. Novel inputs to primary auditory cortex (AI) from the LP/pulvinar complex and the topography of the MGN-AI projection. J. Comp. Neurol. 298(1): 50-68.

Pantev, C. et al. (2001). Representational cortex in musicians. Plastic alterations in response to musical practice. Ann. N.Y. Acad. Sci. 930: 300-14.

Pascual-Leone, A. and Torres, F. (1993). Plasticity of the sensorimotor cortex representation of the reading finger in Braille readers. Brain 116(Pt 1): 39-52.

Paxinos, G. and Franklin, B.J.K. The Mouse Brain in Stereotaxic Coordinates. 2nd Ed. San Diego: Academic Press, 2001.

Piché, M. et al. (2004). Environmental enrichment enhances auditory takeover of the occipital cortex in anophthalmic mice. Eur. J. Neurosci. 20(12): 3463-72.

Poirier, C. et al. (2006). Auditory motion perception activates visual motion areas in early blind subjects. NeuroImage 31(1): 279-85.

Ponce, C.R., Lombar, S.G., and Born, R.T. (2008). Integrating motion and depth via parallel pathways. Nat. Neurosci. 11(2): 216-23.

Prusky, G.T., West, P.W., and Douglas, R.M. (2000). Experience-dependent plasticity of visual acuity in rats. Eur. J. Neurosci. 12(10): 3781-6.

Ptito, M. et al. (2001). When the auditory cortex turns visual. Prog. Brain Res. 134: 447-58.

Ptito, M. et al. (2008). TMS of the occipital cortex induces tactile sensations in the fingers of blind Braille readers. Exp. Brain Res. 184(2): 193-200.

Putzar, L. et al. (2007). Early visual deprivation impairs multisensory interactions in humans. Nat. Neurosci. 10(10): 1243-5.

Putzar, L., Hotting, K., and Roder, B. (2010) Early visual deprivation affects the development of face recognition and of audio-visual speech perception. Restor. Neurol. Neurosci. 28(2): 251-7.

Quinlan, E.M. et al. (1999). Rapid, experience-dependent expression of synaptic NMDA receptors in visual cortex in vivo. Nat. Neurosci. 2(4): 352-7.

Rauschecker, J.P. et al. (1992). Crossmodal changes in the somatosensory vibrissa/barrel system of visually deprived animals. PNAS 89(11): 5063-7.

Rauschecker, J.P. and Korte, M. (1993). Auditory compensation for early blindness in cat cerebral cortex. J. Neurosci. 13(10): 4538-48.

Rauschecker, J.P. (1995). Compensatory plasticity and sensory substitution in the cerebral cortex. Trends Neurosci. 18(1): 36-43.

Rauschecker, J.P. (1996). Substitution of visual by auditory inputs in the cat's anterior ectosylvian cortex. Prog. Brain Res. 112: 313-23.

Rauschecker, J.P. (2002). Cortical map plasticity in animals and humans. Prog. Brain Res. 138: 73-88.

Rakic, P., Suner, I., and Williams, R.W. (1991). A novel cytoarchitectonic area induced experimentally within the primate visual cortex. PNAS 88(6): 2083-7.

Reinert, K.C. et al. (2004). Flavoprotein autofluorescence imaging of neuronal activation in the cerebellar cortex *in vivo*. J. Neurophyiol. 92:199-211.

Renger, J.J. et al. (2002). Experience-dependent plasticity without long-term depression by type 2 metabotropic glutamate receptors in developing visual cortex. PNAS 99(2): 1041-6.

Rockland, K.S. and Ojima, H. (2003). Multisensory convergence in calcarine visual areas in macaque monkey. Int. J. Psychophysiol. 50(1-2): 19-26.

Roe, A.W. et al. (1990). A map of visual space induced in primary auditory cortex. Science 250(4982): 818-20.

Roeser, T. and Baier, H. (2003). Visuomotor behaviors in larval zebrafish after GFP-guided laser ablation of the optic tectum. J. Neurosci. 23(9): 3726-34.

Romei, V. et al. (2007). Occipital transcranial magnetic stimulation has opposing effects on visual and auditory stimulus detection: implications for multisensory interactions. J. Neurosci. 27(43): 11465-72.

Rouw, R. and Scholte, S. (2007). Increased structural connectivity in grapheme-color synesthesia. 10(6): 792-7.

Rouw, R. and Scholte, S. (2007). Neural basis of individual differences in synesthetic experiences. J. Neurosci. 30(18): 6205-13.

Sadato, N. et al. (1996). Activation of primary visual cortex by Braille reading in blind subjects. Nature 380(6574): 526-8.

Sadato, N. et al. (2002). Critical period for cross-modal plasticity in blind humans: a functional MRI study. NeuroImage 16(2): 389-400.

Saenz, M. et al. (2007). Visual motion area MT+/V5 responds to auditory motion in human sight-recovery subjects. J. Neurosci. 28(20): 5141-8.

Schorr, E.A. et al. (2005). Auditory-visual fusion in speech perception in children with cochlear implants. PNAS 102(51): 18748-50.

Schroeder, C.E. and Foxe, J.J. (2002). The timing and laminar profile of converging inputs to multisensory areas of the macaque neocortex. Brain Res. Cogn. Brain Res. 14(1): 187-98.

Schwab, M.E. (2010). Functions of Nogo proteins and their receptors in the nervous system. Nat. Rev. Neurosci. 11(12): 799-811.

Sharma, J., Angelucci, A., and Sur, M. (2000). Induction of visual orientation modules in auditory cortex. Nature 404(6780): 841-7.

Sheng, M. and Greenberg, M. E. (1990). The regulation and function of *c-fos* and other immediate early genes in the nervous system. Neuron 4:477-85.

Smith, G.B. and Bear, M.F. (2010). Bidirectional ocular dominance plasticity of inhibitory networks: recent advances and unresolved questions. Front. Cell. Neurosci. 4:21.

Sprague, J.M. (1972). The superior colliculus and pretectum in visual behavior. Invest. Ophthalom. 11(6): 473-82.

Stein, B.E., Clamann, H.P., and Goldberg, S.J. (1980). Superior colliculus: control of eye movements in neonatal kittens. Science 210(4465): 78-80.

Stein, B.E. and Stanford, T.R. (2008). Multisensory integration: current issues from the perspective of the single neuron. Nat. Rev. Neurosci. 9(4): 255-66.

Sterr, A. et al. (1998). Changed perceptions in Braille readers. Nature 391(6663): 134-5.

Stone, D.B. et al. (2011). Unisensory processing and multisensory integration in schizophrenia: A high-density electrical mapping study. Neuropsychologia 49(12): 3178-87.

Sugiyama, S. et al. (2008). Experience-dependent transfer of Otx2 homeoprotein into the visual cortex activates postnatal plasticity. Cell 134(3): 508-20.

Sur, M., Garraghty, P.E., and Roe, A.W. (1988). Experimentally induced visual projections into auditory thalamus and cortex. Science 242(4884): 1437-41.

Syken, J. et al. (2006). PirB restricts ocular-dominance plasticity in visual cortex. Science 313(5794): 1795-800.

Theil, C.M., Friston, K.J., and Dolan, R.J. (2002). Cholinergic modulation of experience-dependent plasticity in human auditory cortex. Neuron 35(3): 567-74.

Thomi, M. et al. (2006). Enduring critical period plasticity visualized by transcranial flavoprotein imaging in mouse primary visual cortex. J. Neurosci. 26(45): 11775-85.

Thorton-Wells, T.A. et al. (2010). Auditory attraction: activation of visual cortex by music and sound in Williams syndrome. Am. J. Intellect. Dev. Disabil. 115(2): 172-89.

Vasconcelos, N. et al. (2011). Cross-modal responses in the primary visual cortex encode complex objects and correlate with tactile discrimination. PNAS 108(37): 15408-13.

Vetencourt, J.F.M. et al. (2008). The antidepressant fluoxetine restores plasticity in the adult visual cortex. Science 320(5874): 385-8.

Wallace, M.T., Meredith, M.A., and Stein, B.E. (1992). Integration of multiple sensory modalities in cat cortex. Exp. Brain Res. 91(3): 484-8.

Wallace, M.T., Meredith, M.A., and Stein, B.E. (1993). Converging influences from visual, auditory, and somatosensory cortices onto output neurons of the superior colliculus. J. Neurophysiol. 69(6): 1797-809.

Wallace, M.T. and Stein, B.E. (1997a). Cross-modal synthesis in the midbrain depends on input from cortex. J. Neurophysiol. 70(1): 429-32.

Wallace, M.T. and Stein, B.E. (1997b). Development of multisensory neurons and multisensory integration in cat superior colliculus. J. Neurosci. 17(7): 2429-44.

Wass, S. (2011). Distortions and disconnections: disrupted brain connectivity in autism. Brain and Cognition 75(1): 18-28.

Will, B. et al. (2004). Recovery from brain injury in animals: relative efficacy of environmental enrichment, physical exercise or formal training (1990-2002). Prog. Neurobiol. 72(3): 167-82.

Willi, R. et al. (2010). Constitutive genetic deletion of the growth regulator Nogo-A induces schizophrenia-related endophenotypes. J. Neurosci. 30(2): 556-67.

Williams, L.E. et al. (2010). Reduced multisensory integration in patients with schizophrenia on a target detection task. Neuropsychologia 48(10): 3128-36.

Yaka, R., Yinon, U., and Wollberg, Z. (1999). Auditory activation of cortical visual areas in cats after early visual deprivation. Eur. J. Neurosci. 11(4): 1301-12.

Yaka, R. et al. (2000). Pathological and experimentally induced blindness induces auditory activity in the cat primary visual cortex. Exp. Brain Res. 131(1): 144-8.

Yoshinaga-Itano, C. et al. (1998). Language of early- and later-identified children with hearing loss. Pediatrics 102(5): 1161-71.

Zeng, C. et al. (2009). Cochlear damage changes the distribution of vesicular glutamate transporters associated with auditory and nonauditory inputs to the cochlear nucleus. J. Neurosci. 29(13): 4210-7.

Zheng, W. and Knudsen, E.I. (1999). Functional selection of adaptive auditory space map by GABAA-mediated inhibition. Science 284(5416): 962-5.

Zikopoulos, B and Barbas, H. (2007). Circuits for multisensory integration and attentional modulation through the prefrontal cortex and the thalamic reticular nucleus in primates. Rev. Neurosci. 18(6): 417-38.